SYNTHESIS OF QUINOXALINE-FERROCENE COMPOUNDS AND THEIR MEDICINAL PROPERTIES AGAINST *MYCOBACTERIUM TUBERCULOSIS*

MASTER OF SCIENCE IN CHEMISTRY

L.A. RAPHOKO

2019

SYNTHESIS OF QUINOXALINE-FERROCENE COMPOUNDS AND THEIR MEDICINAL PROPERTIES AGAINST *MYCOBACTERIUM TUBERCULOSIS*

BY

RAPHOKO LERATO AUGUSTINAH

A RESEARCH DISSERTATION SUBMITED FOR THE DEGREE, MASTER OF SCIENCE IN THE DEPARTMENT OF CHEMISTRY, SCHOOL OF PHYSICAL AND MINERAL SCIENCES, FACULTY OF SCIENCE AND AGRICULTURE, UNIVERSITY OF LIMPOPO SOUTH AFRICA.

SUPERVISOR: Prof W NXUMALO

2019

Declaration

I declare that “Synthesis of quinoxaline-ferrocene compounds and their medicinal properties against *mycobacterium tuberculosis*” is my own work submitted for the degree Master of Science at university of Limpopo. It has not been submitted for any degree or examination at any other University, and all sources I have used or quoted have been indicated and acknowledged through complete references.

…… ……..

Ms Raphoko L.A Date

Dedication

The work developed in this study is dedicated to my late mother F. Raphoko, late aunt MJ Molokomme and my family at large.

Acknowledgement

It is by grace of the all Mighty God that the work designed in this study has become a reality, and for that I'm thankful of my supervisor Prof Winston Nxumalo with the support, guidance and encouragement.

I would like to extend my sincere gratitude to every individual and institution that played a role in my studies. The work has been fruitful through your contributions:

- My family for their prayers, support and having faith in me to conquer through it all.
- The department of chemistry at the University of Limpopo for granting me the opportunity to enroll for postgraduate degrees.
- Dr RM Mampa and Dr TC Leboho for the advice and guidance offered through my academic journey.
- Ms TG Ramakadi for her continuous guidance in teaching and training me with running (experiments), maintenance and processing (data) of nuclear magnetic resonance (NMR) instrument.
- Prof T Naicker from the University of Kwazulu natal (UKZN) together with NRF bursary for the financial support.
- The centre for drug delivery and development (H3-D) centre at the University of Cape Town for the anti-Mycobaterium tuberculosis assay experimental data.
- Prof TM Matsebatlela and MA Sibiya for the anticancer assay experimental data.
- University of Stellenbosch for high resolution mass spectrometry analysis.
- My friends KD Mazwi, NG Mutileni and most importantly MD Matseba you have been a great influence.
- Mr K.B Dilebo, Mr N.R Moroane and Mr K Lekgau and for making the lab space a fun place to be.

Scientific contributions

Conference attended:

Oral presentation at:

9th Faculty of Sciences and Agriculture, University of Limpopo Research day, Limpopo, South Africa, 2018

Date: 20-21 September 2018

Synthesis of quinoxaline-ferrocene compounds and their medicinal properties against *Mycobacterium tuberculosis*

LA Raphoko, W Nxumalo
University of Limpopo Department of Chemistry, Private Bag x1106, Sovenga, 0727
email address: leratomaraphoko@gmail.com

Tuberculosis (TB), caused by *Mycobacterium tuberculosis (Mtb)* is an ancient and persistent disease that has plagued mankind since human history [1]. Currently the emergence of drug resistant strains, particularly multi drug resistant TB (MDR-TB) and extensively drug resistant TB (XDR-TB) has become a global concern [2]. This has prompted us to design and synthensise quinoxaline compounds incoporated with ferrocene moiety to enhance the anti-*Mycobacterium tuberculosis* (anti-*Mtb*) activity of the compounds against TB. To achieve this, a series of quinoxaline alkynyl and ferrocene derivatives have been synthesised and confirmed by spectral data (^{1}H-NMR, ^{13}C-NMR and mass spectroscopy). All the synthesised compounds have been tested for in vitro activity against *Mtb* strain $H_{37}R_V$ following the alamar blue assay employing rifampicin as a reference drug. The tested quinoxaline alkynyl and ferrocene derivatives were found to possess anti-*Mtb* activity with Minimum Inhibitory Concentration (MIC) ranging from 0.828 µg/mL to 13.853 µg/mL and 22.099 µg/mL to 50 µg/mL respectively. Therefore, incorporation of quinoxaline-ferrocene is expected to enhance the activity of the compounds.

Oral presentation at:

Frank Warren conference, Drakensburg, South African, 2019

Date: 7-11 July 2019

Synthesis of quinoxaline alkynyl derivatives and their medicinal properties against *Mycobacterium tuberculosis* ($H_{37}R_V$ strain)

Lerato A. Raphoko* and Winston Nxumalo

Department of Chemistry, University of Limpopo, Private Bag x1106, Sovenga, 0727, Polokwane
leratomaraphoko@gmail.com*

Keywords: Quinoxaline, *Mycobacterium tuberculosis*

Tuberculosis (TB), caused by *Mycobacterium tuberculosis (Mtb)* is an ancient and persistent disease that has plagued mankind since human history [1]. Currently the emergence of drug resistant strains, particularly multi drug resistant TB (MDR-TB) and extensively drug resistant TB (XDR-TB) have become a global concern [2]. This has prompted us to design and synthesise quinoxaline alkynyl derivatives and evaluate the antimycobacterial activity of the compounds. A series of quinoxaline alkynyl derivatives were successfully synthesised and confirmed by ^{1}H-NMR and ^{13}C-NMR spectroscopy. The compounds were evaluated for *in vitro* antimycobacterial activity against *Mtb* $H_{37}R_V$ strain following the alamar blue assay employing rifampicin as a reference drug. Preliminary results obtained upon *in vitro* screening were found to possess antimycobacterial activity with Minimum Inhibitory Concentration (MIC_{90}) ranging from 1.13 µM to 68.58 µM. Within this series, three quinoxaline alkynyl derivatives were found to exhibit excellent activity with 3-(6-chloroquinoxalin-2-yl)propiolaldehyde showing the highest activity at MIC_{90} of 1.13 µM followed by 3-(quinoxalin-3-yl)propiolaldehyde and 3-(quinoxalin-3-yl)prop-2-ynyl methanesulfonate at MIC_{90} of 4.55 and 6.47 µM respectively.

Poster presentation at:

43rd SACI National Convention, CSIR-ICC, Pretoria, South Africa, 2018

Date: 2-7 December 2018

Synthesis of quinoxaline-ferrocene compounds and their medicinal properties against *Mycobacterium tuberculosis*

Lerato A. Raphoko and Winston Nxumalo

Department of Chemistry, University of Limpopo, Private Bag x1106, Sovenga, 0727, Polokwane

email address: leratomaraphoko@gmail.com

Keywords: Quinoxaline, Ferrocene, *Mycobacterium tuberculosis*

Tuberculosis (TB), caused by *Mycobacterium tuberculosis (Mtb)* is an ancient and persistent disease that has plagued mankind since human history [1]. Currently the emergence of drug resistant strains, particularly multi drug resistant TB (MDR-TB) and extensively drug resistant TB (XDR-TB) have become a global concern [2]. This has prompted us to design and synthesise quinoxaline compounds incorporated with ferrocenyl moiety to enhance the anti-*Mycobacterium tuberculosis* (anti-*Mtb*) activity of the compounds against TB. To achieve this, a series of quinoxaline alkynyl derivatives have been synthesised and confirmed by spectral data (^{1}H-NMR, ^{13}C-NMR and mass spectroscopy). The compounds were tested *in vitro* against *Mtb* strain $H_{37}R_V$ following the alamar blue assay employing rifampicin as a reference drug. Preliminary results obtained upon *in vitro* screening were found to possess anti-*Mtb* activity with Minimum Inhibitory Concentration (MIC_{90}) ranging from 0.828 µg/mL to 14.600 µg/mL.

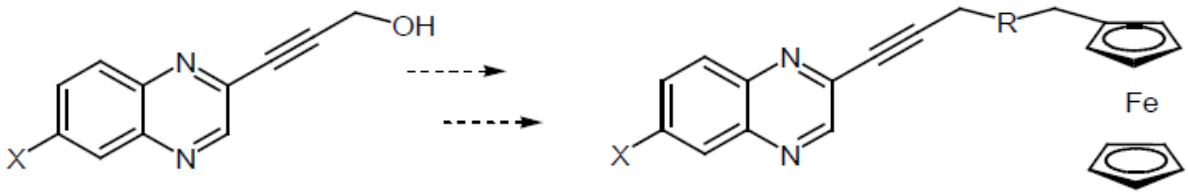

where X = H, Cl

Where R= O, N

Scheme 1 Synthesis of quinoxaline-ferrocene derivatives.

Publication:

molecules

MDPI

Article

Induction of Cell Death in Human A549 Cells Using 3-(Quinoxaline-3-yl) Prop-2-ynyl Methanosulphonate and 3-(Quinoxaline-3-yl) Prop-2-yn-1-ol

Mixo Aunny Sibiya [1], Lerato Raphoko [2], Dikgale Mangokoana [1], Raymond Makola [1], Winston Nxumalo [2] and Thabe Moses Matsebatlela [1,*]

[1] Department of Biochemistry, Microbiology and Biotechnology, School of molecular and Life Sciences, University of Limpopo, Sovenga 0727, South Africa; aunnymixo@gmail.com (M.A.S.); dikgalemangokoana@gmail.com (D.M.); makolaraymond4@gmail.com (R.M.)

[2] Chemistry Department, School of Physical and Mineral Sciences, University of Limpopo, Sovenga 0727, South Africa; leratomaraphoko@gmail.com (L.R.); winston.nxumalo@ul.ac.za (W.N.)

* Correspondence: thabe.matsebatlela@ul.ac.za; Tel.: (+27)-15-268-2337

Received: 10 December 2018; Accepted: 14 January 2019; Published: 23 January 2019

check for updates

Abstract: Despite major advancements in the development of various chemotherapeutic agents, treatment for lung cancer remains costly, ineffective, toxic to normal non-cancerous cells, and still hampered by a high level of remissions. A novel cohort of quinoxaline derivatives designed to possess a wide spectrum of biological activities was synthesized with promising targeted and selective anticancer drug activity. Hence, this study was aimed at determining in vitro anticancer activity effects of a newly synthesized class of 3-(quinoxaline-3-yl) prop-2-ynyl quinoxaline derivatives on A549 lung cancer cells. An assessment of the quinoxaline derivatives ferric reducing power, free radical scavenging activity, cytotoxic activity, and ability to induce reactive oxygen species (ROS) production was performed using the Ferric Reducing Antioxidant Power (FRAP), 2,2-diphenyl-1-picryl-hydrazyl (DPPH), 3-[4,5-dimethylthiazole-2-yl]-2,5-diphenyltetrazolium bromide (MTT) and 2′,7′-dichlorodihydrofluorescein diacetate (H_2DCFDA) assays, respectively. The ability of the quinoxaline derivatives to induce apoptosis in A549 cells was assessed using the Acridine Orange/Ethidium Bromide (AO/EB) and Annexin V-FITC/Dead Cell Assay. Of the four quinoxaline derivatives tested, 3-(quinoxaline-3-yl) prop-2-ynyl methanosulphate (LA-39B) and 3-(quinoxaline-3-yl) prop-2-yn-1-ol (LA-55) displayed a dose-dependent reducing power, free-radical scavenging activity, inhibition of cell viability, and stimulation of ROS production which was accompanied by induction of apoptosis in A549 lung cancer cells. None of the quinoxaline derivatives induced cell death or ROS production in non-cancerous Raw 267.4 macrophage cells. Cytotoxicity was observed in A549 lung cancer, HeLa cervical cancer, and MCF-7 breast cancer cells albeit inhibition was more pronounced in A549 cells. The results of the study suggest that 3-(quinoxaline-3-yl) prop-2-ynyl methanosulphate and 3-(quinoxaline-3-yl) prop-2-yn-1-ol induce apoptotic cell death in A549 lung cancer cells.

Table of Contents

List of abbreviations

A

AIDS	Acquired Immunodeficiency syndrome

B

MCF-7	Breast cancer cell lines
brs	Broad singlet
XTT	(2,3-Bis-(2-Methoxy-4-Nitro-5-Sulfophenyl)-2*H*-Tetrazolium-5-carboxanilide)

C

CNS	Central nervous system
HeLa	Cervical cancer
CQS	Chlorquinoxaline sulfonamide
CQ	Chloroquine
FcB1	Chloroquine resistant strain
F32	Chloroquine sensitive strain
J	Coupling constant
$CDCl_3$	Chloroform-d

D

DMSO	Dimethyl Sulfoxide
DMF	*N,N*-Dimethyformamide
DCM	Dichloromethane
DMAP	Dimethylamino pyridine

DMP	Dess Martin Periodinane
ºC	Degree Celsius
d	Doublet
dd	Double of doublets
MTT	[3-(4,5-Dimethylthiazol-2-yl)-2,5-diphenyltetrazolium Bromide]
E	
EC_{50}	Effective concentration
EMB	Ethambutol
XDR-TB	Extensively drug resistant tuberculosis
Equiv.	Equivalence
F	
FDA	Food and drug administration
Fc	Ferrocene
FTIR	Fourier-transformation infrared spectroscopy
H	
HT29	Human colon cancer cell lines
PC-3	Human prostate cancer cell lines
Huh-7	Human liver cell lines
HIV	Human immunodeficiency virus
HRMS	High resolution mass spectrometry
Hz	Hertz
I	
IC_{50}	Inhibitory Concentration

NAMI	Imidazolium trans-DMSO-imidazole-tetrachlororuthenate
KP-1019	Indazolium trans- [tetra-chlorobis(1-H-indazole)-ruthenate (III)]
L	
A549	lung cancer cell line
RPMI-8226	Leukemia cell lines
M	
µM	Micro molar
MDR-TB	Multri-drug resistant tuberculosis
Mtb	Mycobacterium tuberculosis
mM	Milli molar
MIC	Minimum inhibitory concentration
MHz	Megahertz
mL	Milli litre
min	Minutes
mmol	Millimole
mp	Melting point
m	Multiplet
µL	Micro litre
N	
NMR	Nuclear magnetic resonance
P	
%	Percentage
ppm	part per million

S

NaN_3	Sodium azide

T

TB	Tuberculosis
THF	Tetrahydrofuran
TLC	Thin layer chromatography
t	Triplet
PPh_3	Triphenylphosphine

U

UCT	University of Cape Town

W

WHO	World health organization

Abstract

In an attempt to synthesise quinoxaline-ferrocene compounds with antimycobacterial activity; a series of quinoxaline alkynyl derivatives were successfully synthesised from 3-(quinoxalin-3-yl)prop-2-yn-1-ol **86A** and 3-(6-chloroquinoxalin-2-yl)prop-2-yn-1-ol **86B**. In this series compounds **87A – B**, **90A – B**, and **93A – C** were intermediates obtained in an effort to synthesise quinoxaline-ferrocene compounds. Treatment of either **86A** or **86B** with various acid chlorides afforded quinoxaline alkynyl ester derivatives **97A** - **97B**. Within this series, two quinoxaline-ferrocene compounds 3-(quinoxalin-3-yl)prop-2-ynyl ferrocetate **97A-iv** and 3-(6-chloroquinoxalin-2-yl)prop-2-ynyl ferrocetate **97B-iv** were successfully incorporated with ferrocenoyl chloride and obtained in 42 - 43% yield. The reactions of 3-chloroquinoxaline-2-carbonyl chloride **99** with ferrocenyl alcohol and ferrocenyl amine were unsuccessful. However, 3-chloroquinoxaline-2-carbonyl ester **100A - C** and amide **101A - D** derivatives with various alcohols and amines were obtained. The structures of all the compounds were confirmed by spectroscopic analysis (NMR, FT-IR and HRMS).

The synthesised compounds were all evaluated for preliminary *in-vitro* antimycobacterial activity. The results obtained exhibited compound **90B** with the highest activity against *Mtb* $H_{37}R_V$ strain at MIC_{90} of 1.13 µM, followed by **90A** and **87A** exhibiting MIC_{90} of 4.55 and 6.47 µM, respectively. The quinoxaline alkynyl ester derivatives were found to exhibit poor to good activity. Within this series, three compounds were found to exhibit antimycobacterial activity at MIC_{90} < 20 µM with compound **97A-ii** showing the highest activity at MIC_{90} of 16.18 µM, followed by **97A-i** and **97B-iii** showing MIC_{90} of 18.05 and 19.36 µM, respectively. From the two quixonaline-ferrocene compounds, compound **97A-iv** was found to exhibit antimycobacterial activity at MIC_{90} of 39.90 µM. However, compound **97B-iv** was found to be inactive. The 3-chloroquinoxaline-2-carbonyl ester **100A - C** and amide **101A - D** derivatives were found to be inactive. However, compound **99-C** was found to exhibit antimycobacterial activity at MIC_{90} of 40.66 µM.

Compounds **86A**, **86C**, **87A** and **90A** were evaluated for *in-vitro* antiproliferative activity against cancer cell lines. The results of antiproliferative activity showed that compounds

86A and **87A** exhibited excellent activity against A549 lung cancer cell lines. Compound **87A** was found to be the most active against A549 cell line showing 50% viability-inhibition at 25 µM.

Chapter 1

1. Introduction

1.1 Heterocyclic compounds

Heterocyclic compounds are a class of compounds which exhibit a cyclic structure in nature with at least one or more atoms other than hydrogen and carbon in the ring structure [1-2]. Most common atoms include oxygen, nitrogen and sulfur [1]. In accordance with the heteroatom(s) present in the ring structure, heterocyclic compounds can be classified as nitrogen, oxygen and sulfur based within each class [2]. These compounds are grouped on the basis of ring size determined by the total number of atoms in the ring [3]. The type and size of the ring structure, together with different substituents on the core scaffold, impact greatly on the physiochemical properties of the compounds [3]. Introduction of heteroatoms into a molecular scaffold is known to improve the drug-like properties of compounds, enhancing solubility, hydrogen bonding and rigidity [4-5].

Heterocyclic compounds are known to be the largest area of research in organic chemistry worldwide [6-8]. These compounds have been of interest and played a significant role in drug discovery over the years [9]. As a result, heterocyclic compounds have steered to the birth of medicinal chemistry due to their interesting biological properties [2-3]. Heterocyclic compounds have a wide range of applications as they are found among compounds used not only as pharmaceuticals but also as veterinary and agrochemical products [1,8]. These compounds are essential for health and life as they are the cornerstone for most of the drugs available on the market [3,9]. The chemistry of heterocyclic compounds has drawn great attention to researchers to continue investigating these compounds for development of new drugs against various diseases [6]. Furthermore, drugs such as chloroquine, gefitinib and rifampicin currently available on the market for treatment of malaria, cancer and tuberculosis, respectively are no longer effective against drug resistant strains [8-9]. This suggest an urgent search for new

therapeutic agents which can target a novel pathway so as to be effective against drug resistant strains.

1.1.1 Structure and biological application of heterocyclic compounds

1.1.1.1 Oxygen-containing heterocyclic compounds

Oxygen-containing heterocyclic compounds have drawn considerable attention over the years with benzofuran frequently used in the area of drug discovery [6,10]. Benzofuran derivatives possess a wide range of biological application. This include antimicrobial, anticancer, antialzheimers, antitubercular, antiinflamatory, analgesic, central nervous system (CNS) regulants and antiviral properties [11]. Benzofuran is a core skeleton of many clinically approved drugs. For example, compounds such as saprisartan **1** (used for treatment of hypertension and heart failure), benzobromarone **2** (used for treatment of gout), galantamine **3** (used for treatment of mild to moderate alzheimers disease), rifampentine **4** and rifampicine **5** (used for TB treatment) and citalopram **6** (antidepressant) [11-12]. To date over 34 drugs containing benzofuran scaffold have been approved by food and drug administration (FDA) [11].

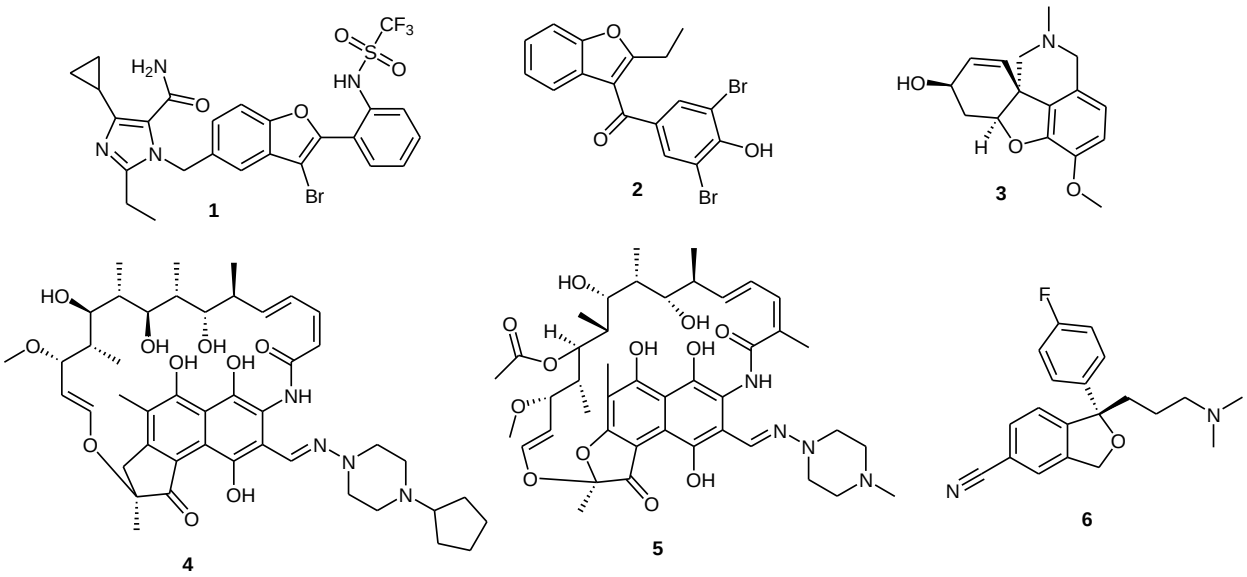

Figure 1: Examples of clinically approved benzofuran derivatives.

1.1.1.2 Sulfur-containing heterocyclic compounds

Thiophene and benzothiophene have a special place in medicinal chemistry due to their low toxicity and good lipophilicity [13]. Thiophene scaffolds are amongst the heterocyclic compounds classified as sulphur containing heterocyclic compounds [13]. These compounds have been extensively used in pharmaceuticals and industrial field [14]. Thiophene derivatives are reported to exhibit various biological properties that include antibacterial, antioxidant, antifungal, local anesthetic activity and anticancer [13-15]. Several studies have shown that minor substitutions on the thiophene structure improves biological and pharmacological activity of these compounds [14-15]. For example 2-amino thiophene derivatives are known to be used as pesticides, dyes and pharmaceuticals [14]. Furthermore compounds such as **7** (a potent apoptosis inducer), **8** (a potential antiinflamatory and antiosteroporosis agents) and **9** (an agonist of allosteric enhancer at the adenoside A_1 receptor) are reported as biologically active multisubstituted 2-aminothiophene derivatives [14].

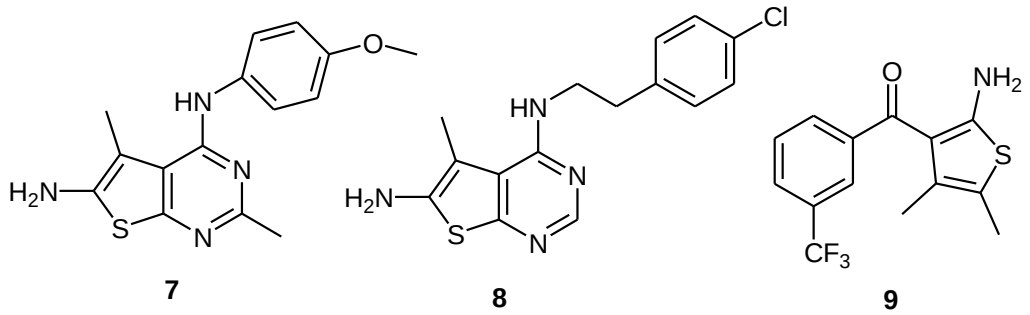

Figure 2: Examples of thiophene derivatives with biological activity.

The introduction of 2-aminothiophene derivatives in medicinal chemistry yielded commercially available drugs known as olanzapine and tinoridine [15]. da Franca Rodrigues and coworkers [16] investigated a series of 2-aminothiophene derivatives for activity against antileishmanial activity on promastigotes. The results obtained showed that all compounds possess antileishmanial activity at IC_{50} values ranging from 3.37 to 189.3 µM and EC_{50} values ranging from 15.82 to 212.73 µM when assayed against axenic amastigotes. Within this series, compounds **10A - C** showed highest activity with IC_{50} of 3.37, 3.65 and 7.37 µM, respectively.

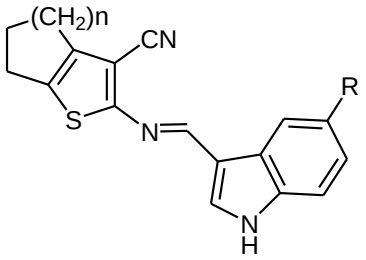

Where n = 3, R = H **(A)**
n = 2, R = 5-bromo **(B)**
n = 3, R = 5-bromo **(C)**

10A - C

Figure 3: Example of 2- aminothiophine derivatives with antileishmanial activity.

1.1.1.3 Nitrogen-containing heterocyclic compounds

Within the family of heterocyclic compounds, *N*-containing heterocyclic compounds have been of interest and play a major role in drug discovery [1-2]. *N*-heterocyclic compounds are a class of compounds distinguished by the presence of nitrogen atom(s) within the ring structure as shown by compounds **11**-**19** in **Figure 4**.

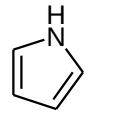

pyrrole
11

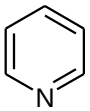

pyridine
12

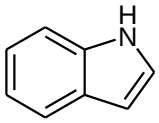

indole
13

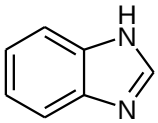

benzimidazole
14

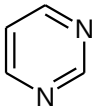

pyrimidine
15

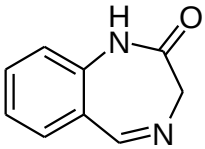

1.4-benzoiazepin-2-one
16

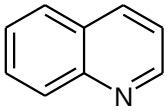

quinoline
17

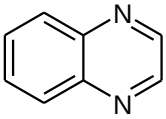

quinoxaline
18

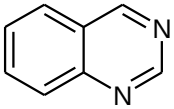

quinazoline
19

Figure 4: Examples of N-heterocyclic compounds.

Like many other heterocyclic compounds, nitrogen containing compounds are also found in several pharmacologically active compounds due to their wide spectrum of biological properties [1]. The biological importance of nitrogen containing compounds are regarded as a template for development of new drugs for various diseases [1]. Delamanid **20** and bedaquiline **21** were reported to respond positively against MDR-TB and XDR-TB [17-18]. These drugs are currently used for treatment of MDR-TB in various parts of the world,

including South Africa [18]. Bedaquiline was approved in 2012 by FDA after 40 years of struggle in drug development stages, whereas in 2014 European Medicines Agency approved delamanid for treatment of MDR-TB [17]. Many drugs containing *N*-heterocyclic compounds are currently used in medical practices. These includes pyrazine **22**, isoniazid **23**, levofloxacin **24** and ethionamine **25** which are used for TB treatment [17]; while quinine **26**, pyrimethamine **27** and chloroquine **28** are used to treat malaria [19-20].

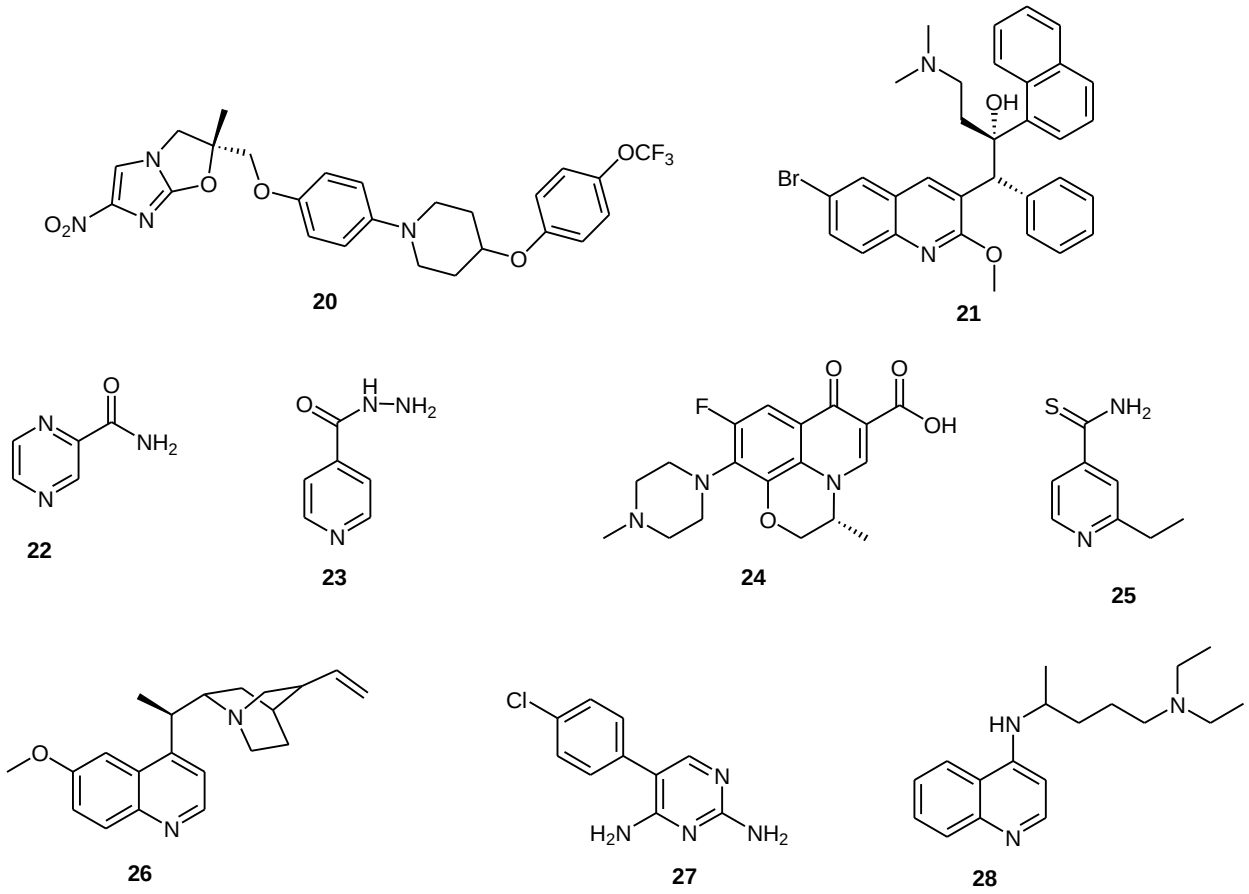

Figure 5: Examples *N*-heretocyclic compounds currently used in medicinal application.

Quinoline containing compounds are reported in literature to exhibit excellent antitubercular and anticancer activities [19-20]. Eswaran and coworkers [19] reported a series of fluorine containing quinoline hydrazine derivatives and evaluated them for their *in vitro* antitubercular activity against *Mtb* $H_{37}R_v$. In their study, they reported that compounds **29 - 32** demonstrated good antitubercular activity with MIC of 6.25 µM against *Mtb* $H_{37}R_V$ and MDR-TB. Furthermore, Arafa and coworkers [20] synthesised a series of quinoline

hydrazine derivatives and screened them for anticancer activity against HT29 and MDA-MB cell lines. From this study, compound **33** was found to be active against HT29 and MDA-MB cell lines with IC_{50} of 4.7 and 4.6 mM, respectively.

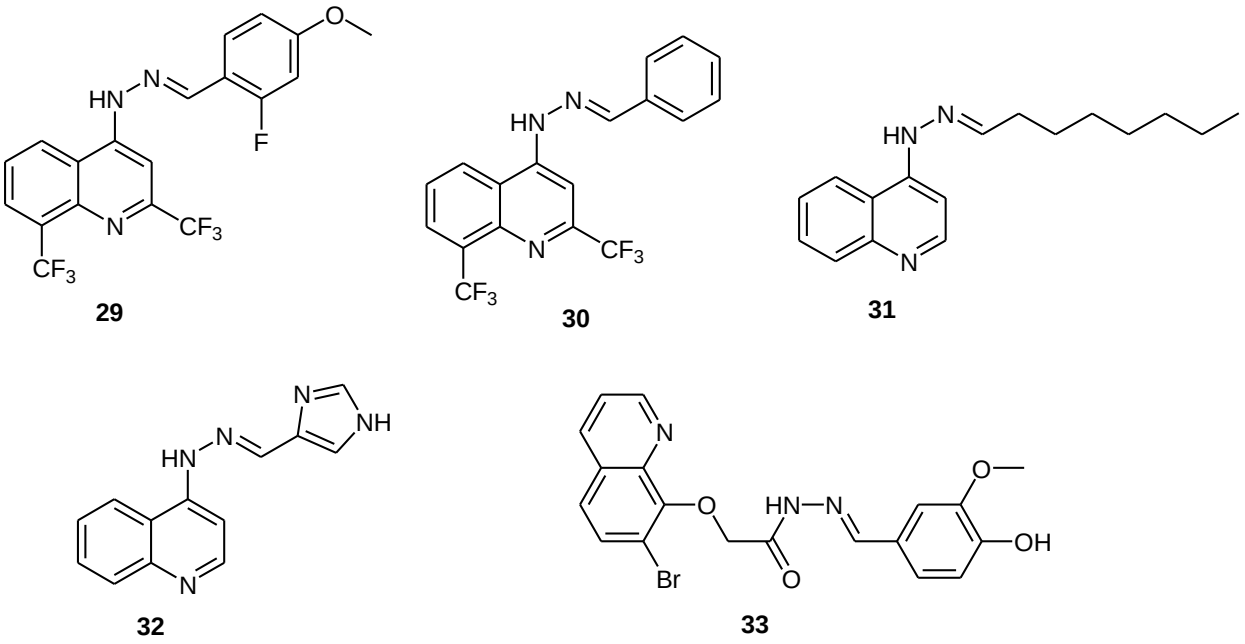

Figure 6: Examples of quinoline derivatives with anticancer and antitubercular activities.

Quinoline containing compounds have been previously studied for activity against various diseases including TB [21]. Quinoline **17** is described as a bioisoster of quinoxaline **18** and are known to exhibit similar biological properties [22]. Quinoxaline, characterised by a benzene ring fused to a pyrazine ring at two adjacent carbon atoms has been frequently found in a variety of pharmacologically active compounds [22].

1.2 Quinoxaline compounds

Among the heterocyclic compounds, quinoxaline **18** has emerged as one scaffold that has attracted continuing interest in medicinal chemistry because of its diverse biological properties [7]. The properties include antibacterial, antifungal, antiviral, antimalarial, antitubercular, anticancer and antiinflammatory properties [22-27]. Therefore, quinoxaline derivatives are regarded as an important class of *N*-heterocyclic compounds in organic synthesis and drug discovery [5,22]. Apart from medicinal application, quinoxaline

derivatives have also found applications as organic semiconductors, dyes, efficient electron luminescent materials and building blocks for synthesis of anion receptor [24]. The quinoxaline nucleus makes all these activities to be feasible [22].

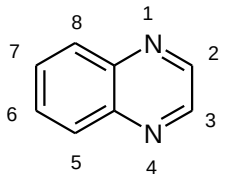

18

Figure 7: Structure of quinoxaline **18**.

Quinoxaline is one of the easiest *N*-containing heterocyclic compounds to synthesise [7]. It is synthesised by cyclocondensation of an *O*-phenylenediamine and oxaldehyde at room temperature [25]. Due to its diversity, several methods for synthesis of quinoxaline derivatives are available [25]. Various methods include condensation of substituted 1,2-diamines with ∝-diketones and 1,4 addition of 1,2 diamine to daizenylbutenes [7,25,27]. Quinoxaline acts as a precursor to assemble a large number of compounds for various applications [22]. Quinoxaline and its derivatives are important components with several compounds that are pharmacologically active [28].

1.2.1 Biological applications of quinoxaline derivatives

Several biological studies on quinoxaline derivatives have been published hitherto, providing an acceptable explanation for the interest of these compounds as anticancer, antimalarial, antitubercular and antibacterial agents [30]. Many drugs containing quinoxaline moiety are currently used in medical practice [28]. These includes compounds such as quinoxidine **34** and dioxidine **35**, which possess significant chemotherapeutic activity and are used against bacterial infections that other antimicrobial agents fail to treat [29]. In addition, these compounds are known to inhibit growth of gram-positive bacteria [28]. On the other hand, echinomycin **36** and levomycin **37** are widely used in medical practice as antibiotics [31]. Both compounds have similar composition, *i.e.,* consist of two quinoxaline-2-carboxylic acid moieties attached to a cyclic octadepsipeptide containing a sulfur cross linkage [32]. These antibiotics are known to possess other

biological properties that include adenosine receptor antagonist, antihelmintic, anticancer, antiinflammatory and antidepressant [31]. Quinoxaline containing drug clofazimine **38** is currently used for treatment of multi drug resistant TB [32]. It was previously unconsidered for TB treatments following several studies suggesting poor activity in humans with pulmonary tuberculosis [33-34]. Clorofazine is now included in second line regimen which is believed to significantly shorten the duration and improve the outcome of treatment in patients with MDR-TB [35]. Brimonidine **39** is a drug bearing quinoxaline core structure used as an antiglaucoma agent. It acts by reducing intraocular pressure, thus mitigating the symptoms of glaucoma [22,36].

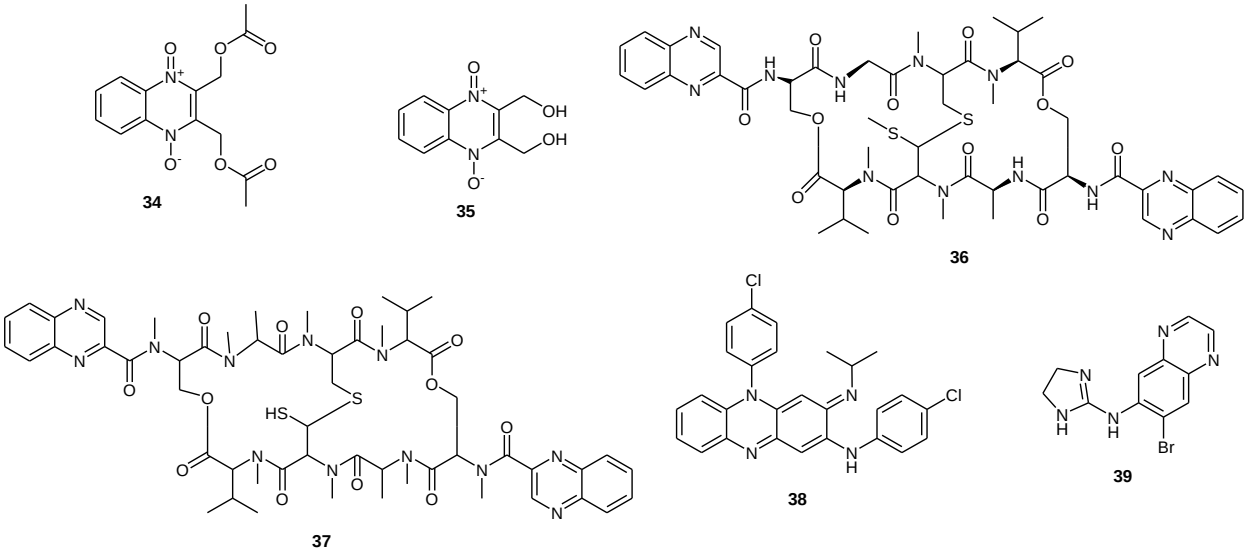

Figure 8: Examples of quinoxaline core drugs used in medical applications.

1.2.1.1 Quinoxaline derivatives as anticancer agents

Quinoxaline derivatives have appeared at the forefront of anticancer agents, with several compounds currently under clinical trials [5]. Among them, XK469 **40** and Chloroquinoxaline sulfonamide (CQS) **41** which are regarded as antineoplastic quinoxaline topoisomerase II inhibitors for anticancer therapeutic purposes [26, 37]. Tseng and coworkers [38] synthesised a novel series of indeno[1,2b]quinoxaline derivatives for antiproliferative evaluation against cancer cell lines using XTT assay. Among them, was 11-{[3-(dimethylamino)propoxy]imino}-N-[3-(dimethylamino)propyl]-11H-indeno[1,2b]-quinoxaline-6-carboxamide **42**, which was found to exhibit excellent cytotoxicity against

MDA-MB231, PC-3 and Huh-7 cancer cell lines with IC_{50} values of 0.87, 0.82 and 0.64 µM, respectively. The antiproliferative activity of the compound was reported to have improved by the presence of an aminoalkoxyimino side chain on *C*-11 position of this amide derivative [38]. Furthermore, a study by Rahul and coworkers [23] presented sulphonamido-quinoxaline derivatives with anticancer properties. The synthesised compounds were investigated for *in vitro* cytotoxicity against leukemia RPMI-8226 cell line, with compound **43** showing the highest activity at IC_{50} of 1.11µM followed by compound **44** with IC_{50} of 1.43 µM. Moreover, Al-Marhabi and coworkers [24] reported compounds **45, 46A – B** as potential anticancer agents with great *in vitro* cytotoxic activity against human breast cell lines (MCFF7), non-small cell lung cancer NCIH460 and CNS cancer SF-268 with IC_{50} values ranging from 0.01 to 0.06 µg/mL.

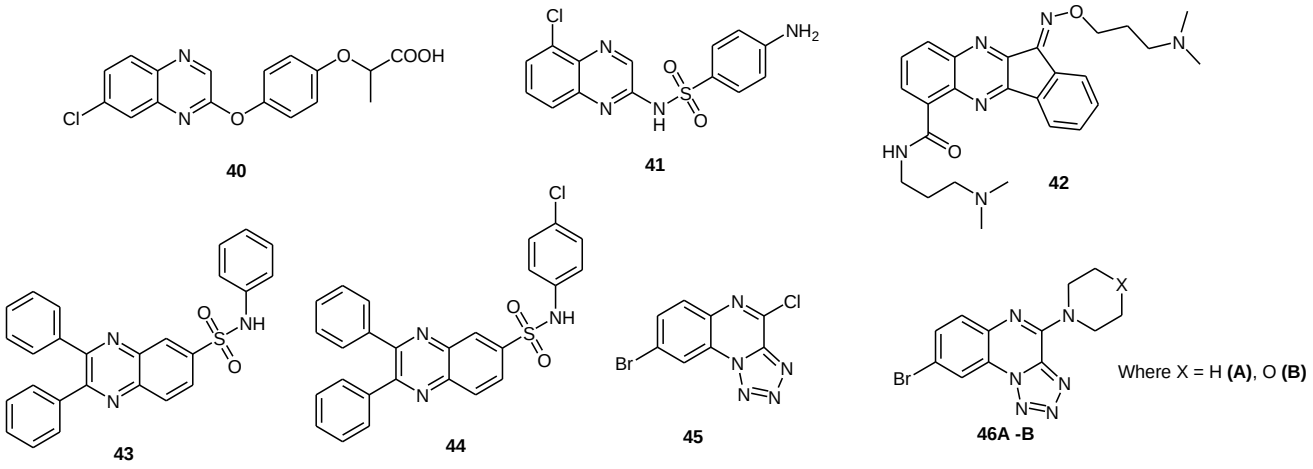

Figure 9: Examples of quinoxaline derivatives with anticancer properties.

1.2.1.2 Quinoxaline derivatives as antitubercular agents

On the search for new and improved compounds with an advanced mechanism of action that can prevent mutation of drug resistant strains, quinoxaline derivatives presented relevant activity against TB [22]. Some of the quinoxaline derivatives have displayed *Mycobacterium tuberculosis* growth inhibition ranging from 90 - 99% [22,30,40]. This shows that compounds of this nature are interesting for development of new antitubercular drugs [30]. Quinoxaline core derivatives with *N*-oxide groups are reported to be most suitable

antitubercular leads [39]. Therefore, several studies have been described concerning the biological activity of 1,4-di-*N*-oxide quinoxaline derivatives as potential antitubercular agents [39-41]. The studies have indicated that the antimycobacterial activity of the compounds entirely depends on the presence of *N*-oxide groups. Furthermore, it is reported that the loss of *N*-oxide groups in the quinoxaline moiety reduces the antimycobacterial activity of the compounds [40].

An example of 1,4-di-*N*-oxide quinoxaline derivative with antituberculosis activity is 3-methyl-2-phenylthioquinoxaline-1,4-dioxide **47**. This compound presented good activity against *Mtb* and showed MIC_{90} between 0.3 and 0.75 µg/mL [22]. Some of 1,4-*N*-dioxide quinoxaline derivatives with different substituents at positions 2, 3, 6 and 7 have been investigated and found to retain antitubercular properties of the quinoxaline moiety. Introduction of electron withdrawing groups (Cl, F, CF_3) at position *C*-6 or *C*-7 in the benzene moiety are found to significantly increase the antitubercular activity against *Mtb* $H_{37}R_V$ [39 – 40]. Furthermore, different substituents at *C*-2 position of 1,4-di-*N*-oxide quinoxaline derivatives displayed excellent antitubercular activity which suggest that substituents at this position play a prominent role in their antitubercular activities [40].

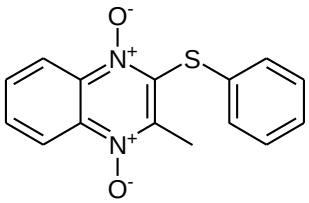

47

Figure 10: Structure of 3-methyl-2-phenylthioquinoxaline-1,4-dioxide.

Santivanez-Veliz and coworkers [30] reported on 1,4-di-*N*-oxide quinoxaline derivatives with antitubercular properties, where compound **48A – B** stand out showing MIC_{90} of 1.5 and 0.75 µg/mL, respectively amongst the twenty four compounds evaluated for antimycobacterial activity. These compounds were most potent against rifampicin, isoniazid and ofloxacin resistant strains. Furthermore, they exhibit intracellular activity on infected macrophases, considering log-reduction and cellular viability. Similarly, Pan and coworkers [40] synthesised a series of 1,4-di-*N*-oxide quinoxaline derivatives with different substituents at *C*-2 position and evaluated them for *in vitro* antimycobacterial activity.

Seventeen compounds were found to possess antitubercular properties with MIC ≤6.25 µg/mL, however compound **49** presented excellent activity having MIC_{90} value of 0.39 µg/mL. Furthermore, several studies of 1,4-di-*N*-oxide quinoxaline derivatives bearing ester groups at *C*-2 position showed significant antitubercular activity with MIC_{90} values of 1.5 µg/mL **50** and 0.2 µg/mL **51**, while the analogs with amide groups at *C*-2 are found to exhibit poor activity [40 - 41].

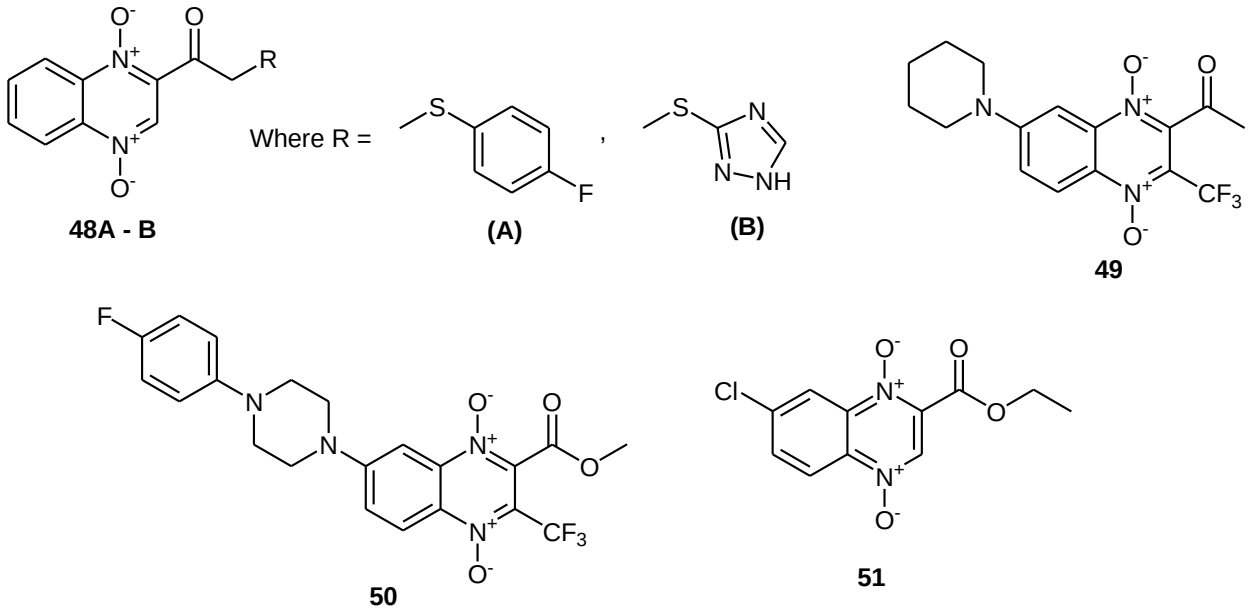

Figure 11: Examples of 1,4-di-N-oxide quinoxaline derivatives with different substituents at *C*-2 showing antitubercular properties.

1.3 Organometallic compounds

Medicinal chemistry has traditionally been the realm of organic chemistry and a thriving area of research with notable exceptions, such as incorporation of organometallic compounds into biomolecules or known drugs [41]. The use of organometallic compounds in medicinal chemistry has increased significantly in recent years [43,44,57]. These compounds offer a large structural variety and are often relatively lipophilic uncharged molecules [45]. The lipophilicity improves the compounds cellular uptake into the mitochondrial pockets [45]. Therefore, incorporation of organometallic compounds leads to profound changes in a drug's biological activity [42,46,47].

1.3.1 Biological application of organometallic compounds

Organometallic compounds have provided a promising alternative to traditional organic drugs [42]. The success of cisplatin **52** and other platinum based drugs (carboplatin **53** and oxaliplatin **54**) have yielded great benefits in medicine as anticancer agents [43,48]. These compounds have demonstrated that the use of metals in medicinal application can be a useful strategy in drug design and drug development [42, 49]. Furthermore, this led to exploration of new transitional metal complexes with interesting biological properties [50 – 51]. Transition metals offer an excellent platform as they can easily adopt various geometries based on the number of coordination bonds present, for example octahedral, square planar, square pyramidal, and trigonal pyramidal [42, 52]. This helps increase the structural diversity of metal complexes [52]. Furthermore, it can enhance flexibility in drug design allowing metal compounds to effectively interact with the binding site of target biomolecules [43, 53].

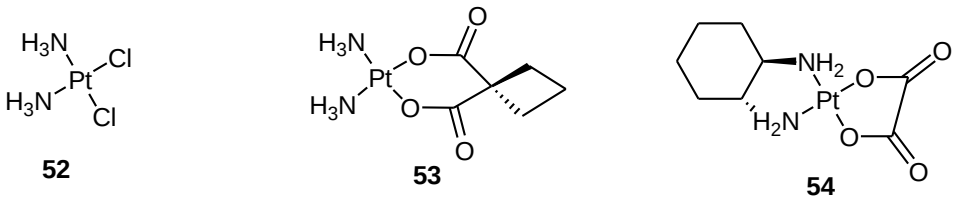

Figure 12: Examples of platinum based drugs used for treatment of cancer.

Non-platinum based compounds containing metals such as iridium, titanium, ruthenium, osmium and iron complexes are gaining more attention and have shown significant potential to become alternatives of platinum based metal drugs [43, 54]. The new class of compounds containing these metals has since found application as anticancer, antimalarial and radiopharmaceuticals [54]. Titanocene chloride **55** was previously investigated for anticancer activity due to it showing resemblance to cisplatin and has entered phase II clinical trials [48, 55]. Ruthenium containing compounds such as imidazolium trans-DMSO-imidazole-tetrachlororuthenate (NAMI-A) **56** and indazolium trans- [tetra-chlorobis(1-H-indazole)-ruthenate (III)] (KP-1019) **57** have shown excellent antiproliferative activity and have passed through to phase II and III clinical trials [51].

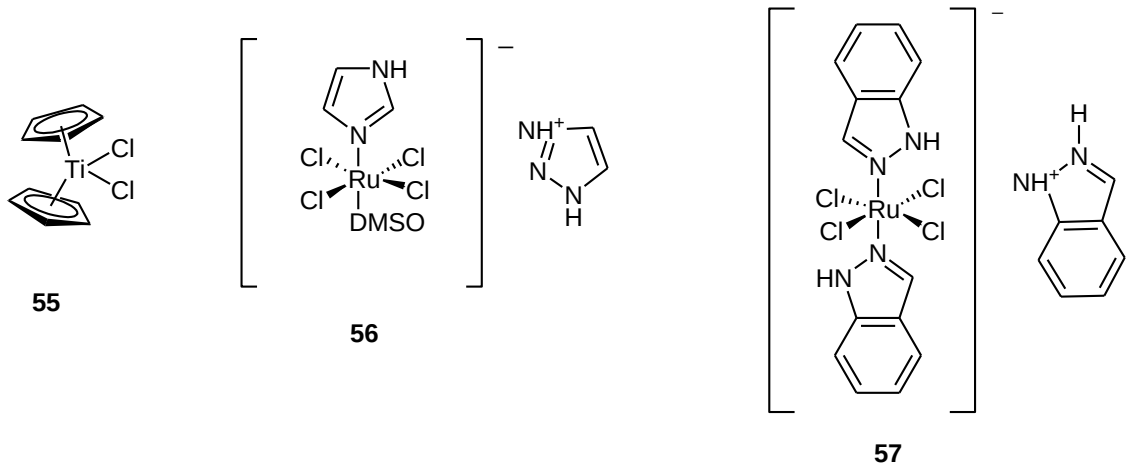

Figure 13: Examples of biologically active organometallic compounds.

Iron complexes have had a successful pathway in drug discovery. Ferrocene (an iron containing complex) is widely used in development of new anticancer and antimalarial drugs [65].

1.4 Ferrocene and its derivatives

Ferrocene (Fc) **58** with its distinctive "sandwich" like structure is a well-known organometallic compound with an interesting history [63]. This complex is susceptible to a wide range of reactions common in organic chemistry, yielding easy access to many organometallic compounds [62]. The physico-chemical properties of Fc and its derivatives present themselves to exhibit special features for various applications in electrochemistry, catalysis and material science [65]. The presence of iron in ferrocene and its derivatives has sparked a tremendous influence in medicinal chemistry [63, 66]. Since its discovery in 1951 by Pauson and Kealy, a comprehensive list of Fc-containing drug candidates have been synthesised and characterised [57, 58, 65, 67]. Furthermore, the chemistry of ferrocene and its derivatives is well known and they are often appreciated for their outstanding stability, lipophilic character, non- toxic nature and ease of derivatisation [65, 68].

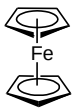

58

Figure 14: Structure of Ferrocene (Fc) **58**.

1.4.1 Medicinal application of ferrocene derivatives

Ferrocene has become a crucial entity in medicine due to it being non-toxic in nature [65, 68]. In 1969 Yeary [69] conducted a study in dogs and found that daily oral intake of 300 mg.kg $^{-1}$ of Fc for a period of 6 months resulted in haemosiderosis (a form of iron overload disorder). However, no latent adverse effect of haemosiderosis were seen for dogs continuing with the daily oral administration for 12-26 months after the 6 months treatment period [69]. Compounds with ferrocenyl moiety are found to possess interesting biological properties such as antibacterial, antimalarial and anticancer [63, 70]. As a result, it has brought significant changes in the field of bio-organometallic chemistry [63]. The activity brought by the attachment of the ferrocenyl group serves as a building block for development of new drugs or to improve the biologically relevant compounds or compounds that do not display biological activity of their own [47, 63].

Introduction of ferrocenyl moiety into organic molecules was first reported in the 1960s. In the 1970s, Ferrocenone **59** was reported to be the first ferrocenyl drug to be approved for medical purpose and used for treatment of anaemia [65, 69]. More successful studies upon incorporation of ferrocenyl moieties into known drugs led to the development of Fc derivatives containing penicillin **60** and cephalosporns **61** and were found to possess moderate antibacterial activity [68].

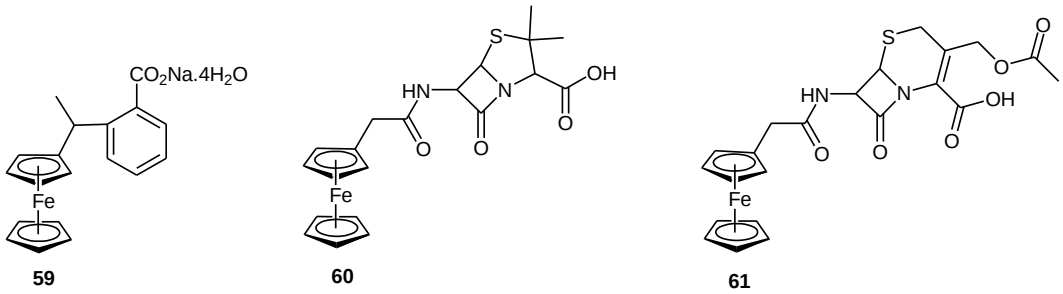

Figure 15: Examples of ferrocenyl derivatives with medicinal applications.

One successful application where bio-organometallic approach was fruitful is in the field of malarial and cancer agents [44], when ferroquine **62** and ferrocifen **64** were separately

discovered [69]. Ferroquine **62**, which is a ferrocenyl derivative of a well-known antimalarial drug chloroquine **28** [63]. Ferroquine has passed through to phase IIb clinical trial and was founds to be remarkably effective against CQ-resistant *P.falciparum* with no observable immunotoxic effect in valve and infected rats [57, 71]. It acts on hematic and cause the inhibition of hemozoin formation [72]. Ferrocifen **64**, which is a ferrocene modified derivative of tamoxifen **63** is another successful example of bio-organometallic chemistry [62]. Ferrocifen is found to possess substantial antiproliferative effects on hormone independent as well as hormone dependent breast cancer cell lines where tamoxifen is found to be inactive [62 - 63]. The success of these compounds led to more investigations of other ferrocenyl-containing compounds for treatment of various disease.

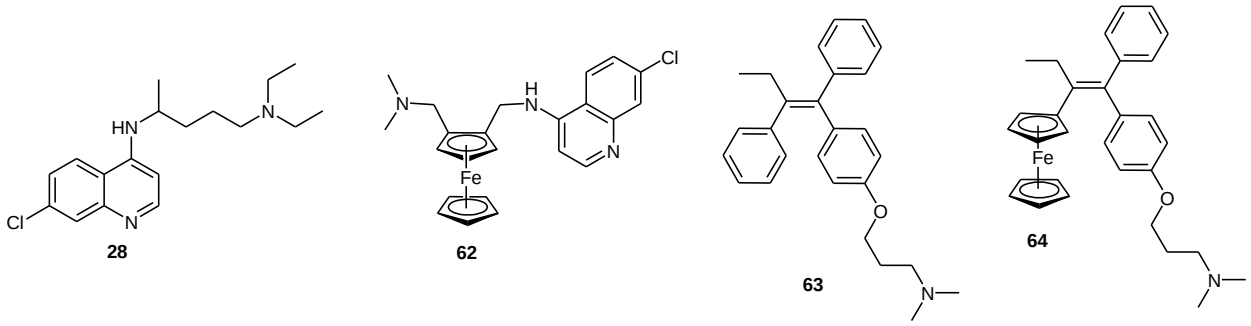

Figure 16: structures of chloroquine (**28**), ferroquine (**62**), tamoxifen (**63**) and ferrocifen (**64**).

Quirante and coworkers [57] developed a series of Ferrocene-indole hybrids for anticancer and malaria therapy. Preliminary results obtained in this study revealed compounds **65A - D** with the highest antiproliferative activity at IC_{50} below 10 µM. Within this series compound **65B** showed excellent activity with an IC_{50} of 5 µM. Antimalarial activity results obtained showed non-substituted ferrocenic indole **65D** as the most active compound with IC_{50} below 28.2 µM against eight parasite strains. Moreover, the results obtained in this study showed that there was no correlation between the anticancer and antimalarial activities of these compounds.

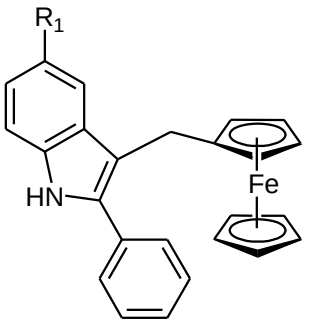

where R_1 = OCH_3 **(A)**, NO_2 **(B)**, Cl **(C)** and H **(D)**

65A - D

Figure 17: Examples of ferrocene indole hybrids with anticancer and antimalarial activity.

Esparza-Ruiz and coworkers [59] investigated a series of ferrocenyl aminoquinoline carboxamide conjugates *in vitro* against cancer. The *in vitro* antiproliferative activity against colon carcinoma (caco-2, HTN-37) and human breast cancer (MDA-MB-4356, HTB-129) showed that compounds containing ferrocenyl moiety exhibit excellent activity as compared to their organic parent compounds. Compound **66,** with two ferrocenyl groups within the structure was highly potent than compound **67** containing one ferrocenyl group with IC_{50} of 0.33 and 0.28 µM against HTB-129 and caco-2, respectively.

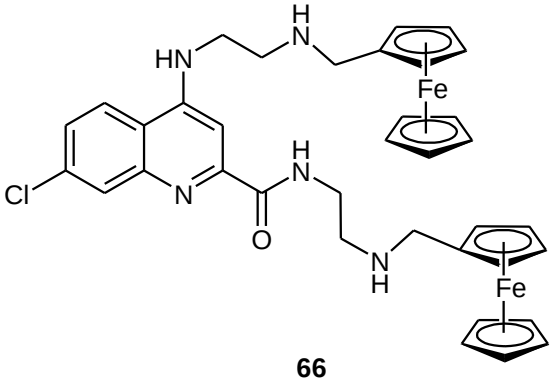

66

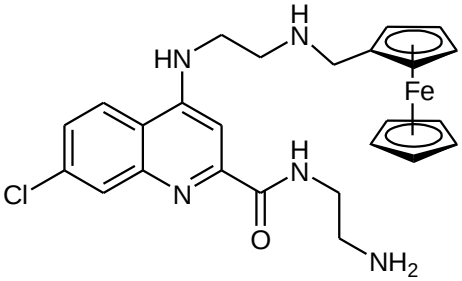

67

Figure 18: Examples of ferrocenyl aminoquinoline carboxamide conjugates with anticancer properties.

Recently, ferrocene based hydrazones **68 – 70** were reported to show excellent activity against *Mtb*. In this study, a quinoline ferrocene hybrid **68** exhibited significant activity against TB with MIC_{90} of 2.5 – 5 µg/mL as compared to EMB (with MIC of 2.5 µg/mL) used as a reference drug. It is reported that the excellent activity of this compound may

be due to the presence of the quinoline ring [58]. As previously mentioned quinolines share similar biological properties with quinoxalines [21]. Previous studies show that ferrocenyl compounds containing quinoxaline moiety possess antimalarial activity.

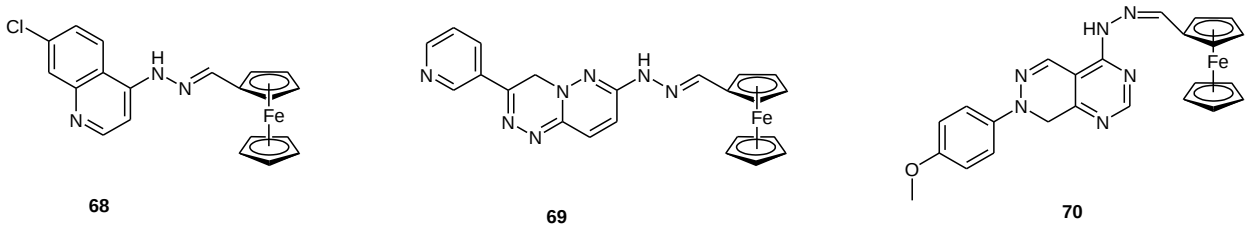

Figure 19: Ferrocenyl derivatives with anticancer and antitubercular activity.

1.4.2 Ferrocenyl compounds based on quinoxaline

There are few literature reports on quinoxaline derivatives incorporated with ferrocene. However, a series of quinoxaline ferrocene derivatives have been reported to overcome chloroquine resistant strains of malaria [60 – 61]. A study conducted by Guillon and coworkers [60] revealed a new series of ferrocenic pyrrolo[1,2-a]quinoxaline derivatives with potent antimalarial activity. In this study, compound **71** had an outstanding IC_{50} of 16.6 ± 1. 2 nM and was found to be six times more active than chloroquine with IC_{50} of 105.3 ± 16.2 nM upon *in vitro* screening against Chloroquine resistant strain FcB1. Likewise, Guillon and coworkers [61] reported another series of ferrocenic pyrrolo[1,2-a]quinoxaline derivatives with antimalarial activity in 2011. In this series, compounds with a benzyl substituted *bis*-(3-aminopropyl)piperazine linker were found to have the highest activity as compared to those with a piperazine link **73A - B**. Among the compounds with 1,4-*bis*-(3-amonipropyl)piperazine linker substituted by a terminal benzyl group, it was observed that the *ortho*, *meta* and *para* nitro substituents on the benzyl group **72A – C** were the most active compounds against *P.falcipurum* CQ-sensitive strain F32 with IC_{50} values ranging from 0.038 to 0.085 µM and CQ-resistant strain FcB1 with IC_{50} values ranging from 0.1423 to 0.380 µM.

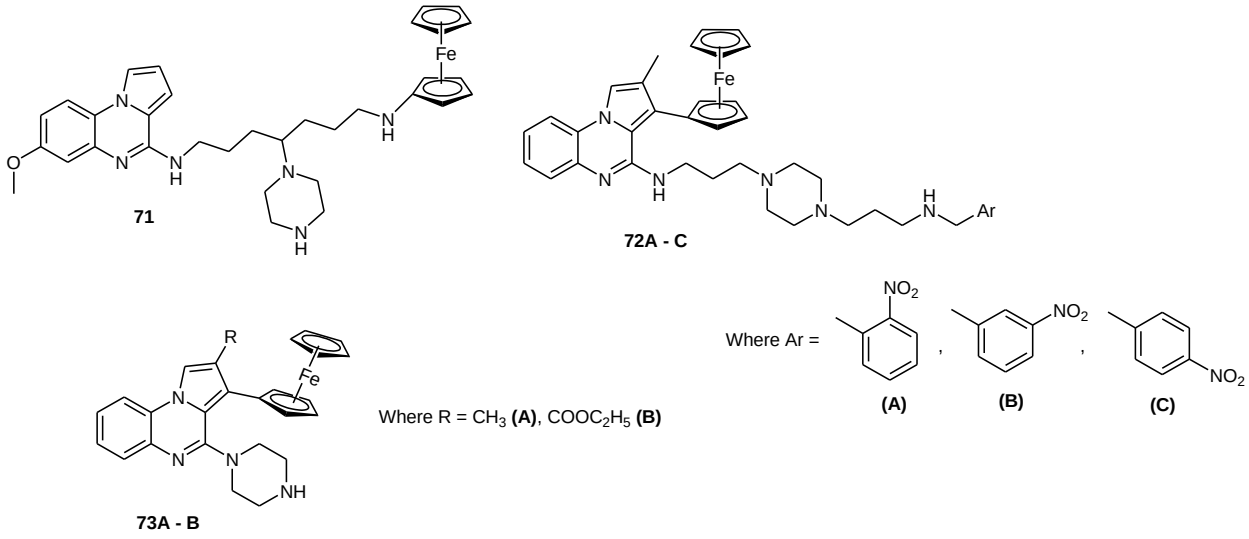

Figure 20: Ferrocenic pyrrolo[1,2-a]quinoxaline derivatives with antimalarial properties.

1.5 Summary

Medicinal chemistry has grown significantly worldwide [42]. Over the years, organic compounds were the most important compounds for drug development. These compounds are known to possess excellent biological properties against various diseases [5, 22, 23]. Most of the drugs that are commercially available on the market are faced with a serious challenge against mutation of drug resistance strains [60]. Even though they are faced with some drawbacks, they still find application within the pharmaceutical industries. Delamanid and bedaquiline have been approved for treatment of MDR-TB and currently used in some parts of the world [17 -18]. The discovery of cisplatin showed that metals can play a vital role in medicinal application. Cisplatin was the first metal complex to be applied for anticancer studies [43, 48]. Its success led to investigation of other transitional metal complexes such as ruthenium complexes (NAMI-A and KP-1019), which are now in phase II of clinical trials for cancer treatment [51]. Introduction of metal complexes into organic molecules has brought a prominent change in drug discovery leading to the birth of bioorganometallic compounds [41, 42, 47]. Merging of these components has shown to improve drug like properties of the desired compounds. A successful application where bioorganometallic compounds were most fruitful is when ferrocifen and ferroquine were discovered [44]. Ferrocifen (anticancer agent) and

ferroquine (antimalarial agent) are both in phase II of clinical trials [57, 62]. The success of these compounds has attracted scientist to further explore this field of study.

1.6 Purpose of the study

In light of the pre-mentioned properties of quinoxaine and ferrocene, a limited number of quinoxaline containing ferrocenyl compounds for biological studies have been reported. Moreover, this shows that there is a need to further broaden this field of study in order to investigate how introduction of an organometallic moiety to quinoxaline motif affects the biological activity of quinoxaline moiety. We then envisaged to synthesise a series of new quinoxaline alkynyl derivatives incorporated with ferrocenyl moiety and evaluate their *in vitro* activity against *Mycobaterium tuberculosis* and cancer cell lines.

1.6.1 Tuberculosis

Tuberculosis (TB) is an ancient and persistent disease, it has been a life threatening disease over a century [73]. TB is ranked above Human Immunodeficiency Virus/Acquired Immuno Deficiency Syndrome (HIV/AIDS) as the deadliest disease worldwide, with an estimated 1.3 million TB deaths (including 374 000 people with HIV/AIDS), according to the latest updates by World Health Organisation (WHO) 2018. In 2016, there were about 10.4 million people infected with TB disease [74]. Tuberculosis is mainly caused by a bacterial pathogen called *Mycobacterium tuberculosis* (*Mtb*) [30, 40]. In the early 1900s, the only known cure for an individual infected with *Mycobaterium tuberculosis* was a regimen of rest, sunshine, fresh air and healthy diet [76]. This approach remained the standard of care until the first antitubercular drug streptomycin was introduced by Schatz in 1944. Presently, antitubercular drugs such as isoniazid, rifampicin, pyrazinamide, and ethambutol are administered as treatment of TB for a period of 6 to 9 months [40]. Despite having several drugs available for treatment, TB is still a major public health concern [77 - 78]. The current regimens available on the market are no longer effective due to continuous emergence of drug resistant strains particularly multi drug resistant (MDR) and extensively drug resistant (XDR) TB [77]. This has prolonged sustainability of TB and made the disease almost impossible to cure [40, 74, 75].

1.6.1.1 Current TB drugs on clinical trials

The success of delamanid **20** and bedaquiline **21** in clinical trials has generated considerable attention in drug development. The presence of diarylquinoline and nitroimidazole moiety in these compounds brings hope for tuberculosis regimen. There are several antitubercular drugs lined up in clinical trials. SQ109 **74** is now in phase II of clinical trials and is currently available for treatment of MDR-TB and XDR- TB [17]. Delpazolid (an anoxazolidinone antibiotic) **75** and PBTZ169 (a benzothiazinone) **76** are currently in phase II of clinical trials [79]. In 2017, an imidazopyridine amide (Q203) **77** drug completed phase I of clinical trials, whereas TBA7371 **78** entered phase I of clinical trials [79]. A total of 14 drug candidate for drug susceptible, MDR and latent TB are now in the clinical stages of drug development. Of the 14 drug only nine are novel and three have been approved *i.e.,* delamanid **20,** bedaquiline **21** and sutezolid **79** [17,79].

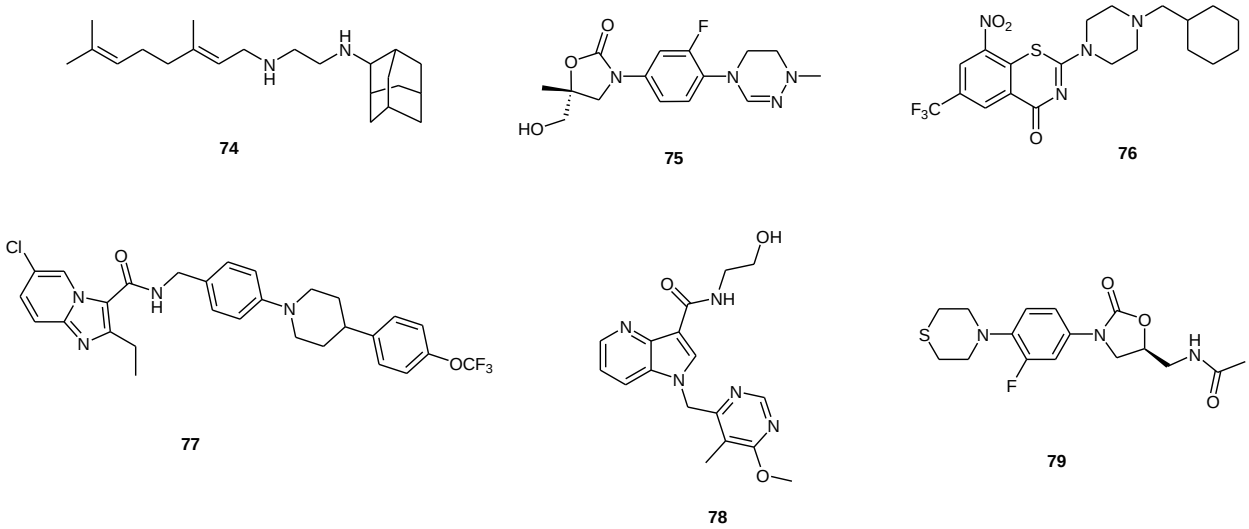

Figure 21: TB drugs currently in clinical trials.

1.6.2 Cancer

Cancer is well known as a collection of diseases that can affect body organs [20]. It is mostly known for its rapid generation of abnormal cells that grow past their usual boundaries thus spreading to other parts of the body [24,82]. Cancer is one of the leading cause of death, particularly in developing countries [43]. According to the statistics

revealed by World Health Organization (WHO 2018), the incidents attributed to this disease showed a total of 9.6 million deaths. The current treatment for cancer includes the use of platinum based drugs like cisplatin [82]. Cisplatin and its derivatives have played a major role in cancer therapy [43]. However, they still face serious challenges such as intensive side effects, reduced treatment efficiency, systemic toxicity and intrinsic resistance [43,53,54]. Cancer is known to affect various parts of the body resulting in breast cancer, cervical cancer, prostate cancer, brain tumor, bone cancer and lung cancer.

1.6.2.1 Lung cancer

Lung cancer is the number one cause of death from cancer related deaths in the world [84–86]. It is the most frequently diagnosed cancer with more than 3 million cases reported in 2015. Subsequently 1.7 million lung cancer related deaths were recorded worldwide in 2015 [84]. Individuals diagnosed with lung cancer at an early stage stand at least 50% chance of survival. However, proper methods of treating lung cancer remain a challenge [83]. Furthermore, the current treatment is expensive, incompetent, non-specific to cancerous cells and causes serious side effects [84].

Over the years, various quinoxaline derivatives (**Scheme 1)** have been synthesised in our laboratory by developing methods of introducing substituents on the quinoxaline nucleus and employing various chemical transformation reaction [87–88]. To date, the substituents on the quinoxaline nucleus have been introduced via Sonogashira cross coupling reactions. The previously synthesised compounds were evaluated for their *in vitro* antimycobacterial activity against *Mtb* $H_{37}R_V$ strain and were found to possess antitubercular activity. Compounds **86A** and **86B** have shown prominent activity against *Mtb* with MIC_{90} values of 52.77 and 1.63 µM, respectively. Comparing the two structures, we found that quinoxaline structure with chlorine atom at *C*-6 enhanced the activity of the compounds. Furthermore, the position of the progargylic alcohol presented an opportunity to further functionalise these compounds. The identified compounds will serve as a starting point for development of new quinoxaline derivatives by way of introducing an organometallic compound such as ferrocene. Ferrocene is reported to be a crucial entity

for the development of new drugs and has already yielded great benefits against malaria and cancer [44].

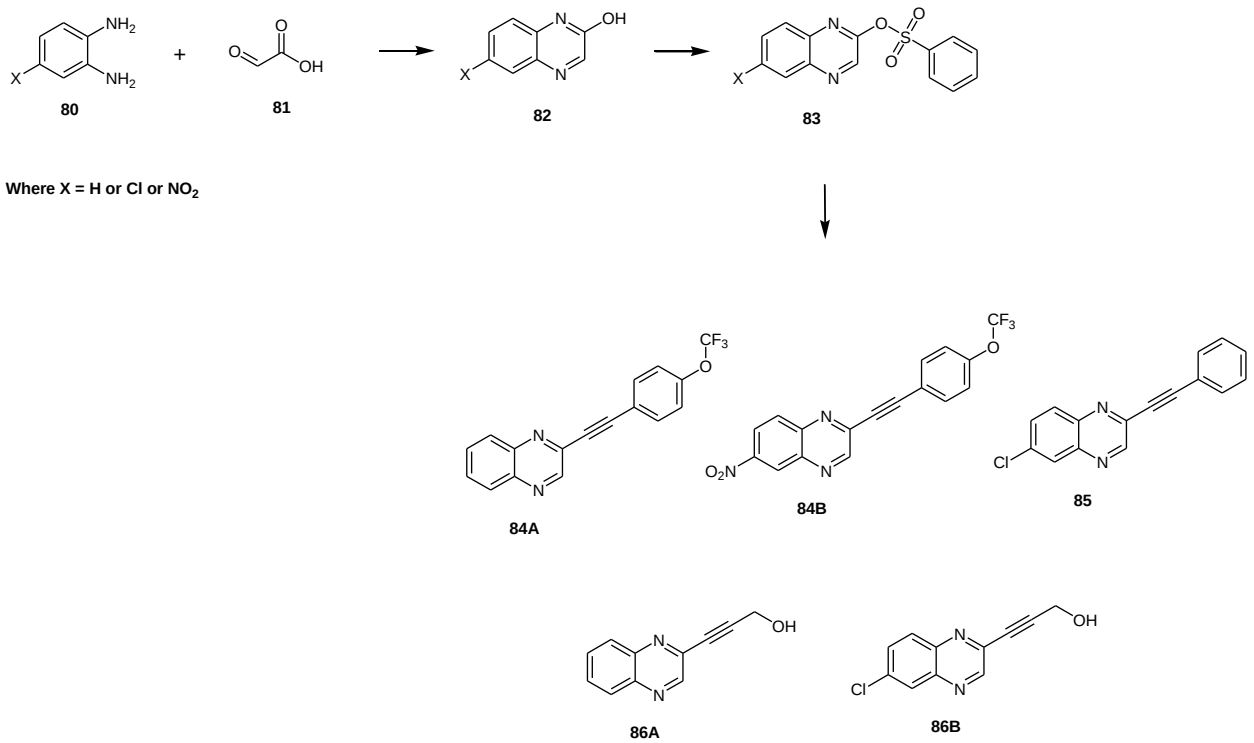

Scheme 1: General synthetic routes to access quinoxaline alkynyl derivatives.

1.7 Aim and Objectives of the study

1.7.1 Aim

The aim of this study was to synthesise quinoxaline-ferrocene compounds and evaluate their biological activity against *Mycobacterium tuberculosis* ($H_{37}R_V$ strain) and cancer.

1.7.2 Objectives were to;

i. Synthesise quinoxaline derivatives and incorporate with ferrocene derivatives via: esterification or reductive amination.
ii. Evaluate the synthesised compounds for *in vitro* activity against *Mtb* $H_{37}R_V$ strain.

iii. Evaluate the synthesised compounds for in vitro activity against A549 lung cancer cell lines.
iv. Perform cytotoxicity assays to check the safety of the compounds.

References

[1] Arora, P., Arora, V., Lamba, H.S. and Wadhwa, D., 2012. Importance of heterocyclic chemistry: A review. *International Journal of Pharmaceutical Sciences and Research*, *3*(9), pp.2947.

[2] Al-Mulla, A., 2017. A Review: Biological Importance of Heterocyclic Compounds. *Der Pharma Chemica*, *9*(13), pp.141-147.

[3] Martins, P., Jesus, J., Santos, S., Raposo, L., Roma-Rodrigues, C., Baptista, P. and Fernandes, A., 2015. Heterocyclic anticancer compounds: recent advances and the paradigm shift towards the use of nanomedicine's tool box. *Molecules*, *20*(9), pp.16852-16891.

[4] Gomtsyan, A., 2012. Heterocycles in drugs and drug discovery. *Chemistry of Heterocyclic Compounds*, *48*(1), pp.7-10.

[5] Gu, W., Wang, S., Jin, X., Zhang, Y., Hua, D., Miao, T., Tao, X. and Wang, S., 2017. Synthesis and evaluation of new quinoxaline derivatives of dehydroabietic acid as potential antitumor agents. *Molecules*, *22*(7), pp.1154.

[6] Khanam, H., 2015. Bioactive benzofuran derivatives: A review. *European Journal of Medicinal Chemistry*, *97*, pp.483-504.

[7] Ajani, O.O., 2014. Present status of quinoxaline motifs: Excellent pathfinders in therapeutic medicine. *European Journal of Medicinal Chemistry*, *85*, pp.688-715.

[8] Dua, R., Shrivastava, S., Sonwane, S.K. and Srivastava, S.K., 2011. Pharmacological significance of synthetic heterocycles scaffold: a review. *Advances in Biological Research*, *5*(3), pp.120-144.

[9] Mandewale, M.C., Patil, U.C., Shedge, S.V., Dappadwad, U.R. and Yamgar, R.S., 2017. A review on quinoline hydrazone derivatives as a new class of potent antitubercular and anticancer agents. *Beni-Suef University journal of Basic and Applied Sciences*, *6*(4), pp.354-361.

[10] Alper-Hayta, S., Arisoy, M., Temiz-Arpaci, Ö., Yildiz, I., Aki, E., Özkan, S. and Kaynak, F., 2008. Synthesis, antimicrobial activity, pharmacophore analysis of some new 2-(substitutedphenyl/benzyl)-5-[(2-benzofuryl) carboxamido] benzoxazoles. *European Journal of Medicinal Chemistry*, *43*(11), pp.2568-2578.

[11] Chand, K., Hiremathad, A., Singh, M., Santos, M.A. and Keri, R.S., 2017. A review on antioxidant potential of bioactive heterocycle benzofuran: Natural and synthetic derivatives. *Pharmacological Reports*, *69*(2), pp.281-295.

[12] Nevagi, R.J., Dighe, S.N. and Dighe, S.N., 2015. Biological and medicinal significance of benzofuran. *European Journal of Medicinal Chemistry*, *97*, pp.561-581.

[13] Yıldız, E., Köse, M., Tümer, M., Purtaş, S. and Tümer, F., 2017. Thiophene based imine compounds: Structural characterization, electrochemical, photophysical and thermal properties. *Journal of Molecular Structure*, *1150*, pp.55-60.

[14] Huang, X.G., Liu, J., Ren, J., Wang, T., Chen, W. and Zeng, B.B., 2011. A facile and practical one-pot synthesis of multisubstituted 2-aminothiophenes via imidazole-catalyzed Gewald reaction. *Tetrahedron*, *67*(34), pp.6202-6205.

[15] of Aguiar, A.C.V., of Moura, R.O., Junior, J.F.B.M., de Oliveira Rocha, H.A., Câmara, R.B.G. and Schiavon, M.D.S.C., 2016. Evaluation of the antiproliferative activity of 2-amino thiophene derivatives against human cancer cells lines. *Biomedicine & Pharmacotherapy*, *84*, pp.403-414.

[16] da Franca Rodrigues, K.A., de Sousa Dias, C.N., do Nascimento Néris, P.L., da Câmara Rocha, J., Scotti, M.T., Scotti, L., Mascarenhas, S.R., Veras, R.C., de Medeiros, I.A., Keesen, T.D.S.L. and de Oliveira, T.B., 2015. 2-Amino-thiophene derivatives present antileishmanial activity mediated by apoptosis and immunomodulation in vitro. *European Journal of Medicinal Chemistry*, *106*, pp.1-14.

[17] Chikhale, R.V., Barmade, M.A., Murumkar, P.R. and Yadav, M.R., 2018. Overview of the development of DprE1 inhibitors for combating the menace of tuberculosis. *Journal of Medicinal Chemistry*, *61*(19), pp.8563-8593.

[18] Lange, C., Chesov, D. and Heyckendorf, J., 2019. Clofazimine for the treatment of multidrug-resistant tuberculosis. *Clinical Microbiology and Infection*, *25*(2), pp.128-130.

[19] Eswaran, S., Adhikari, A.V., Pal, N.K. and Chowdhury, I.H., 2010. Design and synthesis of some new quinoline-3-carbohydrazone derivatives as potential antimycobacterial agents. *Bioorganic & Medicinal Chemistry Letters*, *20*(3), pp.1040-1044.

[20] Arafa, R.K., Hegazy, G.H., Piazza, G.A. and Abadi, A.H., 2013. Synthesis and in vitro antiproliferative effect of novel quinoline-based potential anticancer agents. *European Journal of Medicinal Chemistry*, *63*, pp.826-832.

[21] Subba, K.N., Subba, R.R. and Suryanarayana R.V., 2016. Synthesis and antimicrobial activity of some new quinoxaline derivatives. *Der Pharmacia Lettre, 8(1),* pp. 264-274

[22] Pereira, J.A., Pessoa, A.M., Cordeiro, M.N.D., Fernandes, R., Prudêncio, C., Noronha, J.P. and Vieira, M., 2015. Quinoxaline, its derivatives and applications: a state of the art review. *European Journal of Medicinal Chemistry*, *97*, pp.664-672.

[23] Ingle, R., Marathe, R., Magar, D., Patel, H.M. and Surana, S.J., 2013. Sulphonamido-quinoxalines: search for anticancer agent. *European Journal of Medicinal Chemistry*, *65*, pp.168-186.

[24] Al-Marhabi, A.R., Abbas, H.A.S. and Ammar, Y.A., 2015. Synthesis, characterization and biological evaluation of some quinoxaline derivatives: a promising and potent new class of antitumor and antimicrobial agents. *Molecules*, *20*(11), pp.19805-19822.

[25] Cogo, J., Kaplum, V., Sangi, D.P., Ueda-Nakamura, T., Corrêa, A.G. and Nakamura, C.V., 2015. Synthesis and biological evaluation of novel 2, 3-disubstituted quinoxaline derivatives as antileishmanial and antitrypanosomal agents. *European Journal of Medicinal Chemistry*, *90*, pp.107-123.

[26] Hajri, M., Esteve, M.A., Khoumeri, O., Abderrahim, R., Terme, T., Montana, M. and Vanelle, P., 2016. Synthesis and evaluation of in vitro antiproliferative activity of new ethyl 3-(arylethynyl) quinoxaline-2-carboxylate and pyrido [4, 3-b] quinoxalin-1 (2H)-one derivatives. *European Journal of Medicinal Chemistry*, *124*, pp.959-966.

[27] Carta, A., Paglietti, G., Nikookar, M.E.R., Sanna, P., Sechi, L. and Zanetti, S., 2002. Novel substituted quinoxaline 1, 4-dioxides with in vitro antimycobacterial and anticandida activity. *European Journal of Medicinal Chemistry*, *37*(5), pp.355-366.

[28] Hui, X., Desrivot, J., Bories, C., Loiseau, P.M., Franck, X., Hocquemiller, R. and Figadere, B., 2006. Synthesis and antiprotozoal activity of some new synthetic substituted quinoxalines. *Bioorganic & Medicinal Chemistry Letters*, *16*(4), pp.815-820.

[29] Kumar, J., Chawla, G., Kumar, U. and Sahu, K., 2014. Design and syntheses of some new quinoxaline derivatives containing pyrazoline residue as potential antimicrobial agents. *Medicinal Chemistry Research*, *23*(9), pp.3929-3940.

[30] Santivañez-Veliz, M., Pérez-Silanes, S., Torres, E. and Moreno-Viguri, E., 2016. Design and synthesis of novel quinoxaline derivatives as potential candidates for treatment of multidrug-resistant and latent tuberculosis. *Bioorganic & Medicinal Chemistry Letters*, *26*(9), pp.2188-2193.

[31] Ramalingam, P., Ganapaty, S. and Rao, C.B., 2010. In vitro antitubercular and antimicrobial activities of 1-substituted quinoxaline-2, 3 (1H, 4H)-diones. *Bioorganic & Medicinal Chemistry Letters*, *20*(1), pp.406-408.

[32] Kim, Y.B., Kim, Y.H., Park, J.Y. and Kim, S.K., 2004. Synthesis and biological activity of new quinoxaline antibiotics of echinomycin analogues. *Bioorganic & Medicinal Chemistry Letters*, *14*(2), pp.541-544.

[33] Cholo, M.C., Steel, H.C., Fourie, P.B., Germishuizen, W.A. and Anderson, R., 2011. Clofazimine: current status and future prospects. *Journal of Antimicrobial Chemotherapy*, *67*(2), pp.290-298.

[34] O'Donnell, M.R., Padayatchi, N. and Metcalfe, J.Z., 2016. Elucidating the role of clofazimine for the treatment of tuberculosis. *The International Journal of Tuberculosis and Lung Disease*, *20*(12), pp.52-57.

[35] Tyagi, S., Ammerman, N.C., Li, S.Y., Adamson, J., Converse, P.J., Swanson, R.V., Almeida, D.V. and Grosset, J.H., 2015. Clofazimine shortens the duration of the first-line treatment regimen for experimental chemotherapy of tuberculosis. *Proceedings of the National Academy of Sciences*, *112*(3), pp.869-874.

[36] Li, J.J., 1999. Synthesis of novel 3-substituted pyrrolo [2, 3-b] quinoxalines via an intramolecular heck reaction on an aminoquinoxaline scaffold. *The Journal of Organic Chemistry*, *64*(22), pp.8425-8427.

[37] Ghattass, K., El-Sitt, S., Zibara, K., Rayes, S., Haddadin, M.J., El-Sabban, M. and Gali-Muhtasib, H., 2014. The quinoxaline di-N-oxide DCQ blocks breast cancer metastasis in vitro and in vivo by targeting the hypoxia inducible factor-1 pathway. *Molecular Cancer*, *13*(1), pp.12.

[38] Tseng, C.H., Chen, Y.R., Tzeng, C.C., Liu, W., Chou, C.K., Chiu, C.C. and Chen, Y.L., 2016. Discovery of indeno [1, 2-b] quinoxaline derivatives as potential anticancer agents. *European Journal of Medicinal Chemistry*, *108*, pp.258-273.

[39] Palos, I., Luna-Herrera, J., Lara-Ramírez, E., Loera-Piedra, A., Fernández-Ramírez, E., Aguilera-Arreola, M., Paz-González, A., Monge, A., Wan, B., Franzblau, S. and Rivera, G., 2018. Anti-Mycobacterium tuberculosis Activity of Esters of Quinoxaline 1, 4-Di-N-Oxide. *Molecules*, *23*(6), pp.1453.

[40] Pan, Y., Li, P., Xie, S., Tao, Y., Chen, D., Dai, M., Hao, H., Huang, L., Wang, Y., Wang, L. and Liu, Z., 2016. Synthesis, 3D-QSAR analysis and biological evaluation of quinoxaline 1, 4-di-N-oxide derivatives as antituberculosis agents. *Bioorganic & Medicinal Chemistry Letters*, *26*(16), pp.4146-4153.

[41] Ancizu, S., Moreno, E., Torres, E., Burguete, A., Pérez-Silanes, S., Benítez, D., Villar, R., Solano, B., Marín, A., Aldana, I. and Cerecetto, H., 2009. Heterocyclic-2-carboxylic

acid (3-cyano-1, 4-di-N-oxidequinoxalin-2-yl) amide derivatives as hits for the development of neglected disease drugs. *Molecules*, *14*(6), pp.2256-2272.

[42] Rylands, L.I., Welsh, A., Maepa, K., Stringer, T., Taylor, D., Chibale, K. and Smith, G.S., 2019. Structure-activity relationship studies of antiplasmodial cyclometallated ruthenium (II), rhodium (III) and iridium (III) complexes of 2-phenylbenzimidazoles. *European Journal of Medicinal Chemistry*, *161*, pp.11-21.

[43] Yang, Y., Guo, L., Ge, X., Tian, Z., Gong, Y., Zheng, H., Du, Q., Zheng, X. and Liu, Z., 2019. Novel lysosome-targeted cyclometalated Iridium (III) anticancer complexes containing imine-N-heterocyclic carbene ligands: Synthesis, spectroscopic properties and biological activity. *Dyes and Pigments*, *161*, pp.119-129.

[44] Wang, Y., Pigeon, P., Mcglinchey, M.J., Top, S. and Jaouen, G., 2017. Synthesis and antiproliferative evaluation of novel hydroxypropyl-ferrociphenol derivatives, resulting from the modification of hydroxyl groups. *Journal of Organometallic Chemistry*, *829*, pp.108-115.

[45] Glans, L., Hu, W., Jöst, C., de Kock, C., Smith, P.J., Haukka, M., Bruhn, H., Schatzschneider, U. and Nordlander, E., 2012. Synthesis and biological activity of cymantrene and cyrhetrene 4-aminoquinoline conjugates against malaria, leishmaniasis, and trypanosomiasis. *Dalton Transactions*, *41*(21), pp.6443-6450.

[46] Beauperin, M., Polat, D., Roudesly, F., Top, S., Vessières, A., Oble, J., Jaouen, G. and Poli, G., 2017. Approach to ferrocenyl-podophyllotoxin analogs and their evaluation as anti-tumor agents. *Journal of Organometallic Chemistry*, *839*, pp.83-90.

[47] Cin, G.T., Verep, G., Topel, S.D. and Ciger, V., 2013. An efficient synthesis of ferrocenyl-containing 1, 3, 4-oxadiazole derivatives via oxidative cyclization reaction. *Chemistry of Heterocyclic Compounds*, *49*(7), pp.1061-1067.

[48] Zhang, P. and Sadler, P.J., 2017. Advances in the design of organometallic anticancer complexes. *Journal of Organometallic Chemistry*, *839*, pp.5-14.

[49] Sekhon, B.S. and Bimal, N., 2012. Transition metal-based antimalarial. *Journal of Pharmaceutical Education and Research*, *20112*(3), pp.52-63.

[50] Renier, O., Deacon-Price, C., Peters, J.E., Nurekeyeva, K., Russon, C., Dyson, S., Ngubane, S., Baumgartner, J., Dyson, P.J., Riedel, T. and Chiririwa, H., 2017. Synthesis and In Vitro (Anticancer) Evaluation of η6-Arene Ruthenium Complexes Bearing Stannyl Ligands. *Inorganics*, *5*(3), pp.44.

[51] Liang, J.X., Zhong, H.J., Yang, G., Vellaisamy, K., Ma, D.L. and Leung, C.H., 2017. Recent development of transition metal complexes with in vivo antitumor activity. *Journal of Inorganic Biochemistry*, *177*, pp.276-286.

[52] Zaki, M., Arjmand, F. and Tabassum, S., 2016. Current and future potential of metallo drugs: Revisiting DNA-binding of metal containing molecules and their diverse mechanism of action. *Inorganica Chimica Acta*, *444*, pp.1-22.

[53] Han, Y., Tian, Z., Zhang, S., Liu, X., Li, J., Li, Y., Liu, Y., Gao, M. and Liu, Z., 2018. Half-sandwich IridiumIIIN-heterocyclic carbene antitumor complexes and biological applications. *Journal of Inorganic Biochemistry*, *189*, pp.163-171.

[54] Li, J., Tian, Z., Ge, X., Xu, Z., Feng, Y. and Liu, Z., 2019. Design, synthesis, and evaluation of fluorine and Naphthyridine–Based half-sandwich organoiridium/ruthenium complexes with bioimaging and anticancer activity. *European Journal of Medicinal Chemistry*, *163*, pp.830-839.

[55] Köpf-Maier, P., 1994. Complexes of metals other than platinum as antitumour agents. *European Journal of Clinical Pharmacology*, *47*(1), pp.1-16.

[56] Lainé, A.L. and Passirani, C., 2012. Novel metal-based anticancer drugs: a new challenge in drug delivery. *Current Opinion in Pharmacology*, *12*(4), pp.420-426.

[57] Quirante, J., Dubar, F., González, A., Lopez, C., Cascante, M., Cortés, R., Forfar, I., Pradines, B. and Biot, C., 2011. Ferrocene–indole hybrids for cancer and malaria therapy. *Journal of Organometallic Chemistry*, *696*(5), pp.1011-1017.

[58] Mahajan, A., Kremer, L., Louw, S., Guéradel, Y., Chibale, K. and Biot, C., 2011. Synthesis and in vitro antitubercular activity of ferrocene-based hydrazones. *Bioorganic & Medicinal Chemistry Letters*, *21*(10), pp.2866-2868.

[59] Esparza-Ruiz, A., Herrmann, C., Chen, J., Patrick, B.O., Polishchuk, E. and Orvig, C., 2012. Synthesis and in vitro anticancer activity of ferrocenyl-aminoquinoline-carboxamide conjugates. *Inorganica Chimica Acta*, *393*, pp.276-283.

[60] Guillon, J., Moreau, S., Mouray, E., Sinou, V., Forfar, I., Fabre, S.B., Desplat, V., Millet, P., Parzy, D., Jarry, C. and Grellier, P., 2008. New ferrocenic pyrrolo [1, 2-a] quinoxaline derivatives: synthesis, and in vitro antimalarial activity. *Bioorganic & Medicinal Chemistry*, *16*(20), pp.9133-9144.

[61] Guillon, J., Mouray, E., Moreau, S., Mullié, C., Forfar, I., Desplat, V., Belisle-Fabre, S., Pinaud, N., Ravanello, F., Le-Naour, A. and Léger, J.M., 2011. New ferrocenic pyrrolo [1, 2-a] quinoxaline derivatives: Synthesis, and in vitro antimalarial activity–Part II. *European Journal of Medicinal Chemistry*, *46*(6), pp.2310-2326.

[62] Claus, R., Lewtak, J.P., Muller, T.J. and Swarts, J.C., 2013. Structural influences on the electrochemistry of 1, 1′-di (hydroxyalkyl) ferrocenes. Structure of [Fe {η 5-C 5 H 4–CH (OH)–(CH 2) 3 OH} 2]. *Journal of Organometallic Chemistry*, *740*, pp.61-69.

[63] Chen, P., Liu, C., Hu, J., Zhang, H. and Sun, R., 2018. Design, synthesis and fungicidal activity studies of 3-ferrocenyl-N-acryloylmorpholine. *Journal of Organometallic Chemistry*, *854*, pp.113-121.

[64] Kulikov, V.N., Nikulin, R.S., Arkhipov, D.E., Rodionov, A.N., Babusenko, E.S., Kovalenko, L.V. and Belousov, Y.A., 2017. Ferrocenecarboxylic acid and microwave-assisted synthesis of ferrocenoyl hydrazones. *Russian Chemical Bulletin*, *66*(3), pp.537-544.

[65] Patra, M. and Gasser, G., 2017. The medicinal chemistry of ferrocene and its derivatives. *Nature Reviews Chemistry*, *1*(9), pp.0066.

[66] García-Barrantes, P.M., Lamoureux, G.V., Pérez, A.L., García-Sánchez, R.N., Martínez, A.R. and San Feliciano, A., 2013. Synthesis and biological evaluation of novel ferrocene–naphthoquinones as antiplasmodial agents. *European Journal of Medicinal Chemistry*, *70*, pp.548-557.

[67] Arbi, M.E., Pigeon, P., Rkhis, A.C., Top, S., Rhouma, A., Rebai, A., Jaouen, G. and Aifa, S., 2011. Antimicrobial effect of ferrocenyl diaryl butenes against olive plantlet diseases. *Journal of Plant Pathology*, pp.651-657.

[68] Verma, S.K. and Singh, V.K., 2015. Synthesis and characterization of ferrocene functionalized transition metal dithiocarbamate complexes: Investigations of antimicrobial, electrochemical properties and a new polymorphic form of [Cu {κ2S, S–S2CN (CH2C4H3O) CH2Fc} 2]. *Journal of Organometallic Chemistry*, *791*, pp.214-224.

[69] Yeary, R.A., 1969. Chronic toxicity of dicyclopentadienyliron (ferrocene) in dogs. *Toxicology and Applied Pharmacology*, *15*(3), pp.666-676.

[70] Corry, A.J., Goel, A. and Kenny, P.T., 2012. The synthesis and structural characterization of N-(ferrocenyl) 2 and N-(ferrocenoyl) 2 cystine dimethyl ester derivatives: Potential anion sensing agents. *Inorganica Chimica Acta*, *384*, pp.293-301.

[71] Yong, J., Jiang, X., Wu, X., Huang, S., Zhang, Q. and Lu, C., 2014. Synthesis and Characterization of Ferrocene Derivatives and Preliminarily Electrocatalytic Oxidation of L-Cysteine at Nafion-Ferrocene Derivatives Modified Glassy Carbon Electrode. *Advances in Chemistry*, *2014*.

[72] Wani, W.A., Jameel, E., Baig, U., Mumtazuddin, S. and Hun, L.T., 2015. Ferroquine and its derivatives: new generation of antimalarial agents. *European Journal of Medicinal Chemistry*, *101*, pp.534-551.

[73] Daniel, T.M., 2006. The history of tuberculosis. *Respiratory Medicine*, *100*(11), pp.1862-1870.

[74] World Health Organization, 2017. Global tuberculosis report 2017, Geneva: World Health Organization; 2017. Licence: CC BY-NCSA.

[75] World Health Organization, 2018. Global tuberculosis report 2018, Geneva: World Health Organization; 2018. Licence: CC BY-NCSA.

[76] Goldberg, D.E., Siliciano, R.F. and Jacobs Jr, W.R., 2012. Outwitting evolution: fighting drug-resistant TB, malaria, and HIV. *Cell*, *148*(6), pp.1271-1283.

[77] Srivastava, G., Tripathi, S., Kumar, A. and Sharma, A., 2017. Molecular investigation of active binding site of isoniazid (INH) and insight into resistance mechanism of S315T-MtKatG in Mycobacterium tuberculosis. *Tuberculosis*, *105*, pp.18-27.

[78] El-Azab, A.S., Mary, Y.S., Abdel-Aziz, A.A., Miniyar, P.B., Armaković, S. and Armaković, S.J., 2018. Synthesis, spectroscopic analyses (FT-IR and NMR), vibrational study, chemical reactivity and molecular docking study and antitubercular activity of condensed oxadiazole and pyrazine derivatives. *Journal of Molecular Structure*, *1156*, pp.657-674.

[79] Tiberi, S., du Plessis, N., Walzl, G., Vjecha, M.J., Rao, M., Ntoumi, F., Mfinanga, S., Kapata, N., Mwaba, P., McHugh, T.D. and Ippolito, G., 2018. Tuberculosis: progress and advances in development of new drugs, treatment regimens, and host-directed therapies. *The Lancet Infectious Diseases*, *18*(7), pp.183-198.

[80] Segretti, N.D., Simoes, C.K., Corrêa, M.F., Felli, V.M.A., Miyata, M., Cho, S.H., Franzblau, S.G. and dos Santos Fernandes, J.P., 2016. Antimycobacterial activity of pyrazinoate prodrugs in replicating and non-replicating Mycobacterium tuberculosis. *Tuberculosis*, *99*, pp.11-16.

[81] Yang, Y., Guo, L., Ge, X., Shi, S., Gong, Y., Xu, Z., Zheng, X. and Liu, Z., 2019. Structure-activity relationships for highly potent half-sandwich organoiridium (III) anticancer complexes with C^ N-chelated ligands. *Journal of Inorganic Biochemistry*, *191*, pp.1-7.

[82] Nitulescu, G.M., Margina, D., JUzeNAS, P., Peng, Q., Olaru, O.T., Saloustros, E., Fenga, C., Spandidos, D.A., Libra, M. and Tsatsakis, A.M., 2016. Akt inhibitors in cancer treatment: The long journey from drug discovery to clinical use. *International Journal of Oncology*, *48*(3), pp.869-885.

[83] Abbas, H.A.S., Al-Marhabi, A.R., Eissa, S.I. and Ammar, Y.A., 2015. Molecular modeling studies and synthesis of novel quinoxaline derivatives with potential anticancer activity as inhibitors of c-Met kinase. *Bioorganic & medicinal chemistry*, *23*(20), pp.6560-6572.

[84] Lee, G., Lee, H.Y., Park, H., Schiebler, M.L., van Beek, E.J., Ohno, Y., Seo, J.B. and Leung, A., 2017. Radiomics and its emerging role in lung cancer research, imaging biomarkers and clinical management: state of the art. *European Journal of Radiology*, *86*, pp.297-307.

[85] van Timmeren, J.E., Leijenaar, R.T., van Elmpt, W., Reymen, B., Oberije, C., Monshouwer, R., Bussink, J., Brink, C., Hansen, O. and Lambin, P., 2017. Survival prediction of non-small cell lung cancer patients using radiomics analyses of cone-beam CT images. *Radiotherapy and Oncology*, *123*(3), pp.363-369.

[86] Thawani, R., McLane, M., Beig, N., Ghose, S., Prasanna, P., Velcheti, V. and Madabhushi, A., 2018. Radiomics and radiogenomics in lung cancer: a review for the clinician. *Lung Cancer*, *115*, pp.34-41.

[87] Mokgoathana, H.D., 2015. Sonogashira coupling of quinoxaline-o-sulfonates leading to heterocyclic compounds with potential medicinal properties against TB (MSc dissertation). http://hdl.handle.net/10386/1633.

[88] Ndlovu, N.T., 2016. *Novel synthetic routs towards the synthesis of mono-, di-and tri-substituted qunoxallines* (MSc dissertation, University of Limpopo). http://hdl.handle.net/10386/1703.

Chapter 2

2. Results and discussion

In an effort to establish new quinoxaline-ferrocene derivatives with biological properties, a series of quinoxaline alkynyl derivatives were generated. Our investigation started with the preparation of quinoxaline-2-ol **83** followed by a series of reactions that include sulfonation, Sonogashira cross coupling and functionalisation of the quinoxaline alkynyl alcohol. **Scheme 2** depicts the envisaged synthetic route for possible synthesis of quinoxaline-ferrocene derivatives proposed in this study.

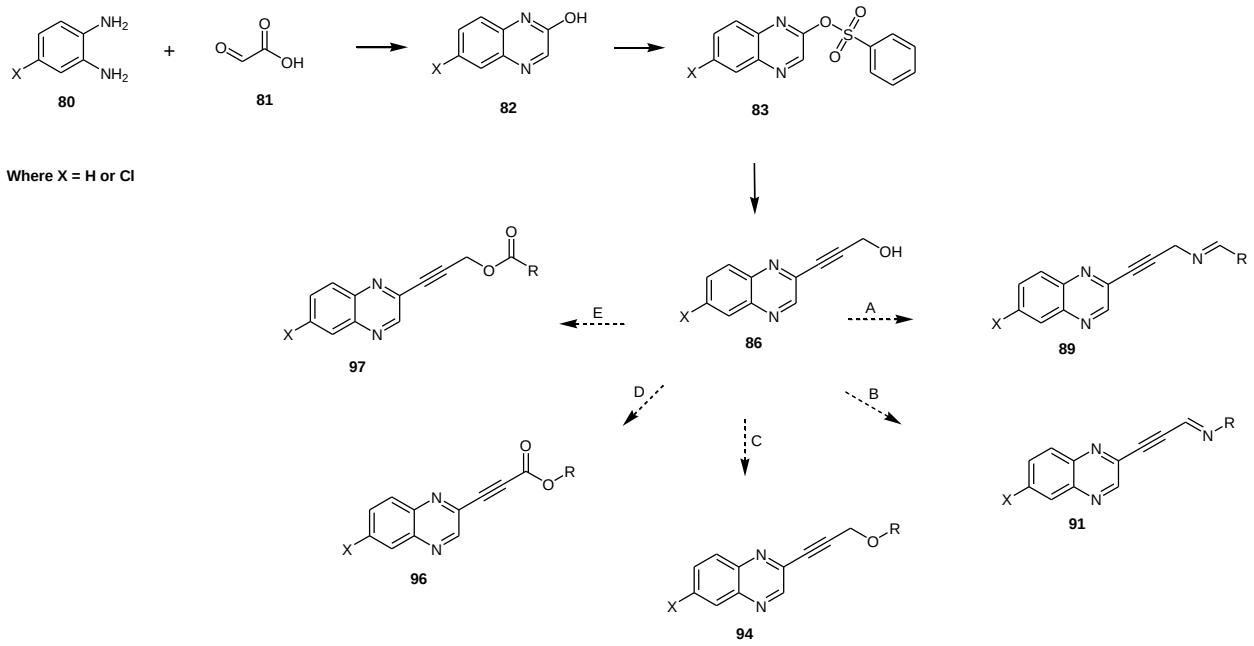

Scheme 2: General synthetic routes to access quinoxaline alkynyl derivatives. (A) Reductive amination, (B) reductive amination, (C) etherification, (D) esterification and (E) esterification.

2.1 Synthesis of quinoxaline intermediates

The first step was to acquire quinoxaline-2-ol **82A**, which was obtained by cyclocondensation of *O*-phenylenediamine and glyoxylic acid to give 70% yield.

Subsequently, sulfonation of quinoxaline-2-ol to generate a good leaving group on *C*-2 position was synthesised in a DMAP catalysed reaction in the presence of Et_3N as a base [1]. Quinoxalin-3-yl benzenesulfonate **83A** was obtained in 83% yield and confirmed using ^{1}H-NMR. The ^{1}H-NMR spectrum confirmed the displacement of the hydrogen on the hydroxyl group with new signals appearing at 7.28, 7.77 and 7.90 ppm accounting for 2:1:2 protons from the benzene sulfonate group. Furthermore, we observed multiplet peaks resonating at 7.79 and 8.08 ppm assigned to the protons on the benzene ring and a characteristic peak of a singlet resonating at 8.89 ppm (–N=C-H) defining the quinoxaline moiety.

Synthesis of 6-chloroquinoxalin-3-yl benzenesulfonate **83B** followed a similar procedure described for synthesis of **83A** while starting with a 6-chloroquinoxalin-2-ol **82A**. From the ^{1}H-NMR spectrum of **83B**, we observed new signals overlapping with the signals from the quinoxaline moiety resonating at 7.60, 7.71, 7.82 and 8.12 ppm which integrated for 2:2:1:3 protons of the compound. Furthermore, a characteristic peak of a singlet resonating at 8.65 ppm (–N=C-H) defining the quinoxaline moiety was observed. Sulfonate intermediates have been previously investigated to be good leaving groups in coupling of pteridines [2, 3]. In this study quinoxalin-3-yl benzenesulfonates **83** serves as excellent coupling partners for sonogashira cross coupling reactions.

Table 1: Summary of the quinoxaline sulfonate intermediates

Entry	**Product**	**% Yield**	**Melting point (ºC)**
1	83A	83	89 – 92 (lit 91 ºC) [1]
2	83B	41	143.7 - 146.5

2.2 Sonogashira cross coupling of quinoxalin-3-yl benzenesulfonate **83A**

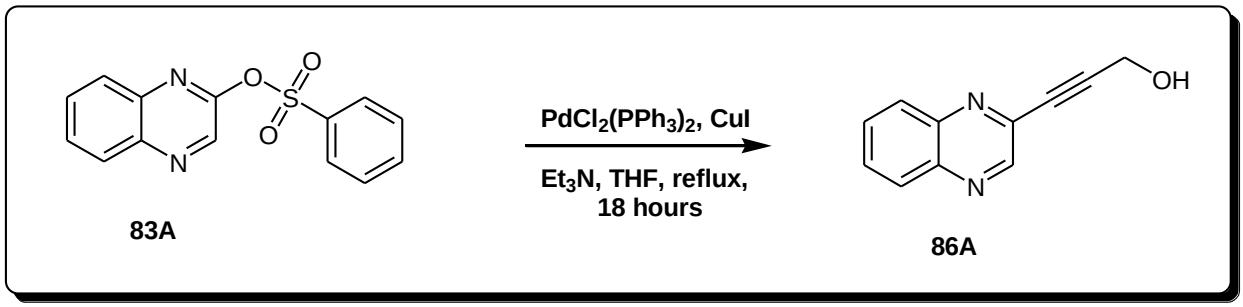

Scheme 3: Synthesis of 3-(quinoxalin-3-yl)prop-2-yn-1-ol **86A**.

The synthesis of 3-(quinoxalin-3-yl)prop-2-yn-1-ol **86A** was achieved via Sonogashira cross coupling reaction (**Scheme 3)**. The substrate quinoxalin-3-yl benzene sulfonate **83A** was successfully coupled with propargyl alcohol by employing $PdCl_2(PPh_3)_2$ (5 mol%), CuI (10 mol%) and Et_3N (2 equiv.) in dry THF [4] to give 3-(quinoxalin-3-yl)prop-2-yn-1-ol **86A** in 60% yield, after recrystallisation form acetone. The ^{1}H-NMR spectrum (**Figure 22)** of 3-(quinoxalin-3-yl)prop-2-yn-1-ol **86A** is described as follows; a singlet peak resonating at 4.61 ppm integrating for 2 protons at *C*–11 is observed. Furthermore, we observe multiplet peaks resonating at 7.79 and 8.08 assigned to the protons on the benzene ring of the quinoxaline moiety and a characteristic peak of a singlet resonating at 8.89 (–N=C-H) defining the quinoxaline moiety. On the ^{13}C-NMR spectrum (**Figure 23)**, the signals attributed to the alkynyl carbons *C*-9 and *C*-10 resonated at 83.0 and 91.9 ppm. Moreover, FT-IR showed the presence of an alcohol stretch at 3275 cm^{-1}. From the mass spectrum, $[M+H]^+$ peak showing m/z 185.0431 was observed. 3-(quinoxalin-3-yl)prop-2-yn-1-ol **86A** was previously reported, therefore all features observed upon characterisation are in agreement with literature [5, 6].

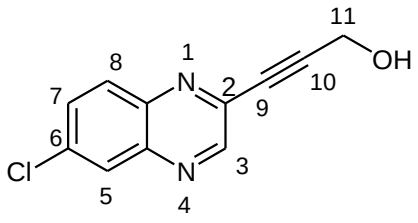

86B

The synthesis of 3-(6-chloroquinoxalin-2-yl)prop-2-yn-1-ol **86B** was achieved by treating 6-chloroquinoxalin-3-yl benzenesulfonate **83B** with propargyl alcohol and obtained in

49% yield. From the ^{1}H-NMR spectrum of 3-(6-chloroquinoxalin-3-yl)prop-2-yn-1-ol **86B**, we observed a singlet peak resonating at 4.60 which integrates for two protons at *C*-11. Furthermore, signals resonating at 7.72, 7.98 and 8.08 ppm of multiplicity (d, dd and d) integrates for 1:1:1 protons from the benzene ring of the quinoxaline moiety. The characteristic peak due to –N=C-H on the quinoxaline moiety was observed at 8.86 ppm. In addition, the alcohol stretch at 3266 cm^{-1} was observed on FT-IR. The mass spectrum of **86B** showed [M+H]$^{+}$ peak with m/z 219.1902 and the appearance of M+2 peak showing m/z 221.0231 due to chlorine isotope was observed.

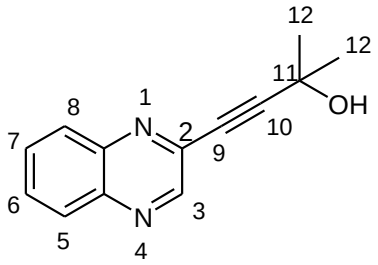

86C

Synthesis of 2-methyl-4-(quinoxalin-3-yl)but-3-yn-2-ol **86C** was achieved by treating quinoxalin-3-yl benzene sulfonate **83A** with 2-methylbut-3-yn-2-ol (1.2 equiv.) and obtained in 78% yield. The ^{1}H-NMR spectrum of **86C** has similar features as **86A,** however the carbon at *C*-11 of **86C** is attached to two methyl groups. The protons on the methyl carbons of **86C** resonate at 1.66 ppm which appears as a singlet integrating for 6 protons. Furthermore, the alcohol stretch was observed at 3290 cm^{-1} on FT-IR spectrum. The mass spectrum of **86C** showed [M+H]$^{+}$ peak with m/z 213.1023. 2-Methyl-4-(quinoxalin-3-yl)but-3-yn-2-ol **86C** was previously reported, therefore all features observed upon characterisation are in agreement with literature [5]. However, melting point and FT-IR data was not reported.

Table 1: Summary of the quinoxaline alkynyl alcohols.

Entry	product	% yield	Melting point (ºC)
1	86A	60	139 – 141 (lit 140 – 141 ºC) [5]
2	86B	49	140.1 – 142.9
3	86C	78	155.3 – 158.4

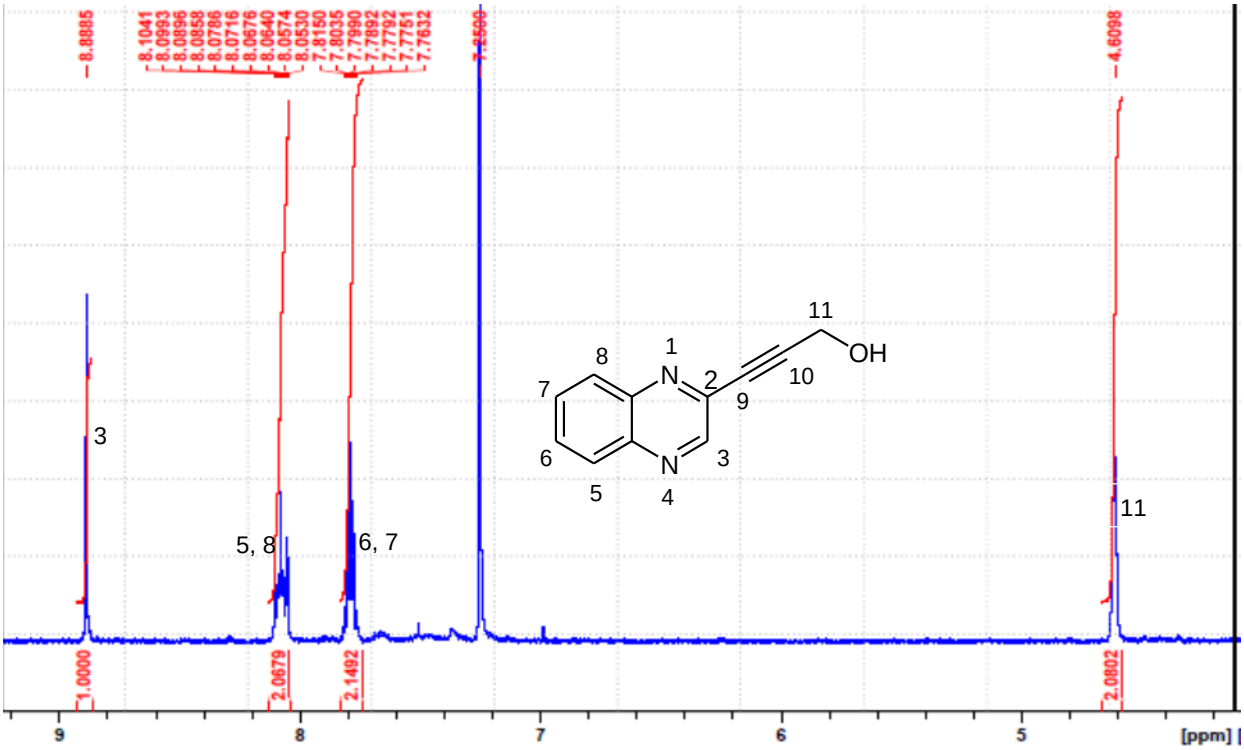

Figure 22: ^{1}H-NMR spectrum of 3-(quinoxalin-3-yl)prop-2-yn-1-ol **86A**.

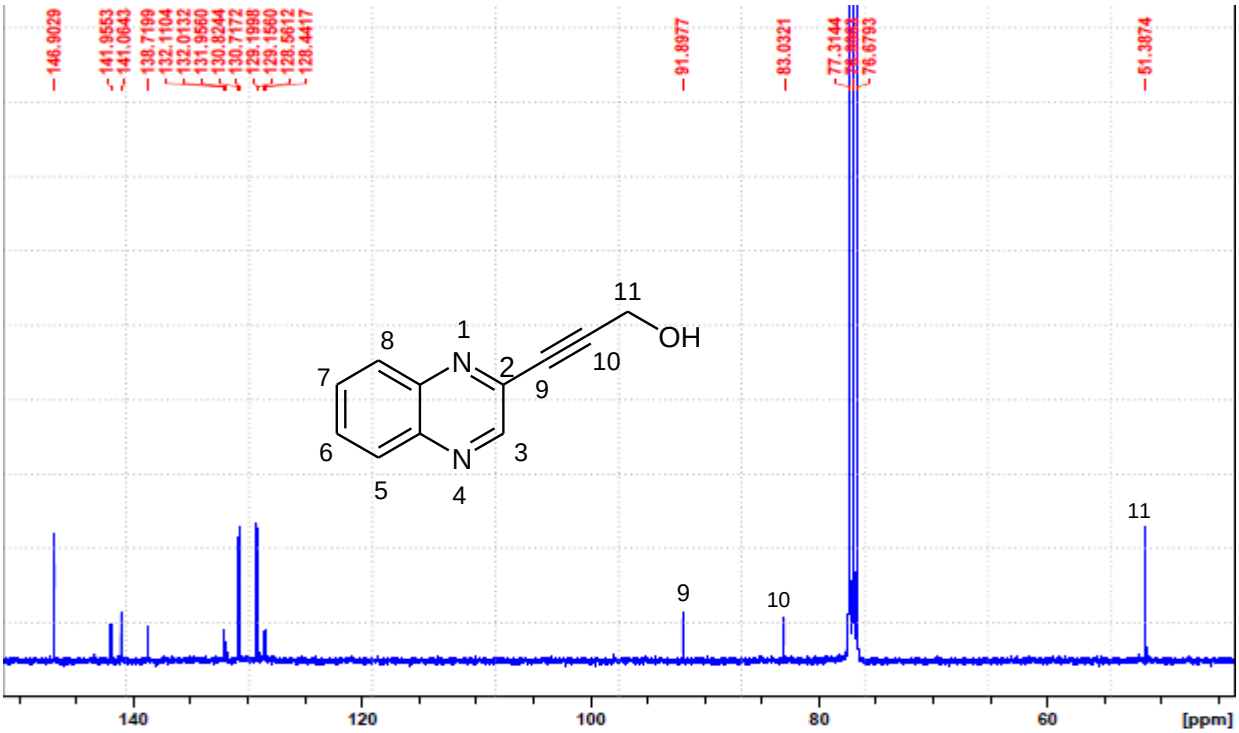

Figure 23: ^{13}C-NMR spectrum of 3-(quinoxalin-3-yl)prop-2-yn-1-ol **86A**.

2.2 Synthesis of quinoxaline alkynyl derivatives

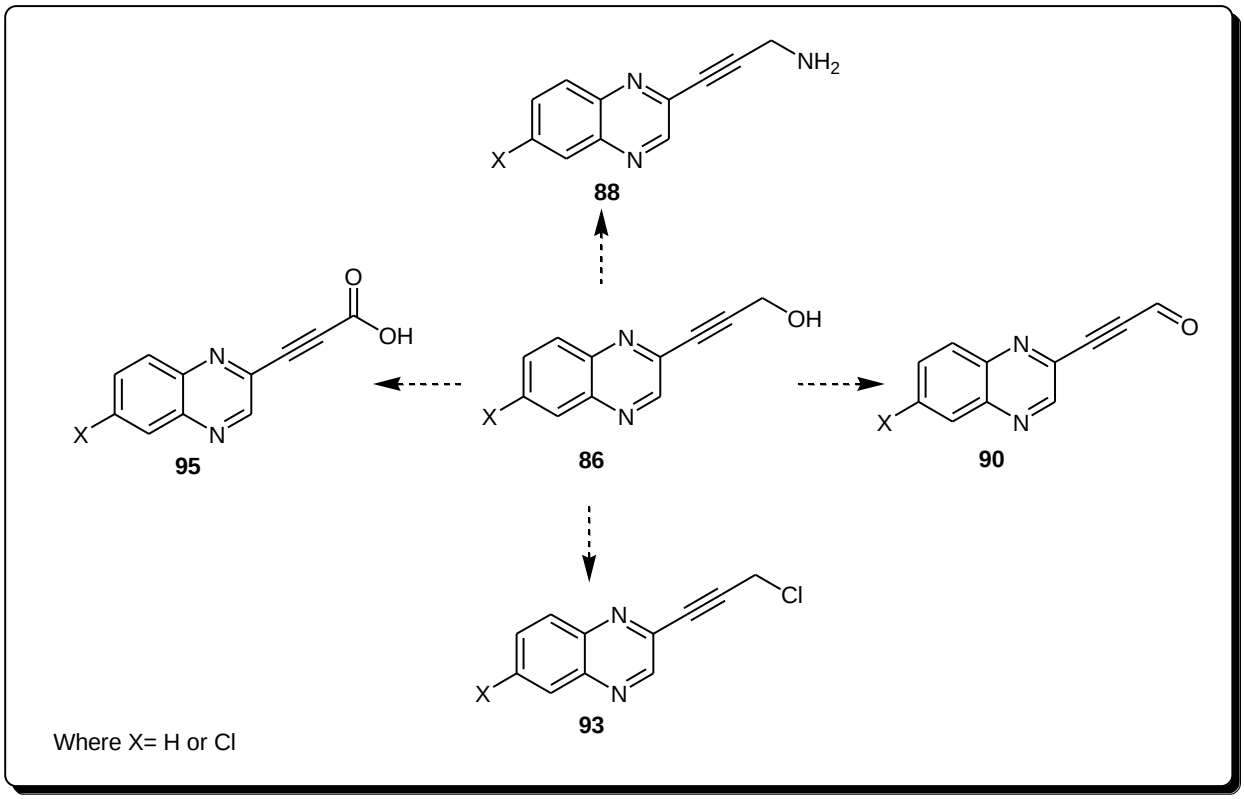

Scheme 4: Possible quinoxaline alkynyl intermediates that can be generated from **87** in order to link ferrocene to quinoxaline moiety.

The quinoxaline alkynyl alcohols (**86A – C)** obtained after sonogashira cross coupling reaction presented an opportunity to link ferrocene into the quinoxaline moiety. For instance, **Scheme 4** shows quinoxaline alkynyl derivatives that can be generated from **86** in order to link the quinoxaline moiety with ferrocene moiety, where quinoxaline can either be introduced as a nucluophile or an electrophile. Therefore, possible links to the ferrocene can be through reductive amination, etherification or esterification. This encouraged us to develop a library of compounds by utilizing the propargylic alcohol available for further functionalisation. In this study, quinoxaline propargylic alcohols were functionalised via substitution and oxidation reactions to satisfy the objectives of this study.

2.2.1 Attempted synthesis of quinoxaline-ferrocene via reductive amination reaction of 3-(quinoxalin-3-yl)prop-2-yn-1-amine 88 (Method A)

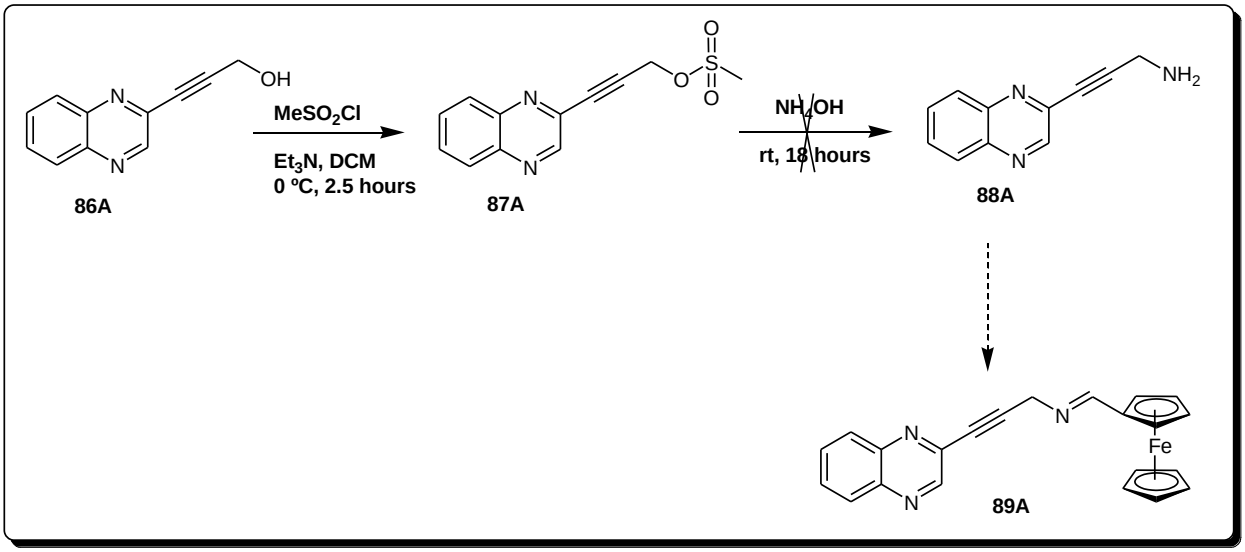

Scheme 5: Attempted synthesis of quinoxaline-ferrocene via reductive amination reaction (Method A).

In an attempt to link ferrocene to quinoxaline moiety through reductive amination (**Scheme 5)**, 3-(quinoxalin-3-yl)prop-2-yn-1-ol **86A** was treated with a mesyl chloride to activate the alcohol and generate 3-(quinoxalin-3-yl) prop-2-ynyl methanesulfonate **87A** in 59% yield as an intermediate with a good leaving group. The formation of **87A** was confirmed by ^{1}H-NMR (**Figure 24)** and we observed the appearance of a new singlet resonating at 3.19 ppm integrating for 3 protons at *C*-12. The singlet integrating for 2 protons at *C*-11 showed a significant downfield shift from 4.61 ppm to 5.16 ppm due to the influence of the electron donating mesyl group attached to the molecule.

3-(quinoxalin-3-yl) prop-2-ynyl methanesulfonate **87A** was treated with excess aqueous ammonia solution (28%) and stirred for 18 hours in an effort to synthesise 3-(quinoxalin-3-yl)prop-2-yn-1-amine **88A**. However, a trace amount of the desired product **88A** and unreacted starting material **87A** was observed. The formation of 3-(quinoxalin-3-yl)prop-2-yn-1-amine **88A** was confirmed by ^{1}H-NMR where an upfield shift on the methylene protons moved from 5.16 ppm to 4.11 ppm due to the influence of an electron donating group (NH_2) attached to the molecule. Furthermore, a singlet resonating at 2.09 ppm

integrating for two protons (NH_2) was observed. The trace amount of **88A** obtained was due to poor solubility of **87A** in aqueous ammonia solution. To improve solubility, **87A** was dissolved in THF and treated with excess ammonia solution (28%) and stirred for 18 hours. Nonetheless, no improvement on the yield was observed.

The reaction was attempted again following a different literature procedure which required the use of NaN_3 in the presence of a mesylated intermediate to generate an azide intermediate, which was later treated with PPh_3 to undergo Staudinger reduction [7]. However, the reaction yielded undesirable product. From the crude ^{1}H-NMR no trace of the desire product and the starting material were observed. As a result, reductive amination reaction through 3-(quinoxalin-3-yl)prop-2-yn-1-amine **88A** was unsuccessful.

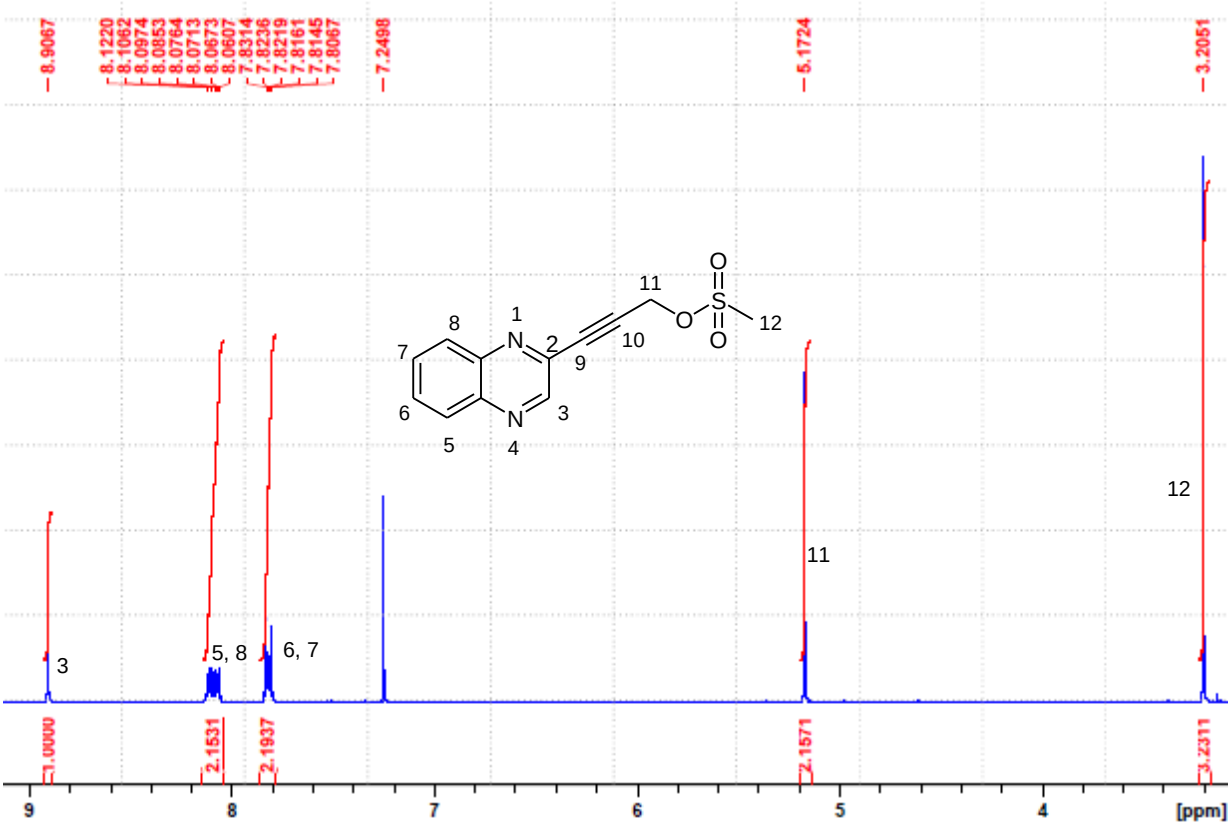

Figure 24: ^{1}H-NMR spectrum of 3-(quinoxalin-3-yl) prop-2-ynyl methanesulfonate **87A**.

2.2.2 Attempted synthesis of quinoxaline-ferrocene via condensation reaction of 3-(quinoxalin-3-yl)propiolaldehyde 90A (Method B)

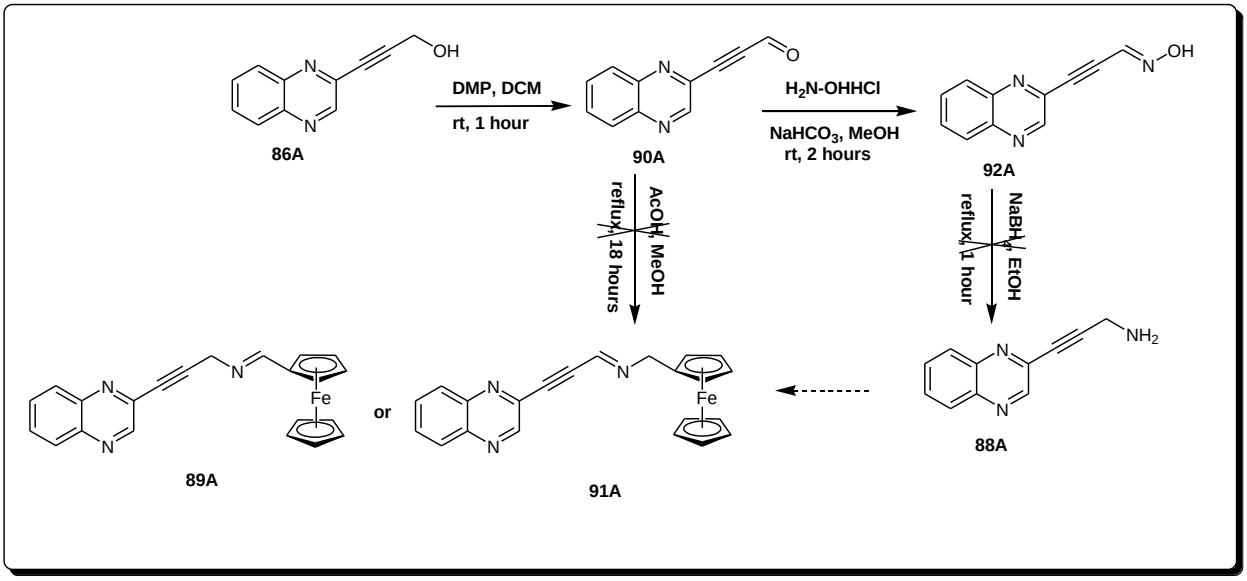

Scheme 6: Synthesis of quinoxaline-ferrocene via reductive amination reaction (Method B).

3-(quinoxalin-3-yl)propiolaldehyde **90A** serves the same purpose as 3-(quinoxalin-3-yl)prop-2-yn-1-amine **88A** in which ferrocene can be linked via reductive amination reaction (**Scheme 6)**. The aldehyde **90A** was successfully synthesised by oxidising **86A** with Dess Martin Periodinane (DMP), however it was obtained in low percentage yield of 28%. The formation of this compound was confirmed in the ^{1}H NMR spectrum (**Figure 25**) by the disappearance of the methylene protons at *C*-11 and a new signal appearing as a singlet integrating for one proton at 9.53 ppm signifying the formation of an aldehyde was observed. The ^{13}C-NMR spectrum (**Figure 26)** confirmed the formation of the desired product **90A** as indicated by the presence of a carbonyl carbon signal resonating at 175.9 ppm assigned to *C*-11. From the mass spectrum, $[M+H]^{+}$ peak showing m/z of 183.0550 was observed. 3-(quinoxalin-3-yl)propiolaldehyde **90A** has previously been reported, therefore all features observed upon characterisation are in agreement with literature [8].

With the aldehyde at hand, we then attempted to synthesise quinoxaline-ferrocene compound **91** through reductive amination. To test the efficacy of literature procedure [9], compound **90A** was treated with fluoroaniline (2 equiv.) and few drops of acetic acid in MeOH under nitrogen atmosphere and heated to reflux for 18 hours. The abovementioned conditions yielded unreacted starting material with no trace of the desired product. Compounds with an imine linker are moisture sensitive and easily undergo hydrolysis. Therefore, water is known to be one of the by-products obtained during reductive amination reactions which plays a role during hydrolysis. The reaction was attempted again in the presence of $NaHCO_3$ (1 equiv.) which traps water produced during the reaction. Unfortunately, the reaction was unsuccessful.

The aldehyde presented an alternative route for condensation reaction with hydroxylamine hydrochloride solution to generate an oxime **92A** which can later be reduced into an amine (3-(quinoxalin-3-yl)prop-2-yn-1-amine) **88A**. The oxime intermediate was successfully synthesised by treating **90A** with H_2N-OH•HCl (1 equiv.) in the presence of $NaHCO_3$ (1 equiv.) in MeOH to yield quantitative amount of the desired product. The oxime intermediated was immediately used for the next reaction without purification. We then attempted an oxime reduction reaction by treating the oxime intermediate with $NaBH_4$ to yield an amine. However, this approach was unsuccessful instead the oxime was isolated. Further attempt with a strong reducing agent $LiAlH_4$, led to an unsuccessful reaction. The crude product analysis showed the presence of the starting material i.e. oxime. Therefore, synthesis of quinoxaline-ferrocene compounds via reductive amination reaction was unsuccessful.

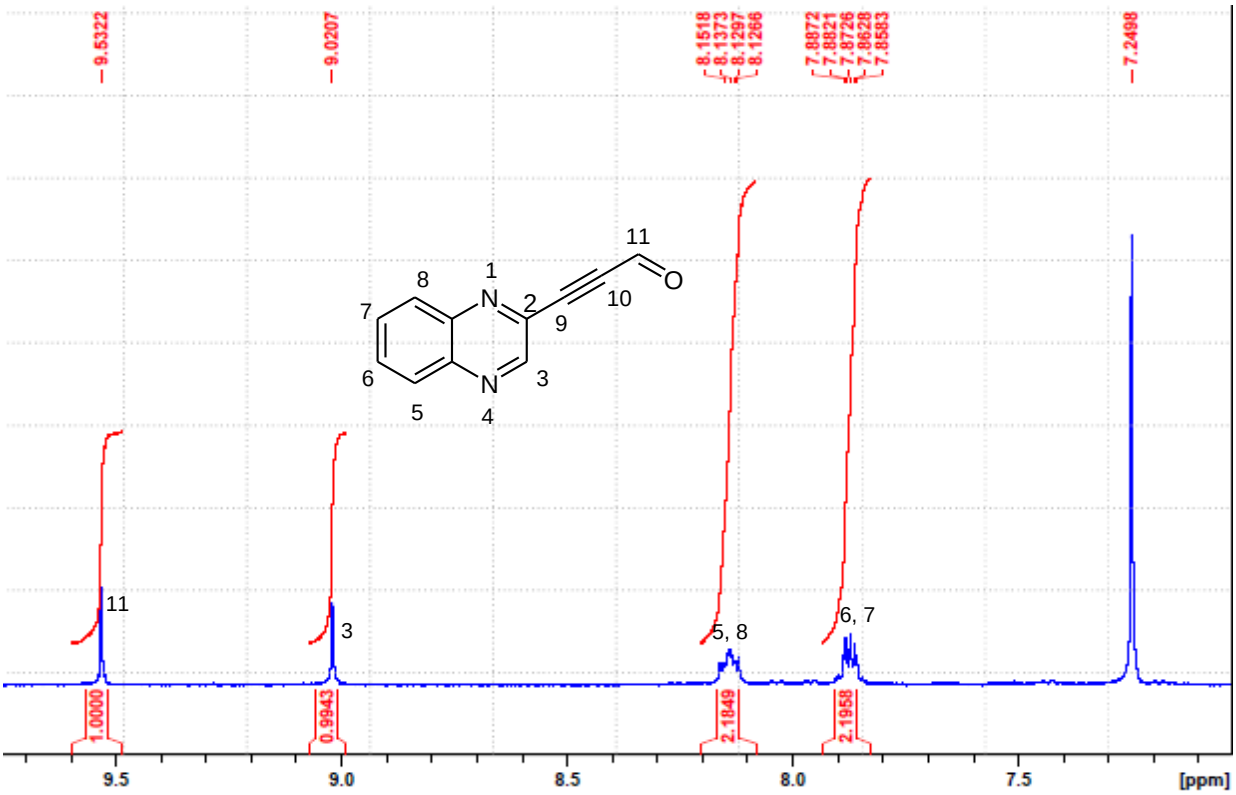

Figure 25: ^{1}H-NMR spectrum of 3-(quinoxalin-3-yl)propiolaldehyde **90A**.

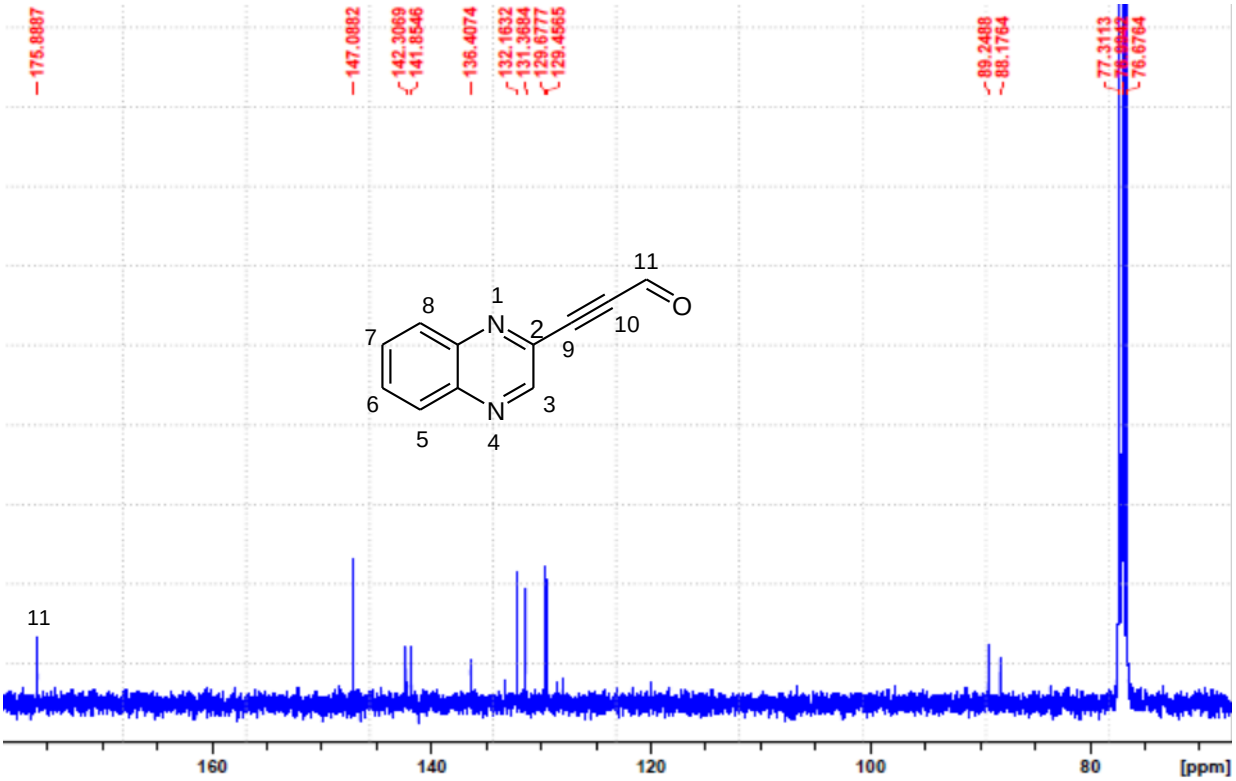

Figure 26: ^{13}C-NMR spectrum of 3-(quinoxalin-3-yl)propionaldehyde **90A**.

2.2.3 Attempted synthesis of quinoxaline-ferrocene compounds via etherification of 2-(3-chloroprop-1-ynyl)quinoxaline 93A (Method C)

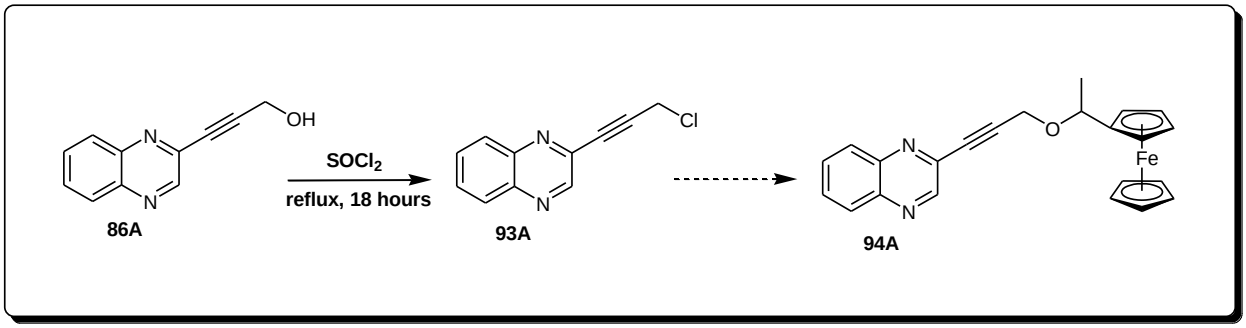

Scheme 7: Synthesis of quinoxaline-ferrocene via etherification reaction (Method C).

We then proposed to link the two moieties via etherification reaction (**Scheme 7**) in which quinoxaline can be introduced as an electrophile. 3-(Quinoxalin-3-yl)prop-2-yn-1-ol **86A** was treated with excess $SOCl_2$ and refluxed for 18 hours to produce 2-(3-chloroprop-1-ynyl)quinoxaline **93A** in 17% yield. From ^{1}H-NMR spectrum (**Figure 27)**, we observed two doublet peaks resonating at 5.44 and 5.88 ppm which integrated for the one proton each at *C*-11. However, the observed chemical shift positions at 5.44 and 5.88 seem not to agree with the inductive effect as a results of oxygen being replaced with chlorine. This observed chemical shift anomaly is supported by ^{13}C-NMR spectrum (**Figure 28**) which indicate carbon *C*-11 resonating at 83.4 ppm contrary to expected chemical shift range of 50 – 60 ppm. Similarly, *C*-9 and *C*-10 also resonate at lower field than anticipated i.e. 137.3 and 141.6 ppm. From the low-resolution mass spectrometry, $[M+H]^+$ peak showing m/z 203.0098 and the appearance of M+2 peak due to the presence of a chlorine isotope was observed. Unfortunately, the same m/z is not observed on high-resolution mass spectrometry. Despite several attempts through variation of reaction conditions such as triethyl amine as a catalyst, the same results were obtained. Therefore, synthesis of quinoxaline-ferrocene compounds via etherification reaction of compound **93A** was unsuccessful.

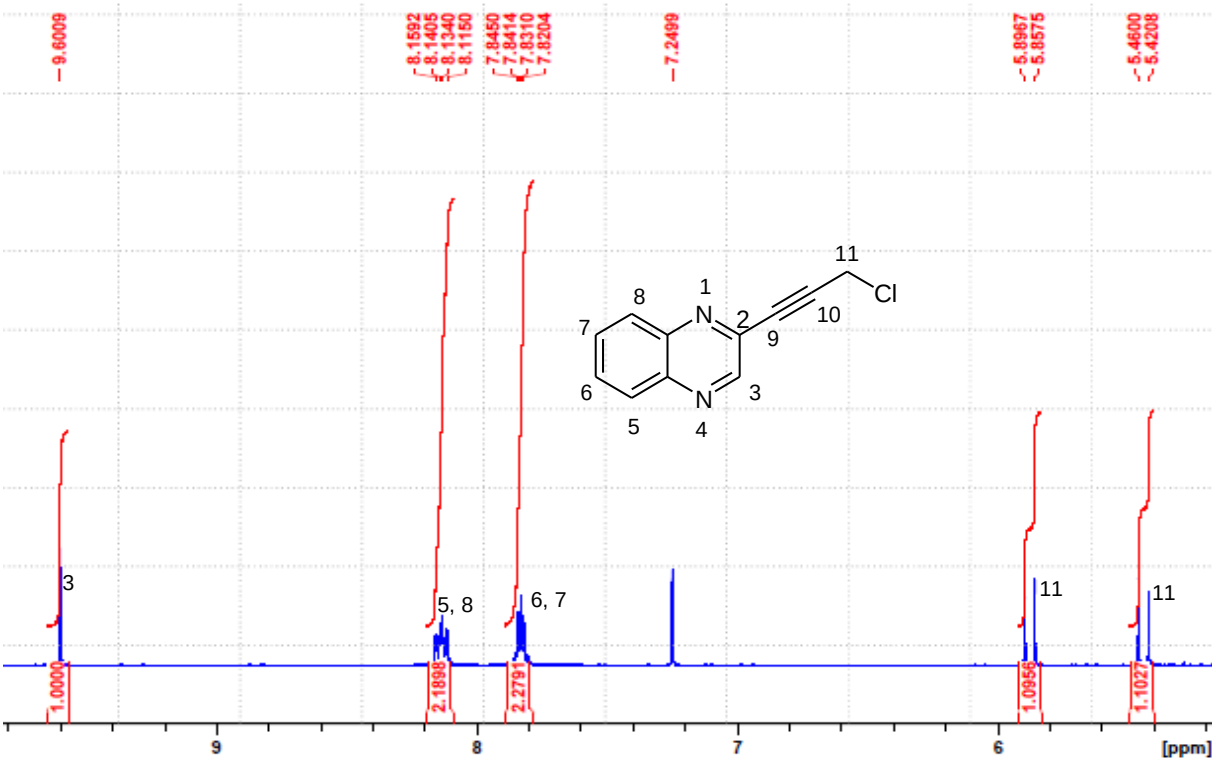

Figure 27: ^{1}H-NMR spectrum of 2-(3-chloroprop-1-ynyl)quinoxaline **93A**.

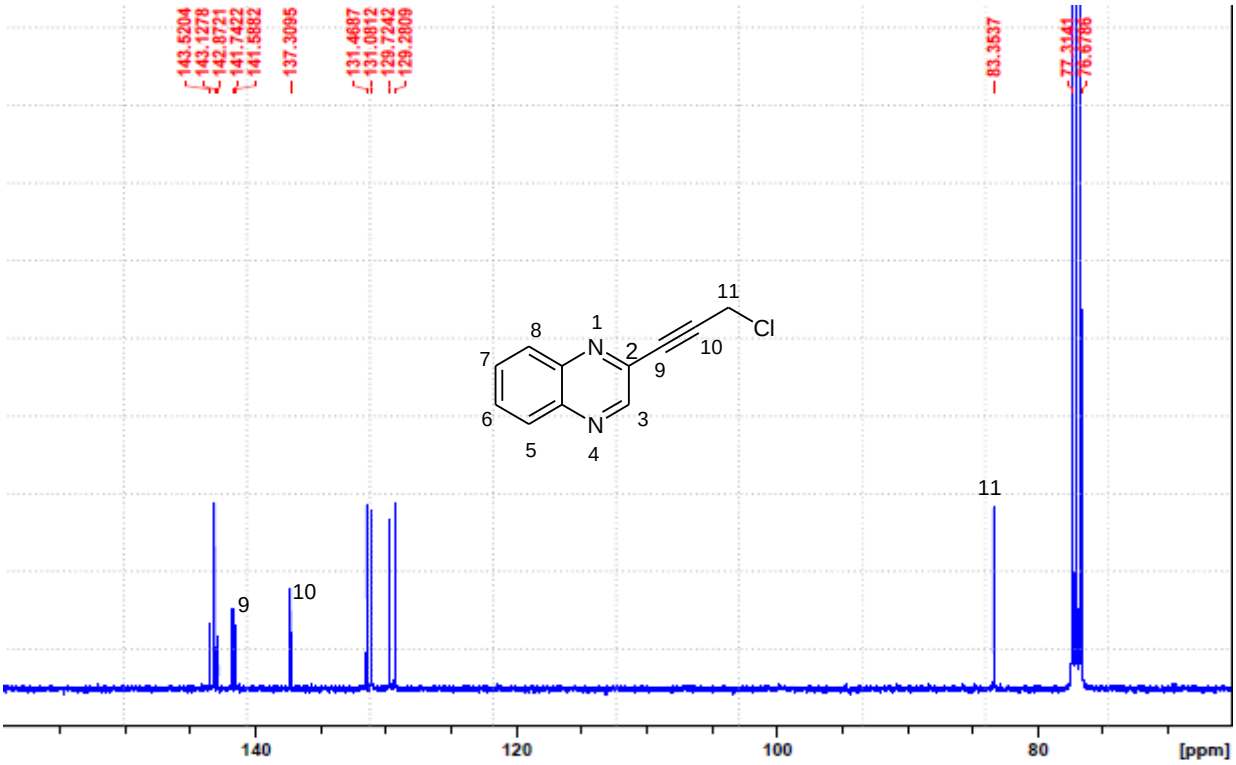

Figure 28: 13C-NMR spectrum of 2-(3-chloroprop-1-ynyl)quinoxaline **93A**.

The mesylated intermediate **87A** presented an alternative to link quinoxaline-ferrocene compounds since it can act as a good leaving group suitable for etherification reaction. Several reactions were attempted following literature procedures [10, 11, 12]. Firstly, isopropanol was treated with 3-(quinoxalin-3-yl) prop-2-ynyl methanesulfonate **87A** in the presence of K_2CO_3. However, the unreacted starting material was recovered with no trace of the desired product. The reaction was attempted again using bases like BuLi and NaH to first deprotonate the alcohol and generate an alkoxide intermediate, but the reaction was unsuccessful. As a result, no trace of the desired product was obtained instead the unreacted starting material was recovered. Therefore, etherification method was unsuccessful.

2.2.4 Attempted synthesis of quinoxaline-ferrocene compounds via esterification reaction of 3-(quinoxalin-3-yl)propiolic acid 95A (Method D)

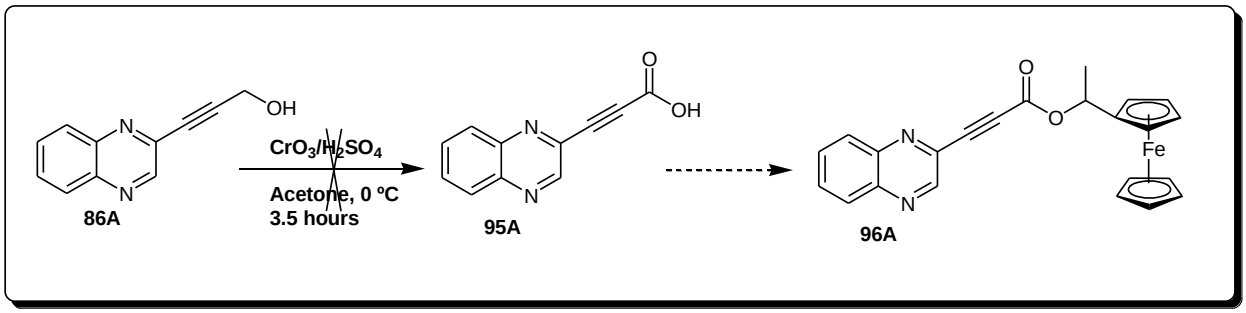

Scheme 8: Attempted synthesis of quinoxaline-ferrocene via esterification reaction (Method D).

We then proposed to link quinoxaline-ferrocene compounds via esterification route (**Scheme 8)** where quinoxaline can be introduced as an acid chloride electrophile. In an effort to synthesis 3-(quinoxalin-3-yl)propiolic acid **95A**, several reactions were attempted. Firstly, **86A** was treated with Jones reagent (CrO_3/H_2SO_4) to oxidise the alcohol into an acid. Unfortunately, the oxidation progressed as far as the aldehyde **90A**. This was confirmed by the presence of an aldehyde proton resonating at 9.53 ppm, while the acid proton was expected to resonate at ~10 – 12 ppm. Further attempts with a

different oxidising agent (H_2IO_6/CrO_3) while varying temperature was conducted. The reaction at 0 ºC for 2.5 hours was unsuccessful with only the unreacted starting material **86A** recovered. The reaction at room temperature progressed to an aldehyde similar to Jones reagent. The reaction of **86A** at 50 ºC yielded a trace amount of the aldehyde and unreacted starting material with no trace of the acid.

The aldehydes obtained through either Dess Martins or Jones oxidizing reagent were further oxidised in an effort to get to the propiolic acid. The aldehyde **90A** was treated with Jones reagent but the reaction was unsuccessful with unreacted starting material recovered. The reaction was attempted again by treating **90A** with H_2IO_6/CrO_3 at room temperature and the unreacted aldehyde **90A** was recovered. Due to unsuccessful attempts to generate the propiolic acid, esterification reaction via 3-(quinoxalin-3-yl)propiolic acid **95** was unsuccessful.

2.2.5 Synthesis of quinoxaline-ferrocene compounds via esterification reaction of 3-(quinoxalin-3-yl)prop-2-yn-1-ol 86A (Method E)

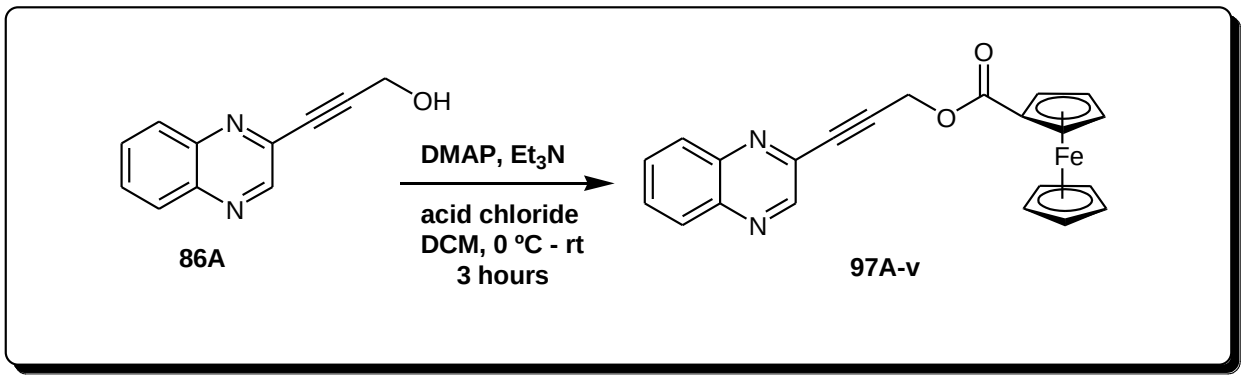

Scheme 9: Synthesis of quinoxaline-ferrocene via esterification reaction (Method E)

The unsuccessful efforts to convert **86A** to an acid chloride (**Scheme 8**) led to the use of **86A** as a nucleophile in the esterification reactions. Thus, 3-(quinoxalin-3-yl)prop-2-yn-1-ol **86A** was subjected to electrophilic substitution reactions to generate a series of ester derivatives. 3-(Quinoxalin-3-yl)prop-2-ynyl acetate **97A-i** was synthesised following a literature procedure [6]. The reaction was achieved by treating **86A** with DMAP (10 mol%),

acetyl chloride (1 equiv.) and Et_3N (3 equiv.) to afford **97A-i** in 70% yield. From the ^{1}H-NMR spectrum (**Figure 29)**, we observed a significant downfield shift from 4.61 ppm to 4.99 ppm at *C*-11 which appears as a singlet integrating for two protons. This is due to the presence of the electron withdrawing acetyl group introduced on the molecule. Furthermore, a singlet peak resonating at 2.15 ppm was assigned to methyl protons at *C*-13. From the ^{13}C-NMR spectrum (**Figure 30)**, an additional 2 peaks were observed and assigned to the methyl carbon (*C*-13) and carbonyl carbon (*C*-12) resonating at 20.7 and 170.1 ppm, respectively. In addition, FT-IR confirmed the formation of **97A-i** wherein the carbonyl stretch representing the formation of an ester was observed at 1732 cm^{-1}. The mass spectrum of **97A-i** showed $[M+H]^+$ peak with m/z 227.0819.

Various ester derivatives were obtained from 3-(quinoxalin-3-yl)prop-2-yn-1-ol **86A** following a similar procedure as described for the synthesis of **97A-i**, using different acid chloride groups. To this series, a quinoxaline-ferrocene compound was successfully synthesised and obtained in yield of 42%. The ^{1}H-NMR spectrum of **97A-iv (Figure 31)** is described as follows; we observe a singlet peak resonating at 4.26 ppm assigned to the protons marked 16 on the lower cyclopentadienyl ring. Furthermore, two sets of triplets resonating at 4.45 and 4.88 ppm assigned to the protons at *C*-14 and *C*-13, respectively are observed. In addition, a significant downfield shift similar to **97A-i** was observed where a singlet integrating for protons at *C*-11 resonates at 5.14 ppm. From the ^{13}C-NMR spectrum (**Figure 32)**, new peaks assigned to the ferrocenyl moiety are observed at 69.5 – 71.8 ppm. Furthermore, a signal assigned to the carbonyl carbon at *C*-12 is observed at 171.1 ppm. A carbonyl stretch representing the formation of an ester was observed at 1709 cm^{-1} on the FT-IR. From the mass spectrum, $[M+H]^+$ peak showing m/z 397.0634 was observed.

Table 2: Summary of 3-(quinoxalin-3-yl)prop-2-ynyl ester derivatives.

Entry	R-Component	Product	%Yield	^{1}H-NMR (δ ppm) R-Component	Ms (m/z)
1	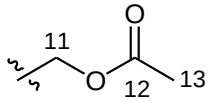	98A-i	70	2.15 (H-13), 4.99 (H-11)	$[M+H]^+$ 227.0819

2	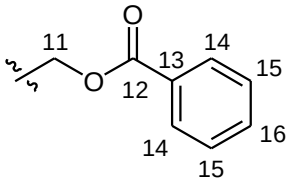	98A-ii	76	5.26 (H-11), 7.47 (H-15), 7.59 (H-16), 8.09 (H-14)	$[M+H]^+$ 289.0561
3	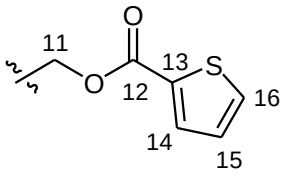	98A-iii	38	5.21 (H-11), 7.12 (H-15), 7.61 (H-16), 7.88 (H-14)	$[M+Na]^+$ 317.1025
4	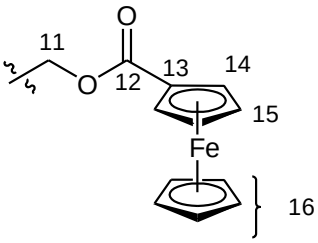	98A-iv	42	4.26 (H-16), 4.45 (H-15), 4.88 (H-14), 5.14 (H-11)	$[M+H]^+$ 397.0634

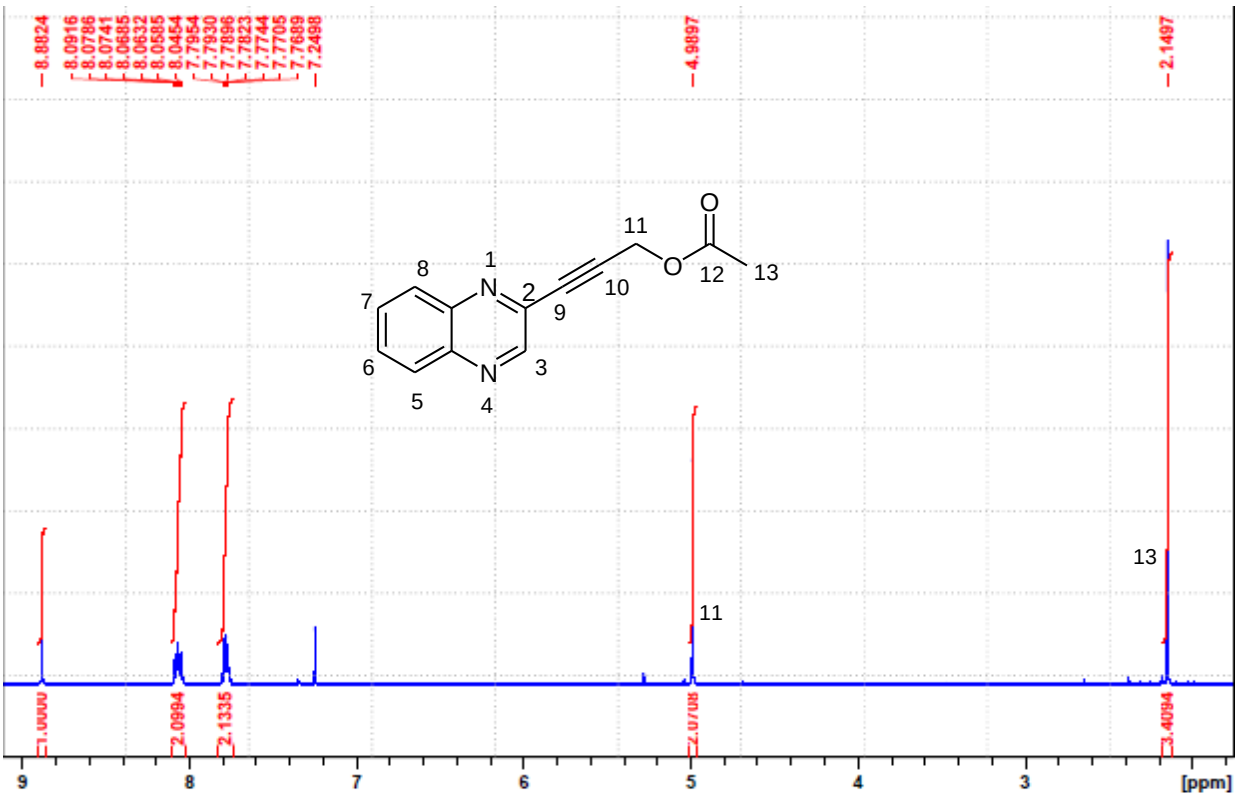

Figure 29: ^{1}H-NMR spectrum of 3-(quinoxalin-3-yl)prop-2-ynyl acetate **97A-i**.

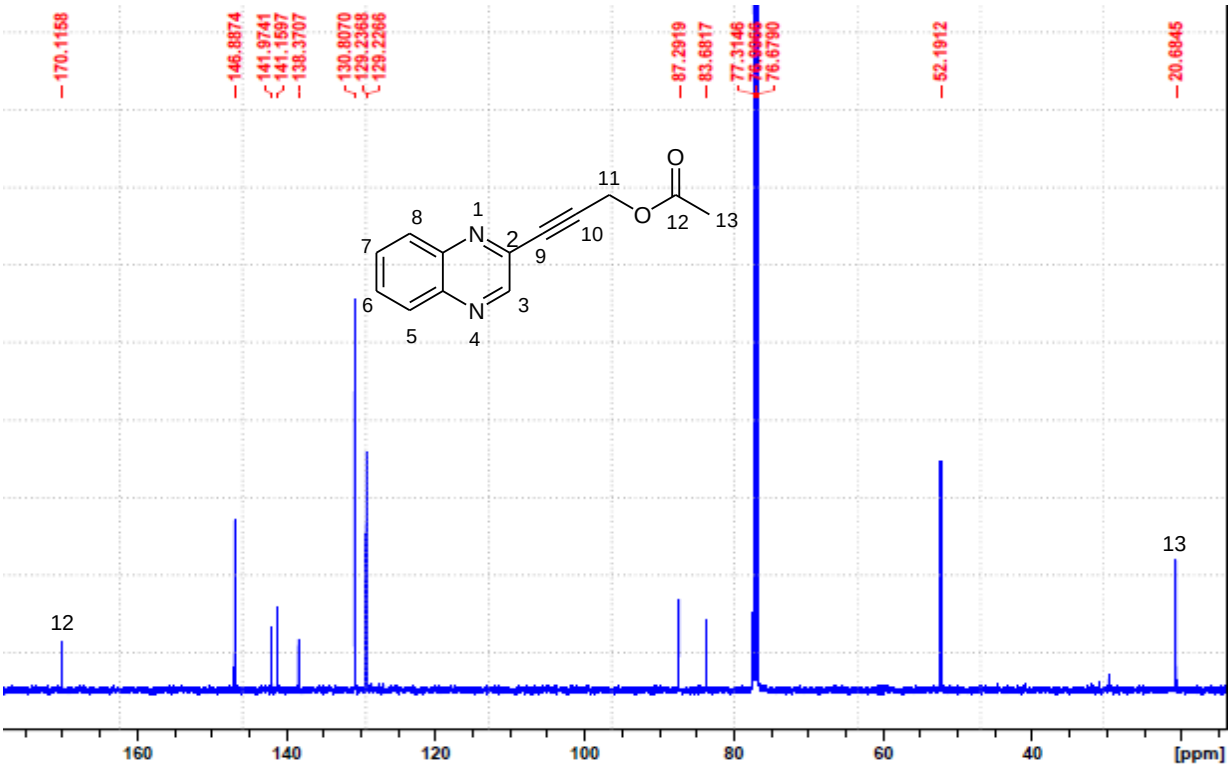

Figure 30: ^{13}C-NMR spectrum of 3-(quinoxalin-3-yl)prop-2-ynyl acetate **97A-i.**

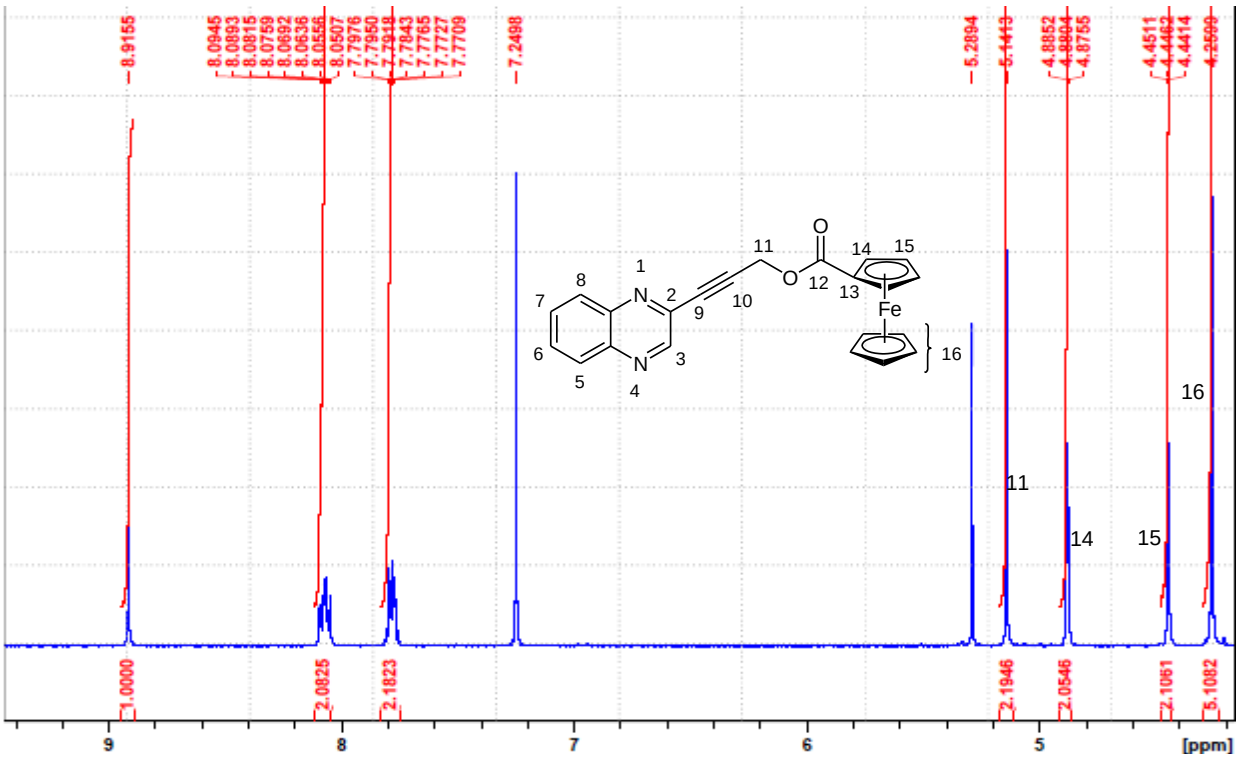

Figure 31: ^{1}H-NMR spectrum of 3-(quinoxalin-3-yl)prop-2-ynyl ferrocetate **97A-iv**.

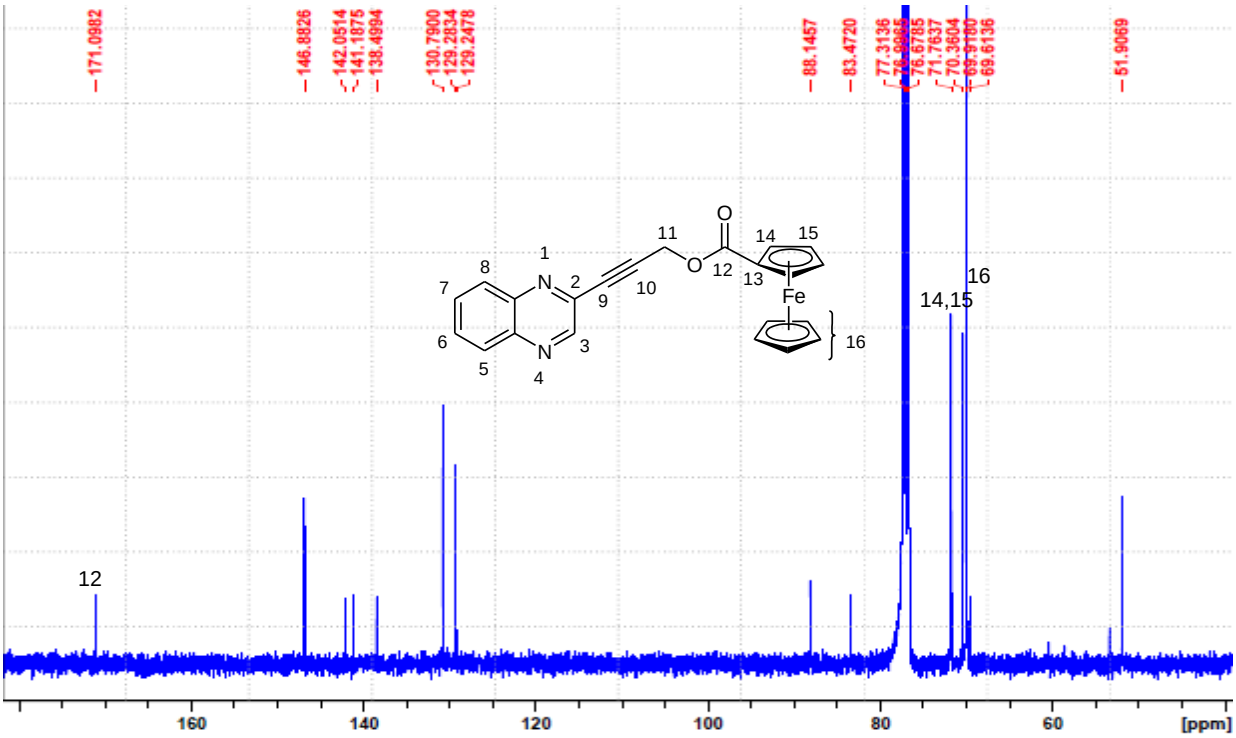

Figure 32: ^{13}C-NMR spectrum of 3-(quinoxalin-3-yl)prop-2-ynyl ferrocetate **97A-iv**.

A series of 6-chloroquinoxaline ester derivatives was also synthesised following a similar procedure as described for the synthesis of **97A** ester derivatives, The successful synthesis of 3-(quinoxalin-3-yl)prop-2-ynyl ferrocetate **97A-iv** encouraged us to develop ester derivatives from 3-(6-chloroquinoxalin-2-yl)prop-2-yn-1-ol **86B** while varying similar acid chloride groups including ferrocenoyl chloride. The 6-chloroquinoxaline ester derivatives synthesised from **86B** were obtained in 13 – 91% yield. The influence of electron withdrawing acetyl groups observed on the 3-(quinoxalin-3-yl)prop-2-yn-1-ol **86A** ester derivatives was again observed on 3-(6-chloroquinoxalin-2-yl)prop-2-yn-1-ol **86B** ester derivatives. For instance, the ^{1}H-NMR spectrum of **97B-iii** (**Figure 33)** showed a significant downfield shift from 4.60 to 5.22 ppm at *C*-11 which appeaed as a singlet integrating for two protons. From the ^{13}C-NMR spectrum, the carbonyl carbon signal of **97B- iii** was observed at 161.3 ppm. A signal due to the formation of an ester functional group was observed at 1704 cm^{-1} on FT-IR. The mass spectrum of compound **97B-iii** showed $[M+H]^{+}$ peak of m/z 329.0156 and the appearance of M+2 peak showing m/z 331.0118 due to the chlorine isotope at *C*-6 was observed.

Table 3: Summary of the 6-chloroquinoxaline ester derivatives.

Entry	R-Component	Product	%Yield	^{1}H-NMR (δ ppm) R-Component	Ms (m/z)
1	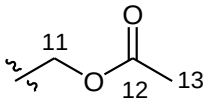	97B-i	91	2.15 (H-13), 4.98 (H-11)	$[M+H]^{+}$ 261.0426
2	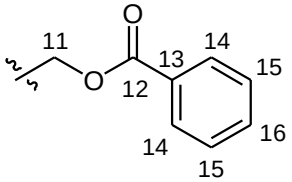	97B-ii	13	5.52 (H-11), 7.47 (H-15), 7.58 (H-16), 8.09 (H-14)	$[M+H]^{+}$ 323.0590
3	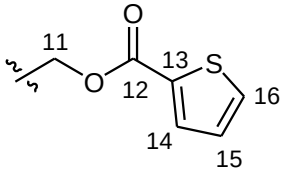	97B-iii	37	5.22 (H-11), 7.14 (H-15), 7.62 (H-16), 7.89 (H-14)	$[M+H]^{+}$ 329.0156
4	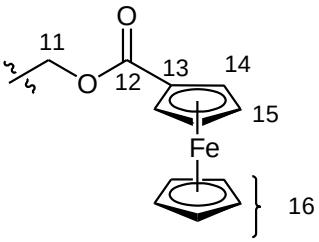	97B-iv	43	4.26 (H-16), 4.45 (H-15), 4.88 (H-14), 5.14 (H-11)	$[M+H]^{+}$ 432.0255

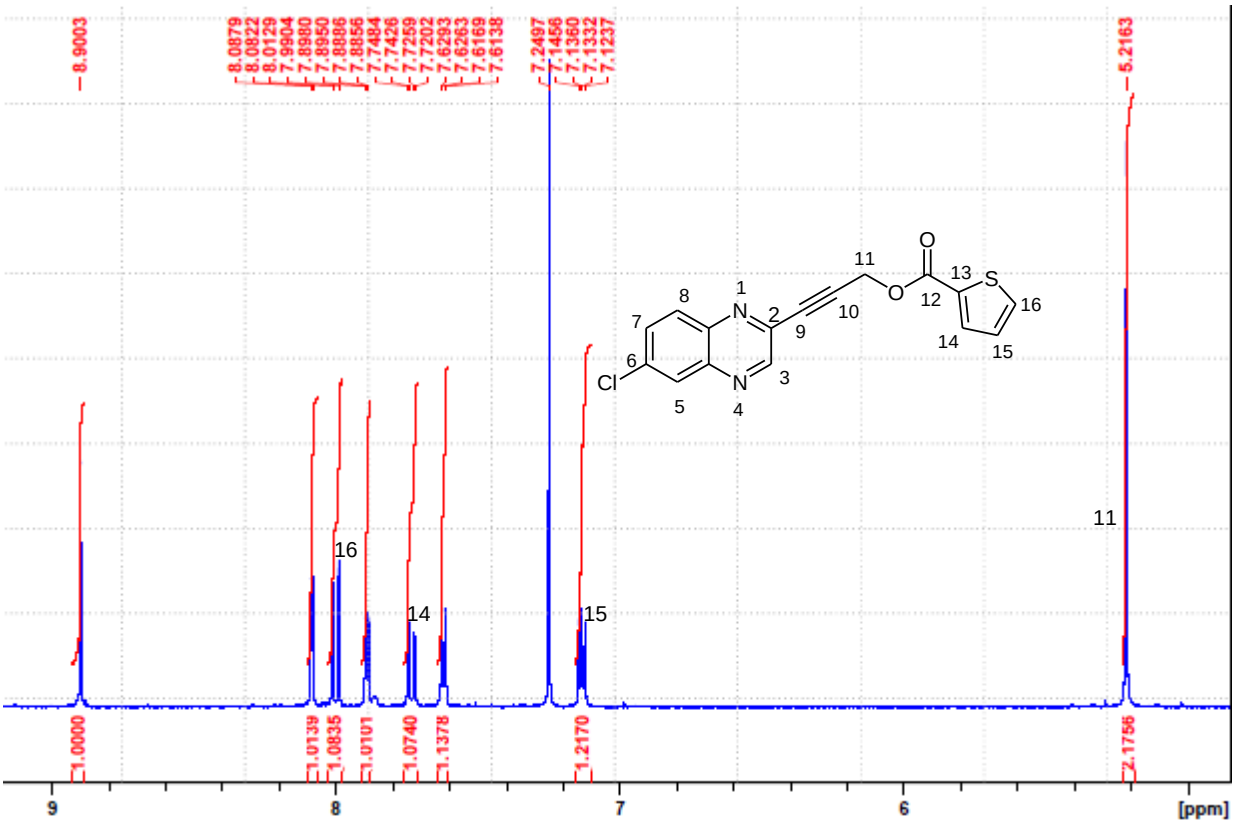

Figure 33: ^{1}H-NMR 3-(6-chloroquinoxalin-2-yl)prop-2-ynyl thiophene-2-carboxylate **97B-iii**.

Similarly, a 6-chloroquinoxaline ester derivative incorporated with a ferrocenyl moiety was successfully synthesised and was isolated in 43% yield. The ^{1}H-NMR spectrum of 3-(6-chloroquinoxalin-2-yl)prop-2-ynyl ferrocetate **97B-iv (Figure 34)**, showed a similar trend where protons at *C*-11 are now appearing at 5.14 ppm. Furthermore, the proton on the ferrocenyl moiety resonated at 4.26, 4.45 and 4.88 which appeared as a singlet and two triplet peaks integrating for 5:2:2 protons, respectively. From ^{13}C-NMR spectrum (**Figure 35)**, signals due to the ferrocenyl moiety are observed at 69.5 – 71.8 ppm and signal due to the carbonyl carbon at C-12 resonating at 171.1 ppm. In addition, a carbonyl signal due to the formation of an ester was observed at 1712 cm^{-1} on FT-IR spectrum. The mass spectrum of **97B-iv** showed $[M+H]^{+}$ peak of m/z 431.0255 and the appearance of M+2 peak showing m/z 433.0231 due to the chlorine isotope at *C*-6 was observed.

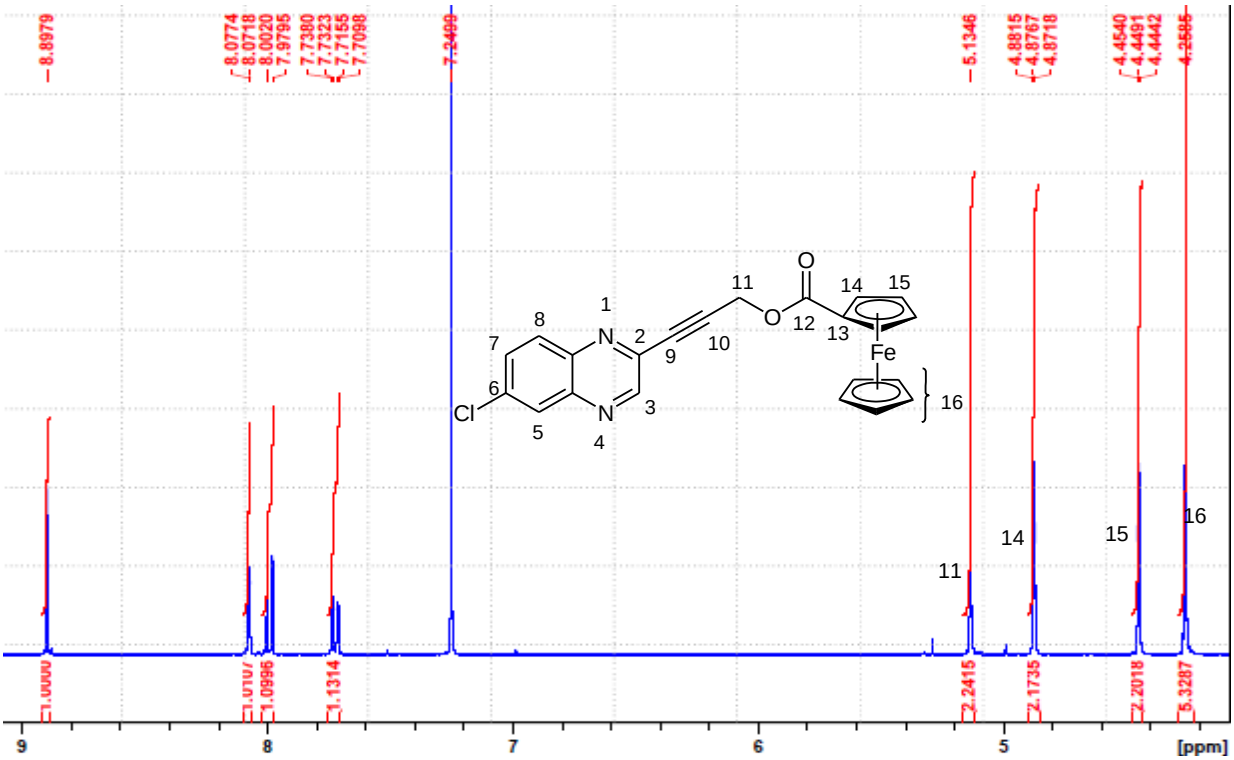

Figure 34: ^{1}H-NMR spectrum of 3-(6-chloroquinoxalin-2-yl)prop-2-ynyl ferrocetate **97B-iv**.

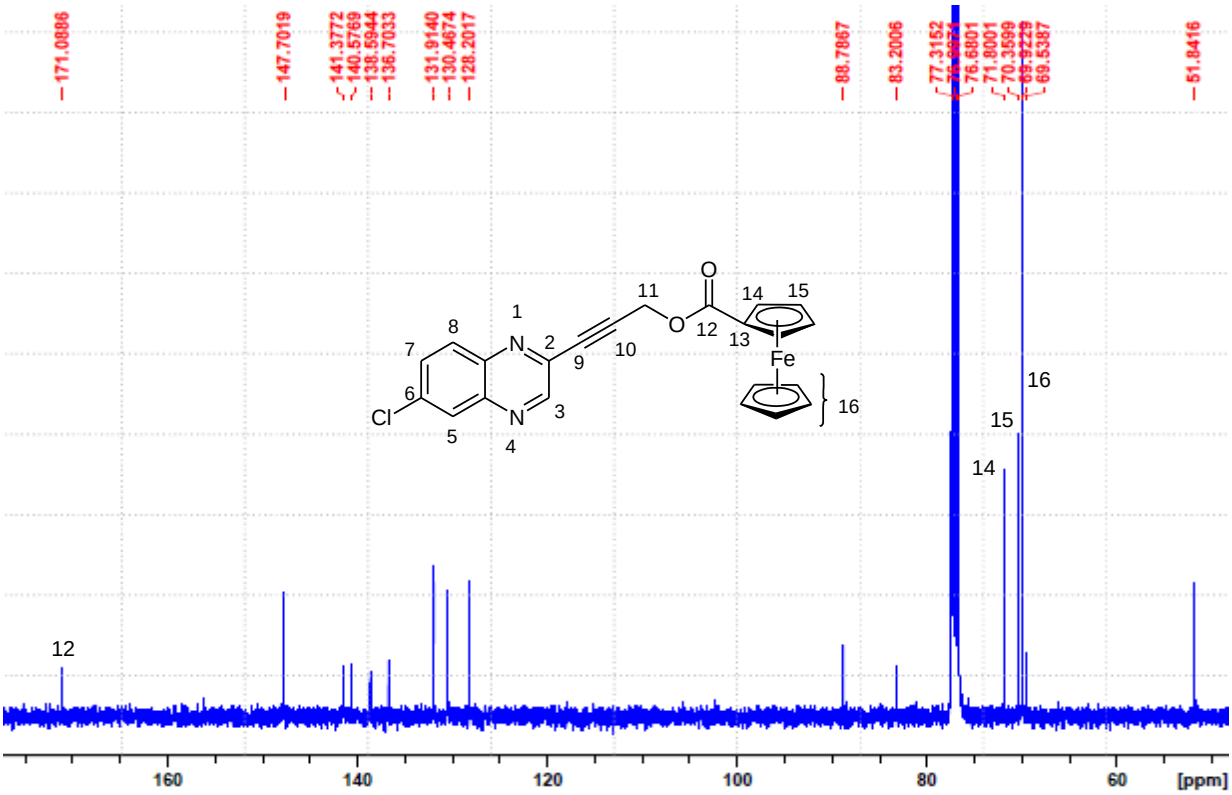

Figure 35: ^{13}C-NMR spectrum of 3-(6-chloroquinoxalin-2-yl)prop-2-ynyl ferrocetate **97B-iv**.

2.3. Synthesis of quinoxaline-ferrocene compound via esterification of 2-methyl-4-(quinoxalin-3-yl)but-3-yn-2-ol 86C (Method E)

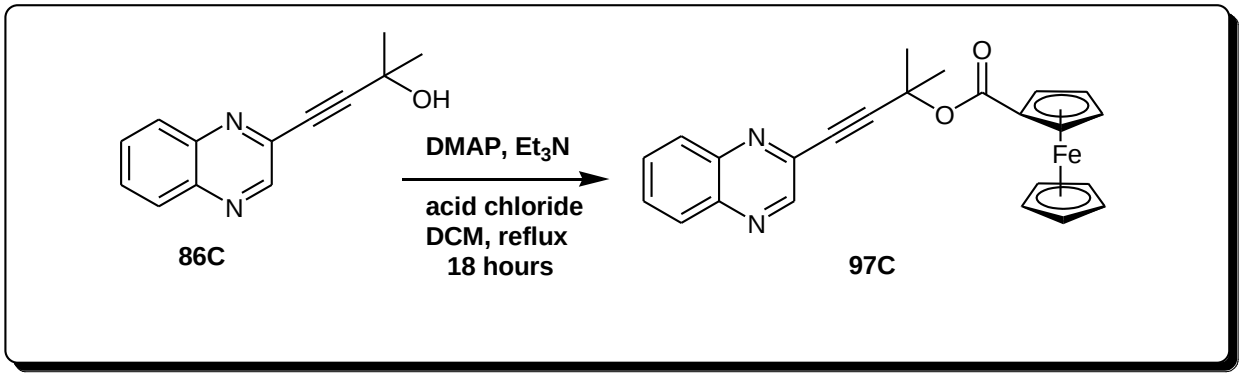

Scheme 10: Synthesis of 4-(quinoxalin-2-yl)-2-methylbut-3-ynyl ferrocetace **97C**.

In an attempt to introduce a ferrocenyl group on 2-methyl-4-(quinoxalin-3-yl)but-3-yn-2-ol **86C** following reaction conditions as described for synthesis **97A-iv**, the reaction was unsuccessful. Instead, we isolated the starting material **86C** and ferrocenoyl chloride. The reaction was again attempted at an elevated temperature (40 ºC) in the presence of DMAP (10 mol%), ferrocenoyl chloride (1 equiv.) and Et_3N (3 equiv.) in DCM. Following this reaction conditions a trace amount of 4-(quinoxalin-2-yl)-2-methylbut-3-yn-2-ol ferrocetate **97C** with unreacted starting materials were isolated. The formation of 4-(quinoxalin-2-yl)-2-methylbut-3-yn-2-ol ferrocetate **97C** was confirmed by a new singlet peak which integrated for six protons attached to the two methyl groups which showed a downfield shift from 1.66 ppm to 1.99 ppm. This was due to the influence of an electron withdrawing ferrocenoyl group introduced to the molecule. Furthermore, the protons due to the ferrocenyl moiety were observed at a range of 4.26 to 4.82 ppm. Protons at 4.40 and 4.82 ppm appeared as triplets which integrated for 2:2 protons, respectively. In addition, a singlet resonating at 4.26 ppm integrating for five protons on the lower cyclopentadienyl ring was observed. The difference in reactivity of **86A** and **86C** arose due to the 2 methyl groups in **86C**, which renders the position of the alcohol to be more substituted and less accessible.

2.4. Synthesis of 3-chloroquinoxaline-2-carbonyl derivatives

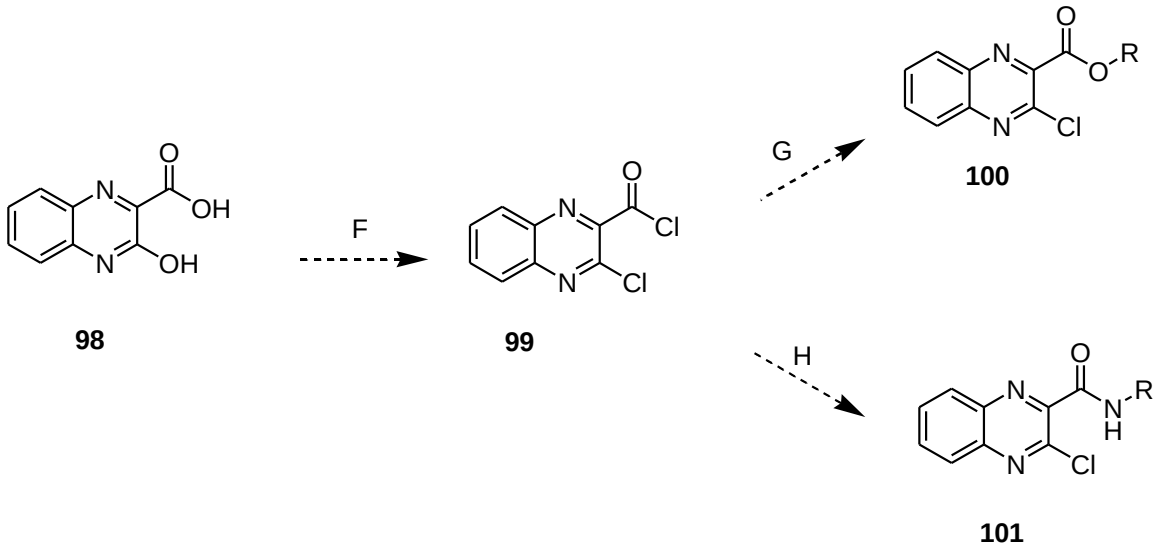

Scheme 11: General synthesis of 3-chloroquinixaline-2-carbonyl derivatives. (F) Chlorination, (G) esterification and (H) amidation.

3-hydroxyquinoxaline-2-carboxylic acid **98** presented an alternative to link quinoxaline-ferrocene compounds in which the quinoxaline can be introduced as an electrophile. A series of 3-chloroquinoxaline-2-carbonyl derivatives were obtained by firstly converting the carbonyl carbon at *C*-9 of 3-hydroxyquinoxaline-2-carboxylic acid **98** into a good electrophile suitable for esterification and amination reactions (**Scheme 11)**. Therefore, 3-chloroquinoxaline-2-carbonyl chloride **99** was synthesised by treating **98** with excess $SOCl_2$ and DMF [13]. Compound **99** was obtained in 93% yield and confirmed on ^{1}H-NMR spectrum (**Figure 36)** described as follows; the protons on the benzene ring are observed at 7.91 – 8.26 ppm. Signals appear as two multiplet and doublets integrating for 1:1:1:1 protons at *C*- 5 to *C*– 8. On the FT-IR a carbonyl stretch resonating at 1770 cm^{-1} due to the carbonyl carbon (*C*-9) was observed. The mass spectrum of **99** showed M-(-COCl) peak of m/z 163.0064 as a result of decarboxylation of the acid at *C*-2 while a calculated m/z 226.9701 was not observed. Furthermore, the appearance of M+2 peak showing 165.0034 due to the chlorine isotope at *C*-3 was observed.

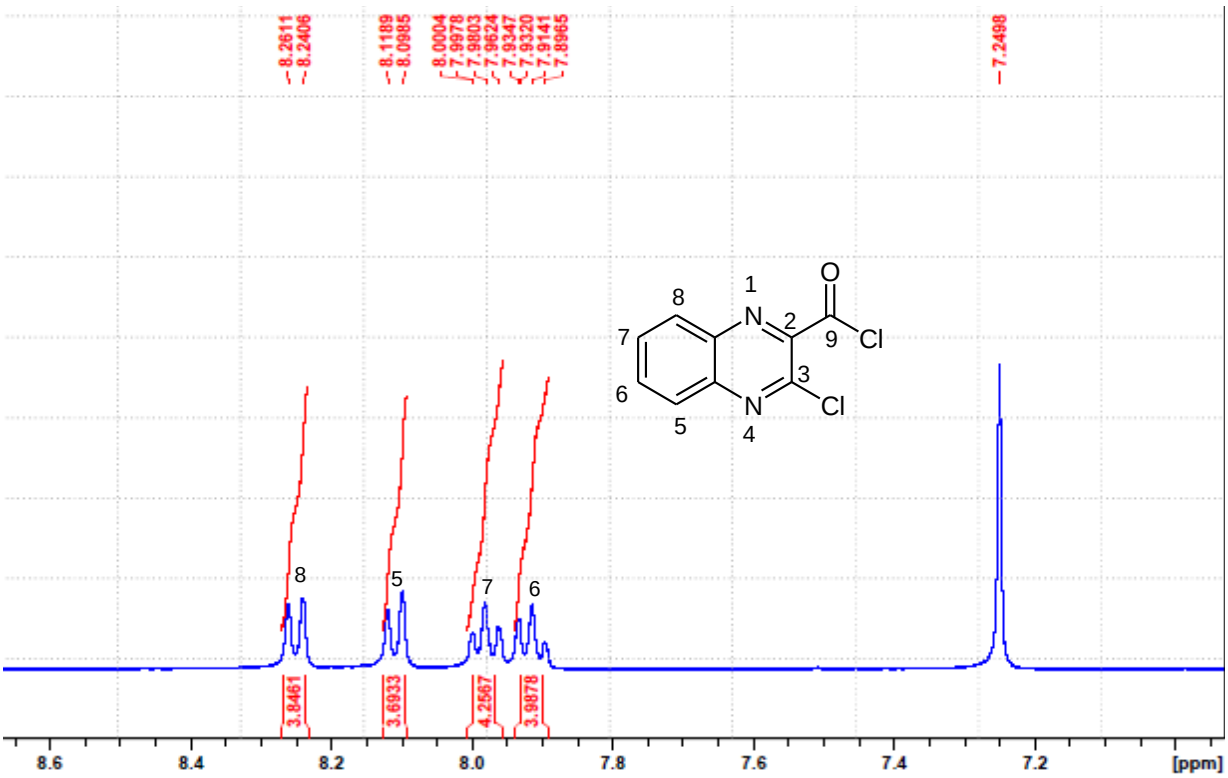

Figure 36: ^{1}H-NMR spectrum of 3-chloroquinoxaline-2-carbonyl chloride **99**.

2.4.1 Synthesis of 3-chloroquinoxaline-2-carbonyl ester derivatives (Method G)

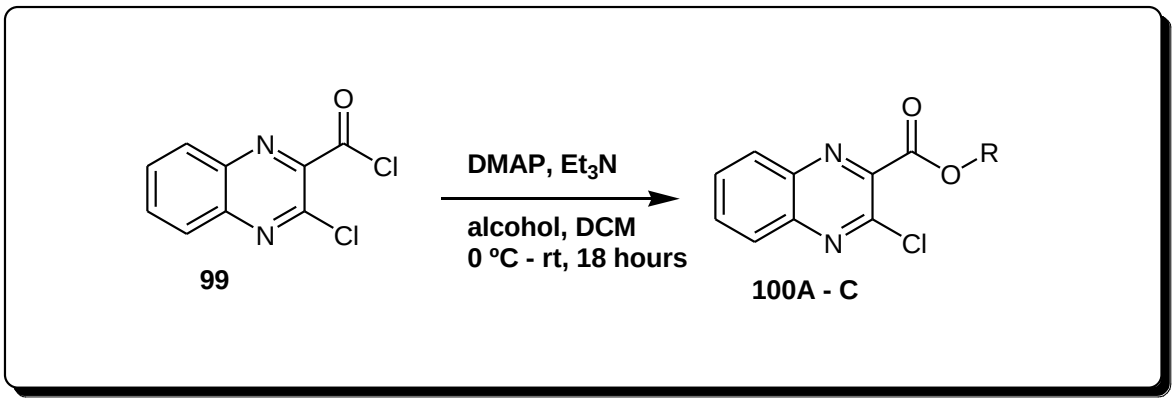

Scheme 12: Synthesis of 3-chloroquinoxaline-2-carbonyl ester derivatives **100A - C**.

The ester derivatives were obtained following a literature procedure [14] described as follows, **99** was treated with DMAP (10 mol %), an alcohol (1.1 equiv.) and Et_3N (3 equiv.) and stirred for 18 hours at room temperature under nitrogen atmosphere. The compounds **100A – C** were obtained in percentage yield of 30 – 78%. While varying the alcohol derivatives, we observed that an ester with propargyl alcohol was obtained in good yield (78%) followed by phenol (63%) and then propan-2-ol (30%). The reactivity of alcohols is influenced by the groups bonded close to the carbon with an alcohol. The formation of these compounds was confirmed by ^{1}H-NMR, ^{13}C-NMR and FTIR. The ^{1}H-NMR spectrum (**Figure 37)** of **100A** showed the presence of 5 protons from the phenol substituent appearing as two multiplet peaks resonating at 7.34 – 7.48 ppm. Furthermore, protons on the benzene ring of the quinoxaline moiety were observed in the range 7.89 – 8.25 ppm. From the ^{13}C-NMR spectrum **Figure 38**, a signal due to the carbonyl carbon at *C*-9 was observed at 162.2 ppm. In addition, a carbonyl stretch due to the carbon at *C*-9 was observed as 1724 cm^{-1} on FT-IR**.** The mass spectrum of compound showed $[M+H]^+$ peak of m/z 285.0415 and the appearance of M+2 peak showing m/z 287.0300 due to the chlorine isotope at *C*-3 was observed.

Table 4: Summary of 3-chloroquinoxaline-2-carbonyl ester derivatives.

Entry	R- component	Product	% Yield	^{1}H-NMR (δ ppm) R-component	Ms (m/z)
1	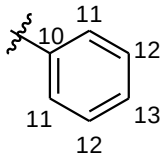	100A	67	7.34 (H_{12-13}), 7.84 (H_{14})	$[M+H]^{+}$ 285.0415
2	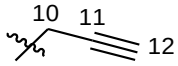	100B	78	2.61 (H_{12}), 5.08 (H_{10})	$[M+Na]^{+}$ 269.0140
3	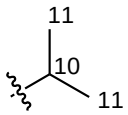	100C	30	1.46 (H_{11}), 5.43 (H_{10})	$[M+Na]^{+}$ 273.0408

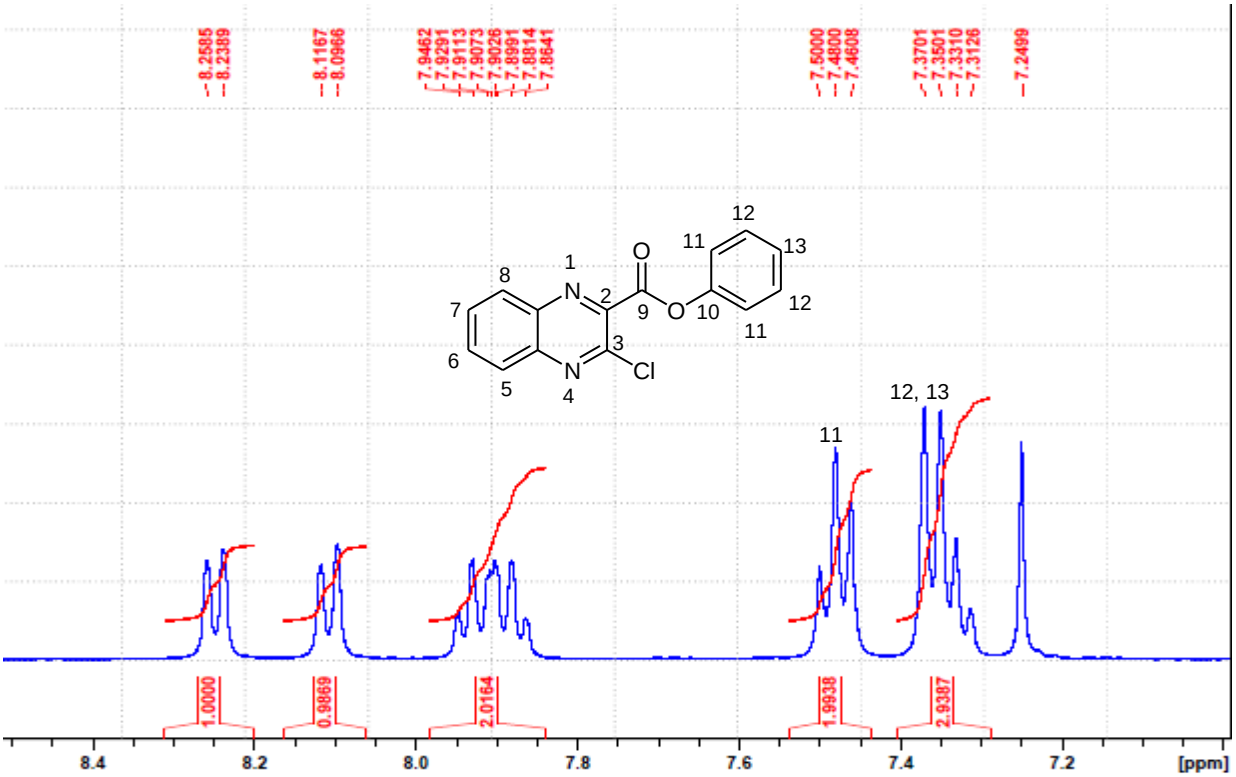

Figure 37: ^{1}H-NMR spectrum of phenyl 3-chloroquinoxaline-2-carboxylate **100A**.

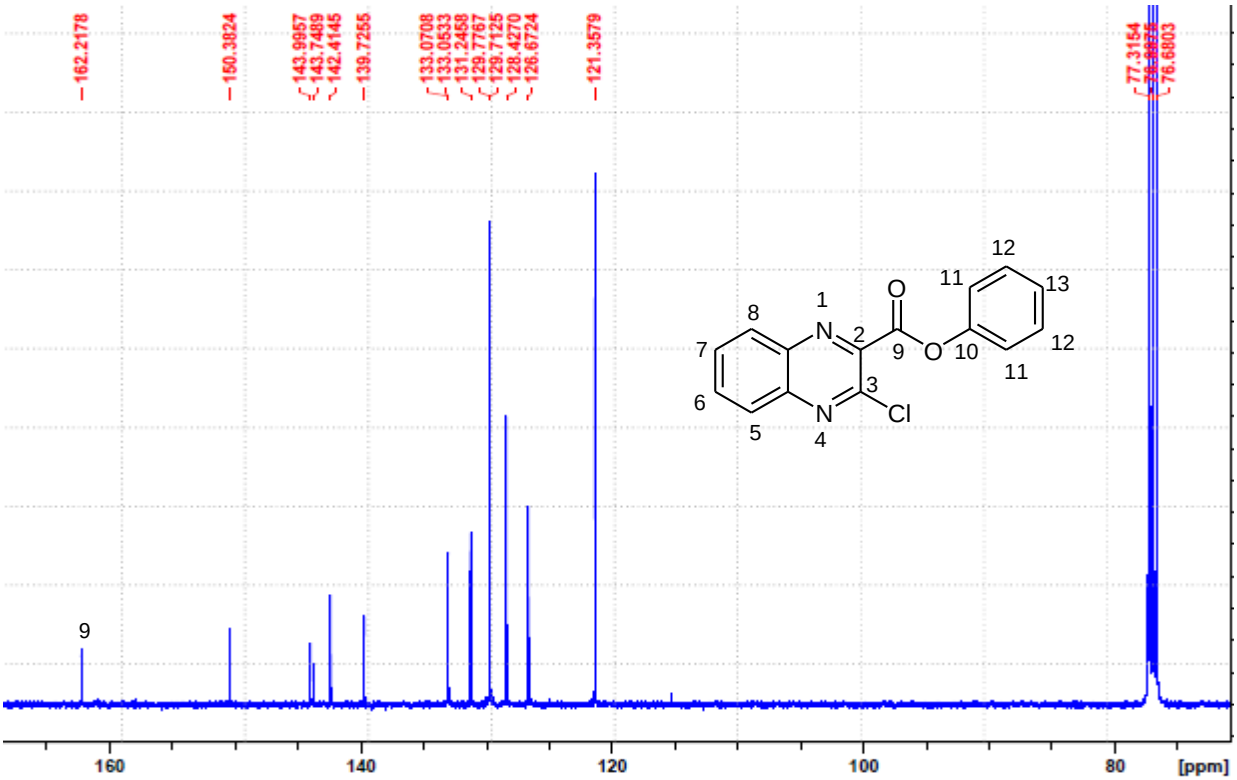

Figure 38: ^{13}C-NMR spectrum of phenyl 3-chloroquinoxaline-2-carboxylate **100A**.

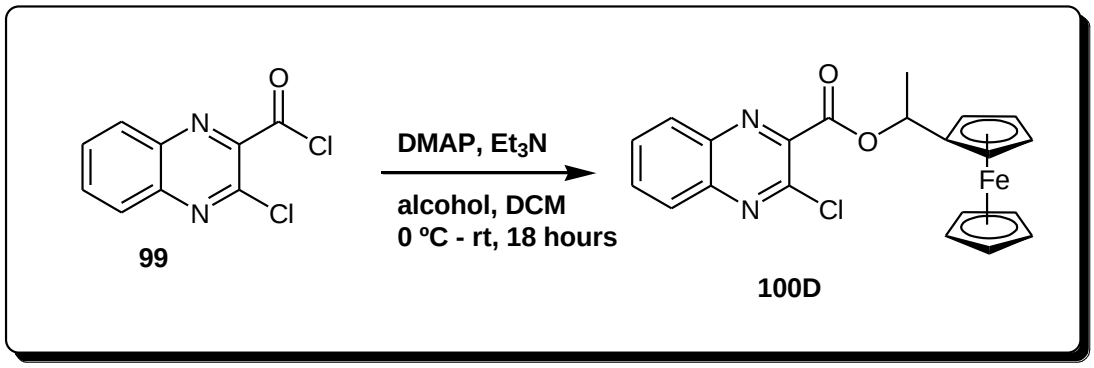

Scheme 13: Synthesis of quinoxaline-ferrocene compounds via esterification (Method G).

In an attempt to introduce a ferrocenyl alcohol on 3-chloroquinoxaline-2-carbonyl chloride **99** following reaction conditions as **100A – C**, a trace amount of the product with unreacted starting material **99** and ferrocenyl alcohol were observed. The crude product

was purified on prep TLC using 30% ethyl acetate/ hexane and we isolated only the above mentioned starting material. The reaction was again attempted using different reaction conditions, thereby employing NaH as a base to first deprotonate the alcohol and treat it with **99**. However, only a trace amount of the product was observed following this reaction conditions. Furthermore, the starting materials were isolated after purification and no trace of the product was isolated. This led to the suggestion that the product hydrolyses back to the starting material during purification. Furthermore, the reaction was attempted by first treating **99** with DMAP (10 mol%) to generate a more electrophilic intermediate while treating the ferrocenyl alcohol with NaH to generate an alkoxide in a separate flask. The two separate mixtures were combined and stirred overnight. However the reaction was unsuccessful.

2.4.2 Synthesis of 3-chloroquinoxaline-2-carbonyl amide derivatives (Method H)

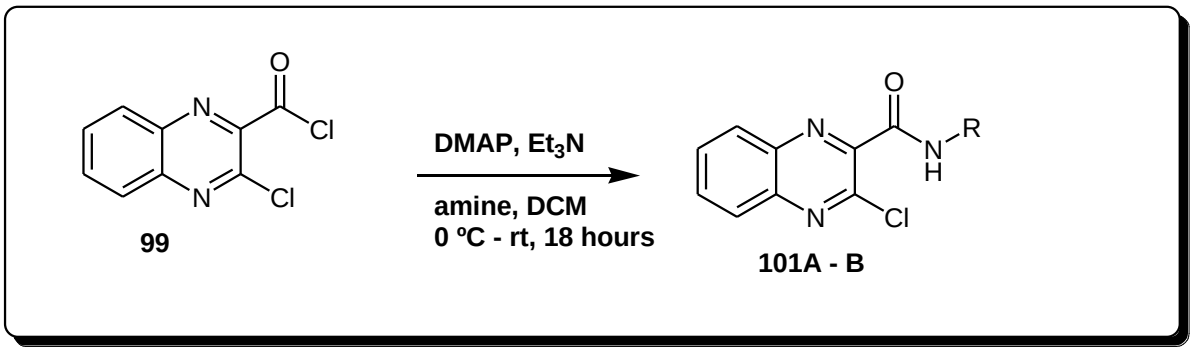

Scheme 14: 3-chloroquinoxaline-2-carbonyl amide derivatives **101A - B**.

The amide derivatives **101A - B** were successfully synthesised following a similar procedure as described for the synthesis ester derivatives **100A - C** while varying amine functionality. These compounds were obtained in yield of 43 – 53%. A signal due to N-H confirming the formation of **101A** was observed on ^{1}H-NMR (**Figure 39)** resonating at 9.44 ppm which appeared as a broad singlet. Furthermore, the methoxy protons are observed at 3.83 ppm as a singlet. Protons at C-12 and C-13 were observed at 6.94 and 7.71 ppm which appeared as doublets. The protons on the benzene ring of the quinoxaline moiety are observed at 7.90 – 8.17 ppm. From ^{13}C-NMR spectrum (**Figure**

40), a signal due to the carbonyl at C-9 resonating at 159.6 was observed. FT-IR was also used for further confirmation of an amide which was observed as a broad stretch resonating at 3275 cm^{-1} (N-H). From the mass spectrum, $[M+H]^+$ peak showing m/z 314.0695 and the appearance of M+2 peak showing m/z 316. 0667 due to the chlorine isotope at *C*-3 was observed.

Table 5: Summary of 3-chloroquinoxaline-2-carbonyl amide derivatives.

Entry	R-component	Product	% Yield	^{1}H-NMR (δ ppm)	Ms (m/z)
1	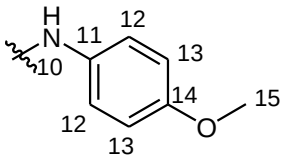	101A	53	3.83 (H_{15}), 6.94 (H_{13}), 7.71 (H_{12}), 9.44 (H_{10})	$[M+H]^+$ 314.0695
2	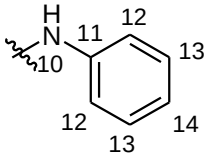	101B	43	7.20 (H_{14}), 7.28 (H_{13}), 7.79 (H_{12}), 9.57 (H_{10})	$[M+H]^+$ 284.0245

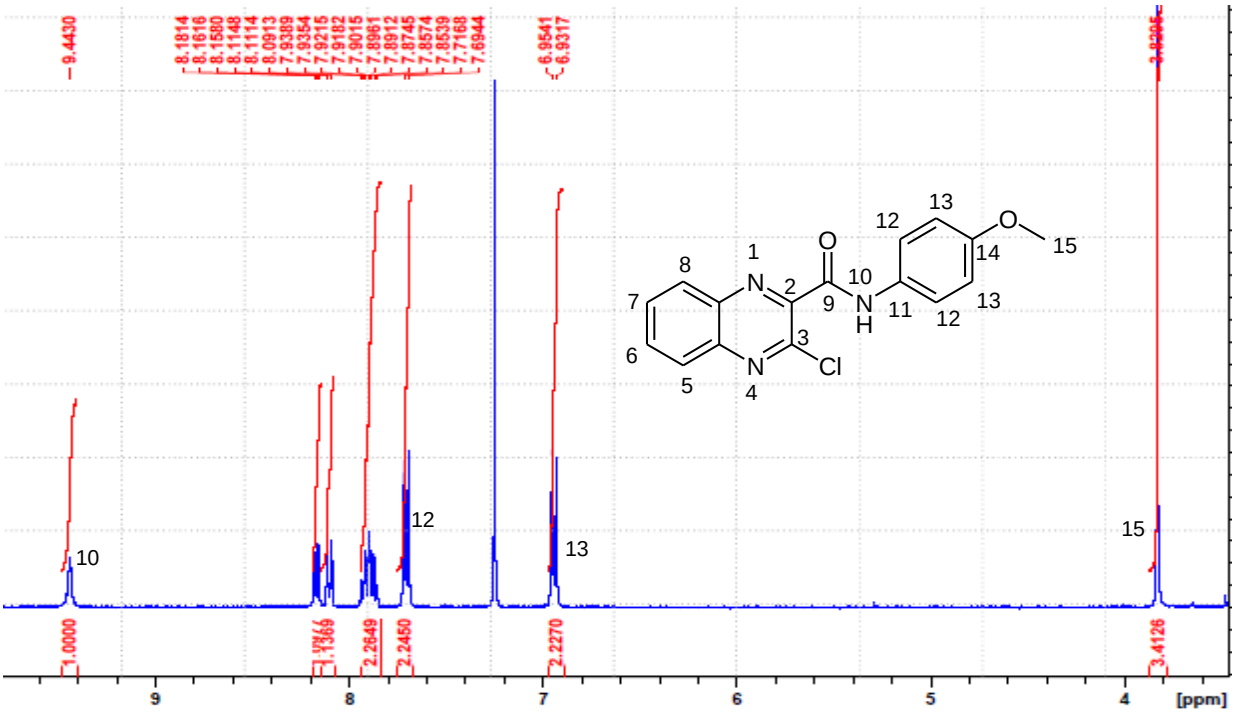

Figure 39: ^{1}H-NMR spectrum of 3-chloro-N-(4-methoxyphenyl)quinoxaline-2-carboxamide **101A.**

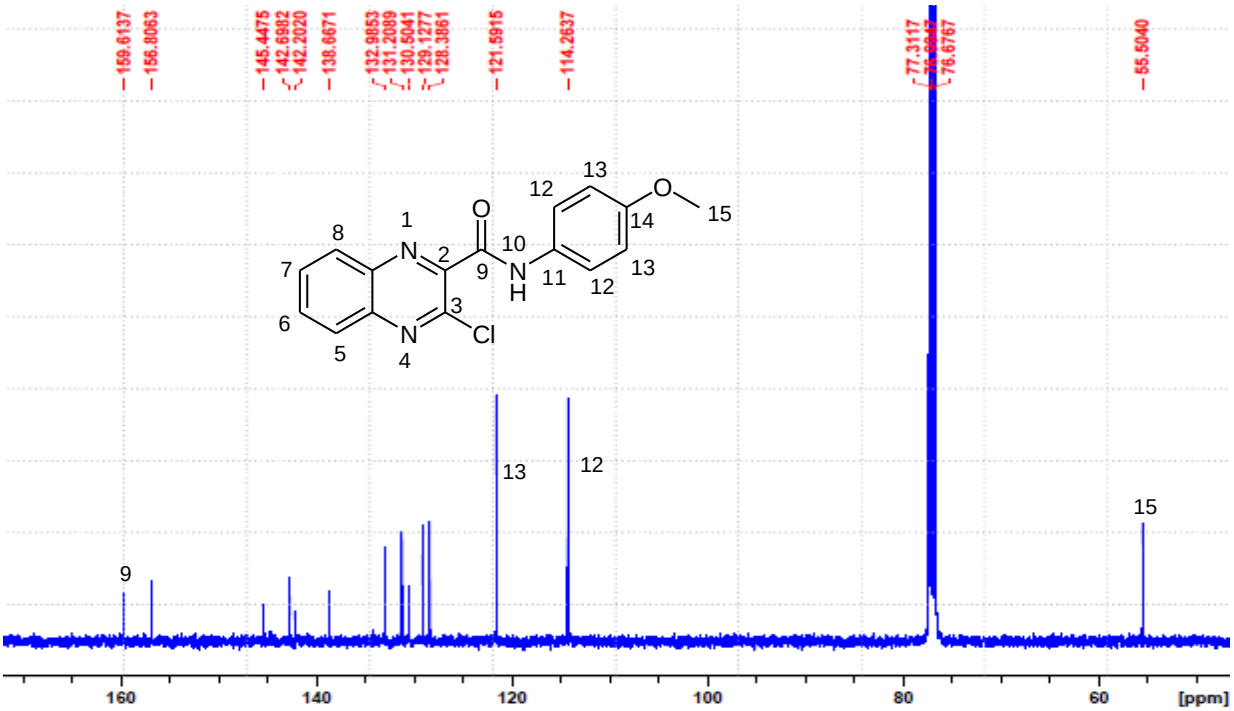

Figure 40: ^{13}C-NMR spectrum of 3-chloro-N-(4-methoxyphenyl)quinoxaline-2-carboxamide **101A**.

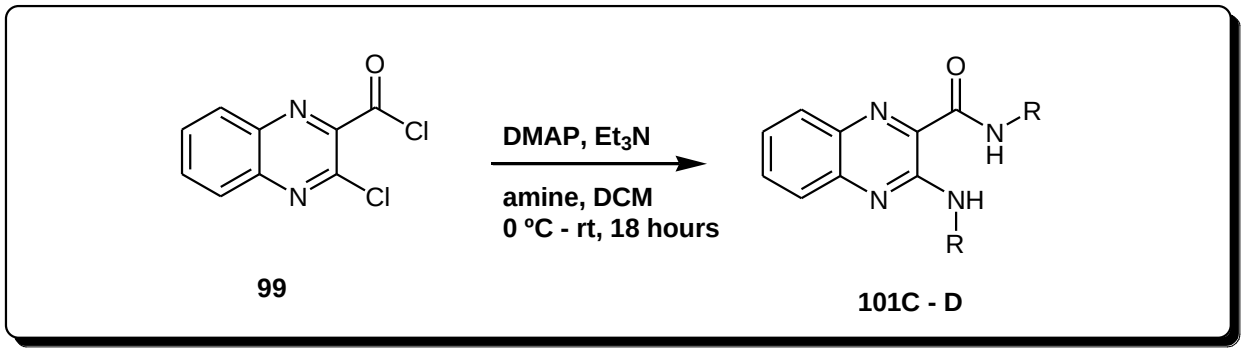

Scheme 15: Synthesis of 3-(amino)quinoxaline-2-carbonyl amide derivatives **101C – D**.

In an attempt to make more amide derivatives using different amine groups, 3-(amino)quinoxaline-2-carboxamide derivatives **101C - D** were obtained. During the reaction, we observed that di-substitution took place at *C*-9 and *C*-3 for compounds **101C** and **101D**. This is due to the electrophilic center at *C*-3. Therefore, there is competition

between the electrophilic center at *C*-9 and *C*-3. We expected the reaction to take place at *C*-9 since it is more electrophilic than *C*-3. As a result, 3-(amino)quinoxaline-2-carboxamide derivatives **101C – D** were isolated in 61 – 30% yield. From, the ^{1}H-NMR spectrum of **101C** (**Figure 41)**, we observed two sets of doublets resonating at 4.65 and 4.82 ppm integrating for protons at C-16 and C-11, respectively. Furthermore, signals due to N-H at position 16 and 10 are observed at 8.59 and 9.21 ppm as broad singlets. From ^{13}C-NMR spectrum (**Figure 42**), two signals resonating at 43.3 and 44.6 due to C-17 and C-11, respectively were observed. Furthermore, a signal due to a carbonyl carbon at *C*-9 resonating at 165.5 was observed. In addition, the amide protons (N-H) at position 10 and 16 were confirmed by FT-IR as it appears at 3364 cm^{-1} region showing broad signal. The mass spectrum of **101C** showed $[M+H]^{+}$ peak with m/z 369.1713.

The ^{1}H-NMR spectrum of **101D (Figure 43)**, showed a multiplet signal which integrated for 12 protons attached to the methyl groups at *C*-18 and *C*-27 which resonated at 1.39 ppm. A signal integrating for two protons at C-17 and C-26 appeared a septed resonating at 4.63 ppm was observed. Furthermore, the N-H signals at position 19 and 10 confirming the formation of the product were observed at 10.23 and 11.29 as broad singlets. In addition, the N-H stretch at 3340 cm^{-1} region was observed from the FT-IR. The mass spectrum of **101D** showed $[M+H]^{+}$ peak with m/z 457.2234.

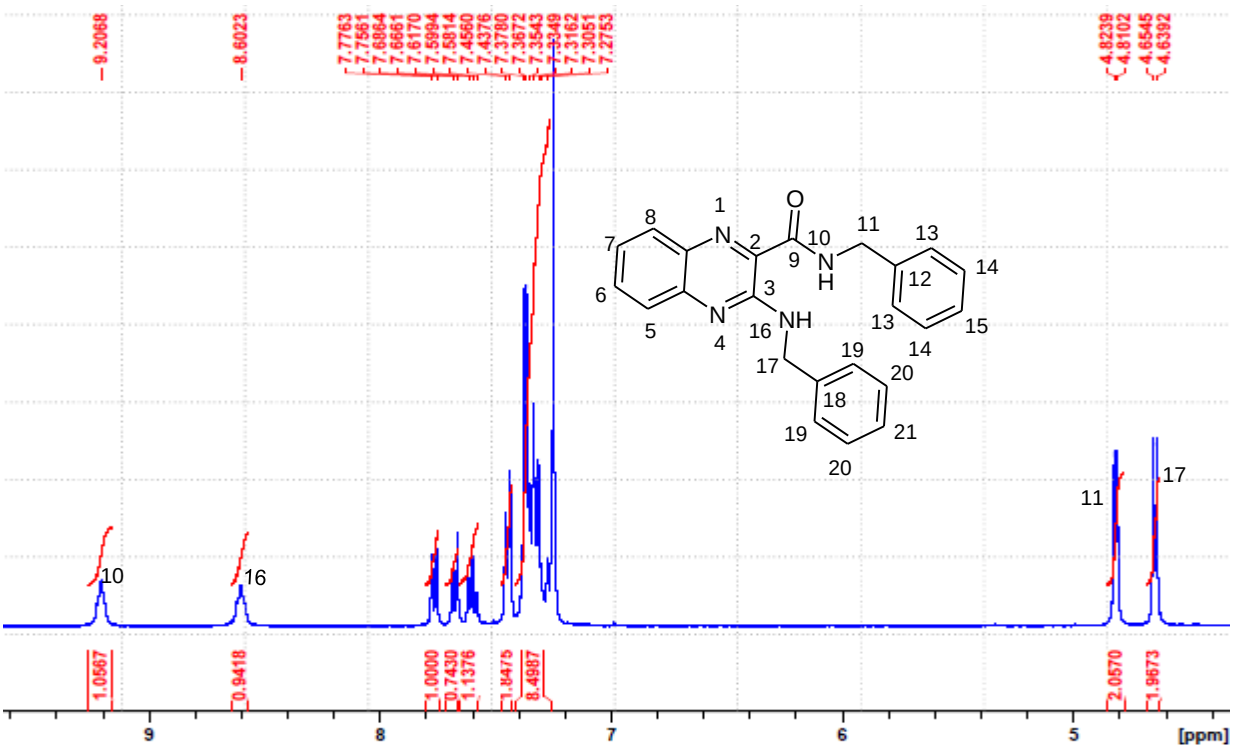

Figure 41: ^{1}H-NMR spectrum of N-benzyl-3-(benzylamino)quinoxaline-2-carboxamide **101C**.

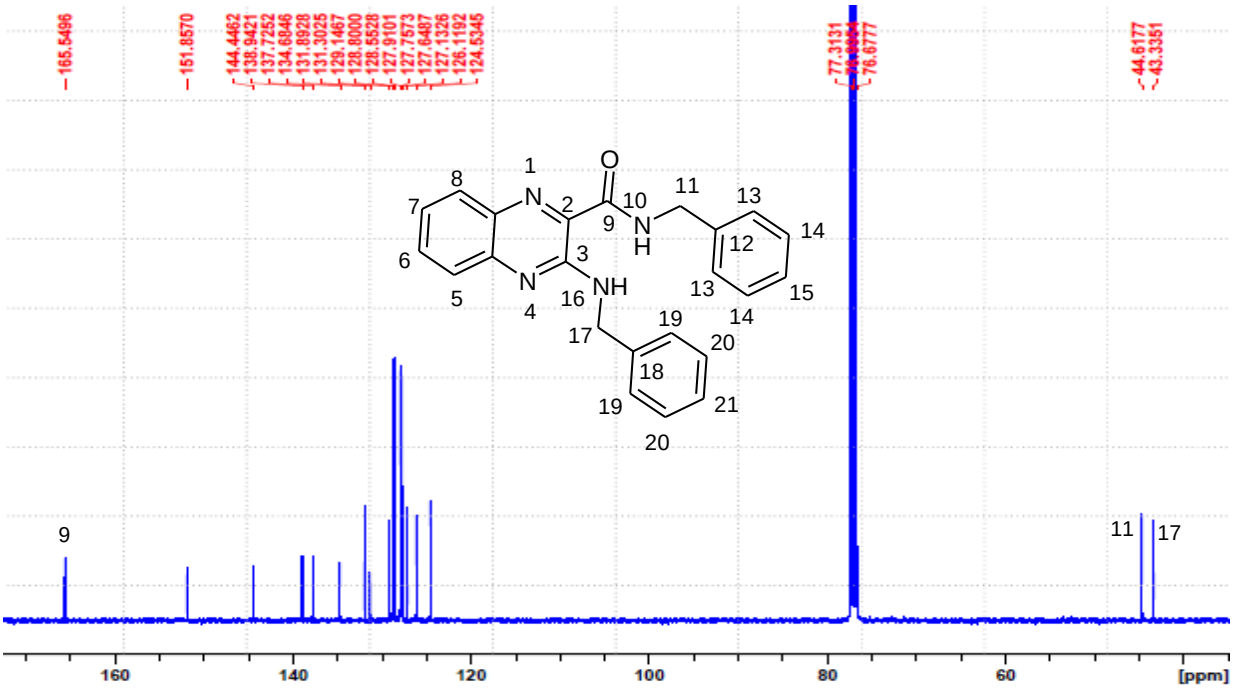

Figure 42: ^{13}C-NMR spectrum of N-benzyl-3-(benzylamino)quinoxaline-2-carboxamide **101C**.

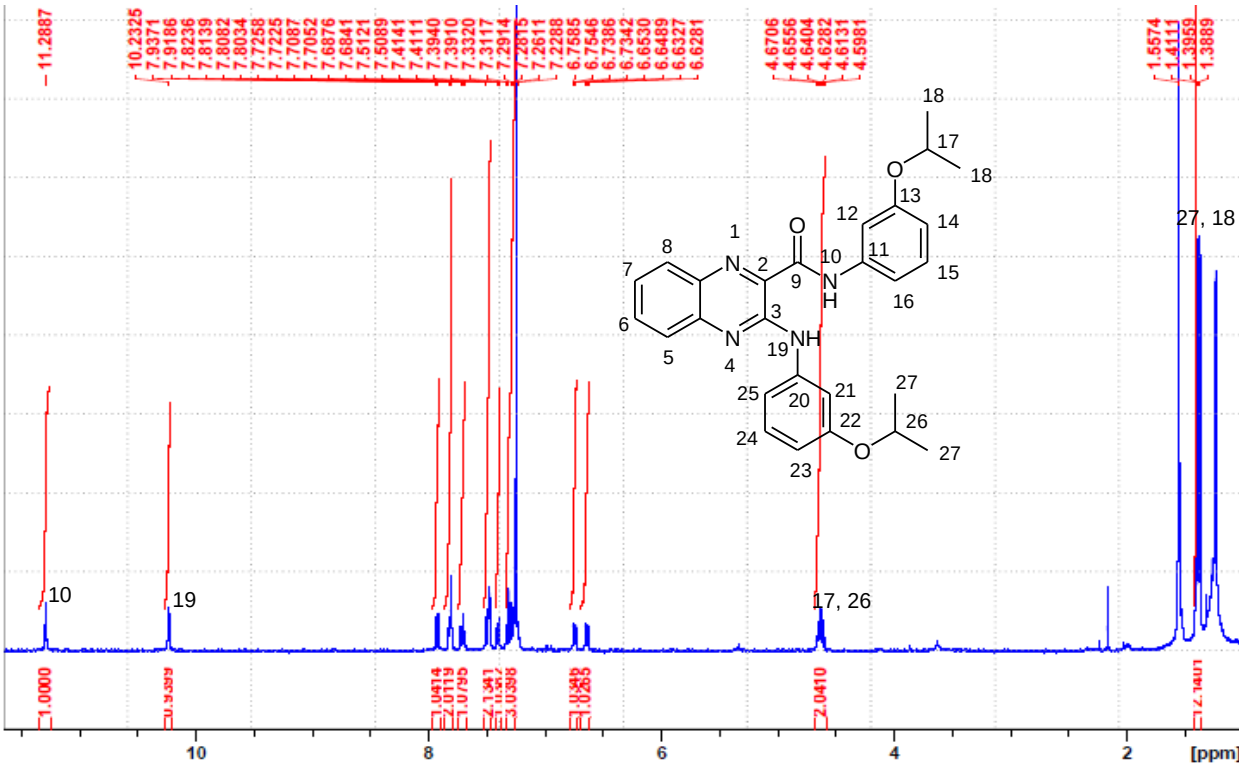

Figure 43: ^{1}H-NMR spectrum of 3-(3-isopropoxyphenylamino)-N-(3-isopropoxyphenyl)quinoxaline-2-carboxamide **101D**.

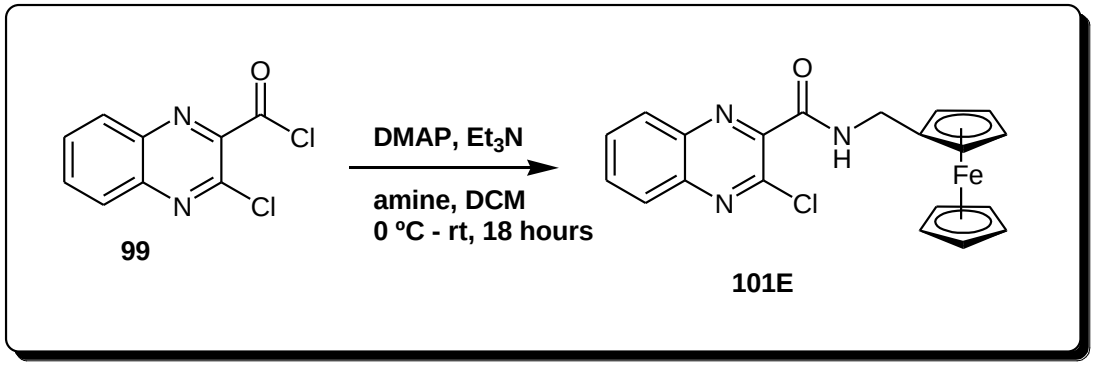

Scheme 16: Synthesis of quinoxaline-ferrocene via amidation reaction (Method H).

In an attempt to introduce a ferrocenyl group into 3-chloroquinoxaline-2-carbonyl chloride **99** via amidation reaction following reaction conditions described for synthesis of **101A - B**, a trace amount of the desired product with unreacted starting material **99** and

ferrocenyl amine were observed. The ^{1}H-NMR of the crude product showed a characteristic peak similar to the one observed in the formation of **101A – B**. A broad singlet resonating at 9.60 ppm due to the N-H proton signifying the formation of an amide was observed. Furthermore, peaks on the quinoxaline and ferrocene moiety signifying the formation of a new product were not properly observed. This is due to the presence of unreacted starting material overlapping with the desired product. However, during purification only the unreacted starting materials were isolated with no trace of the desired product. Similarly, purification of quinoxaline-ferrocene derivatives via esterification of 3-chloroquinoxaline-2-carbonyl chloride **99** yielded unreacted starting material. Due to unsuccessful attempts to introduce ferrocene as an alcohol or amine nuclephile to 3-chloroquinoxaline-2-carbonyl chloride **99** via esterification or amidation reaction, it was then concluded that ferrocene is a poor nucleophile.

2.5 Biological evaluation

In previous studies 3-(quinoxalin-3-yl)prop-2-yn-1-ol **86A** and 3-(6-chloroquinoxalin-3-yl)prop-2-yn-1-ol **86B** found to possess potential antimycobacterial properties with MIC_{90} of 52.77 and 1.63 µM, respectively [4, 5] . The structure activity relationship (SAR) on these compounds showed that introduction of an electron withdraw group (-Cl) at *C*-6 enhanced the antimycobacterial activity of quinoxaline moiety. The two quinoxaline derivatives (**86A** and **86B**) serves as a starting point for development of new quinoxaline derivatives. Therefore, a new series of quinoxaline derivatives developed in this study have been evaluated for their antimycobacterial activity while **86A** (LA-55), **86C** (LA-65C3), **87A** (LA-39B) and **90A** (LA-16) were amongst the first four compounds to be evaluated for anticancer activity.

2.5.1 *In-vitro* antimycobacterial properties of quinoxaline derivatives.

The *in-vitro* antimycobacterial activity of the synthesised compounds was performed at the drug discovery and development center (H3D), university of Cape Town. The preliminary results for *in-vitro* antimycobacterial activity was obtained following broth dilution method in 7H9 CAS GLU TX media. The compounds were assayed within a 14

day period using *Mtb* $H_{37}R_V$ strain with rifampicin as a reference drug. The biological experiments are reported as MIC_{90} and are summarised in **tables 6 - 11**. MIC_{90} is defined as the minimum inhibitory concentration of a compound that is required to inhibit 90% growth of the bacterium. A compound was considered inactive when it showed activity at a concentration >100 μM.

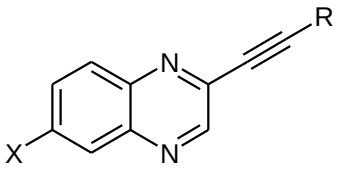

Table 6: Summary of quinoxaline alkynyl derivatives against *Mtb* $H_{37}R_V$ strain.

Entry	X-component	R-component	Product	MIC_{90} (μM) *Mtb* $H_{37}R_V$ strain
1	H-	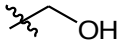	86A	52.77
2	Cl-	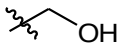	86B	1.63
3	H-	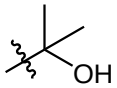	86C	>100
4	H-	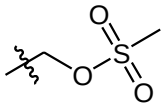	87A	6.47
5	Cl-	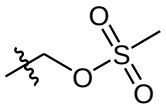	87B	54.50
6	H-		90A	4.55
7	Cl-		90B	1.13
8	H-	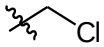	93A	68.58
9	Cl-	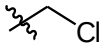	93B	31.88

Quinoxaline alkynyl alcohols (**86A** and **86B**) were found to possess antimycobacterial activity at MIC_{90} of 52.77 and 1.13 µM. However, compound **86C** with a terminal tertiary alcohol was found to exhibit poor antimycobacterial at MIC_{90} > 100 µM. The quinoxaline alkynyl derivatives obtained from **86A** exhibited excellent antimycobacterial activity with the mesylate and aldehyde derivatives showing activity at MIC_{90} of 6.47 and 4.35 µM, respectively. However, compound **93A** with a terminal chlorine atom at C-11 was found to exhibit activity at MIC_{90} of 68.58 µM which was found to be less active compared to the parent quinoxaline derivative **86A** with MIC_{90} of 52.77 µM.

On the other hand, 6-chloroquinoxaline alkynyl derivatives with a mesylate and chlorine atom at C-11 were found to exhibit activity at MIC_{90} of 54.50 and 31.88 µM, respectively. As a result, loss of activity from both compounds was observed. In addition, the terminal aldehyde **90B** exhibited excellent antimycobacterial activity at MIC_{90} of 1.13 µM. According to the results obtained compounds **87A, 90A, 90B** exhibited excellent activity at MIC_{90} <10 µM with compound **90B** showing the highest activity at MIC_{90} of 1.13 µM. Compound **90B** is a derivative of **86B** which exhibited antimycobacterial activity at MIC_{90} of 1.63 µM. It is worth noting that two of the three compounds are a derivative of 3-(quinoxalin-3-yl)prop-2-yn-1-ol **86A**.

While varying the influence of either hydrogen or chlorine atom at *C*-6 of the quinoxaline moiety, we observed that the presence of electron withdrawing group (Cl-) at *C*-11of both **93A** and **93B** exhibited loss of activity as compounds show MIC_{90} of 68.58 and 31.88 µM, respectively. However, the mesyl group introduced in compound **87A** showed an improved activity with MIC_{90} of 6.47 µM as compared to the loss of activity observed in compound **87B** with MIC_{90} of 54.50 µM.

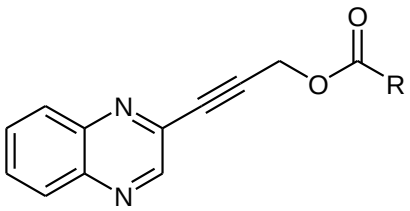

Table 7: Summary of 3-(quinoxalin-3-yl)prop-2-ynyl ester derivatives against *Mtb* $H_{37}R_V$ strain.

Entry	R-component	Product	MIC_{90} (µM) *Mtb* $H_{37}R_V$ strain
1		97A-i	18.05
2	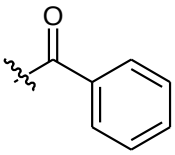	97A-ii	16.18
3	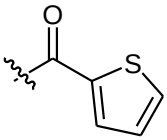	97A-iii	27.01
4	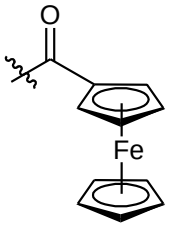	97A-iv	39.39

The ester derivatives obtained from **86A** exhibited potential antimycobacterial activity against *Mtb* $H_{37}R_V$ strain after 14 day period. All acetyl groups introduced to the quinoxaline moiety exhibited an improved activity at MIC_{90} values of 16.18 – 39.39 µM. within this series compounds **97A-i** and **97A-ii** were found with the highest activity at MIC_{90} of 18.05 and 16.18 µM, respectively. Introducing ferrocenyl groups into organic compounds has been reported to enhance the activity of the compounds. Therefore, introducing a ferrocenyl moiety into **86A** has shown potential to improve the antimycobacterial activity of quinoxaline moiety. Compound **97A-iv** was found to exhibit antimycobacterial activity at MIC_{90} of 39.39 µM which shows an improvement on the

quinoxaline moiety as compared to the parent quinoxaline derivative **86A** with MIC_{90} of 57 µM.

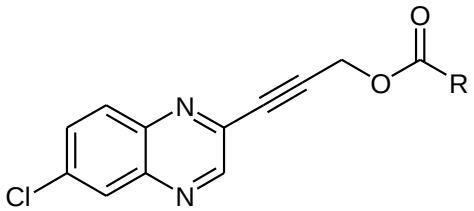

Table 8: Summary of the 6-chloroquinoxaline ester derivatives against *Mtb* $H_{37}R_V$ strain.

Entry	R-component	Product	MIC_{90} (µM) *Mtb* $H_{37}R_V$ strain
1		97B-i	62.31
2	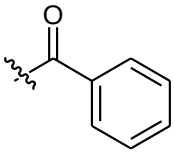	97B-ii	57.64
3	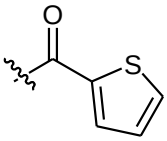	97B-iii	19.36
4	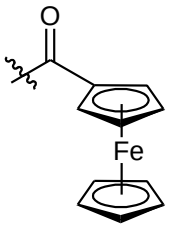	97B-iv	>100

The 6-chloroquinoxaline ester derivatives were found to exhibit loss of activity against *Mtb* $H_{37}R_V$ strain as compared to the parent quinoxaline derivatives **86B** which exhibited antimycobacterial activity at MIC_{90} of 1.63 µM. In addition, the 6-chloroquinoxaline derivative link with ferrocene **97B-iv** was found to be inactive against *Mtb* $H_{37}R_V$ strain. Compound **97B-iv** was found to exhibit poor antimycobacterial activity at MIC_{90} >100 µM. However, compound **97B-iii** was found to be most active amongst the 6-chloroquinoxaline ester derivatives with MIC_{90} of 19.36 µM. It is worth noting that ester

derivatives obtained from **86A** exhibited excellent activity as compared to 6-chloroquinoxaline ester derivatives which exhibited loss of activity. However, from the 6-chloro ester derivatives it was observed that compound **97B-iii** with a thiophenyl acetyl group exhibited excellent activity at MIC_{90} of 19.36 µM as compared to compound **97A-iii** with MIC_{90} of 27.01 µM.

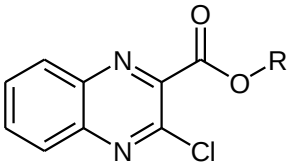

Table 9: Summary of 3-chloroquinoxaline-2-carbonyl ester derivatives against *Mtb* $H_{37}R_V$ strain.

Entry	R-component	Product	MIC_{90} (µM) *Mtb* $H_{37}R_V$ strain
1	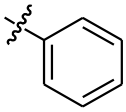	100A	>100
2	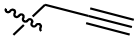	100B	>100
3		100C	>100

The 3-chloroquinoxaline-2-carbonyl ester derivatives **100A – B** were found to be inactive against *Mtb* $H_{37}R_V$ strain.

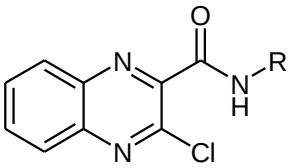

Table 10: Summary of 3-chloroquinoxaline-2-carbonyl amide derivatives against *Mtb* $H_{37}R_V$ strain

Entry	R-component	Product	MIC_{90} (µM) *Mtb* $H_{37}R_V$ strain

1	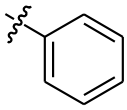	101A	>100
2	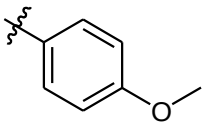	101B	40.66

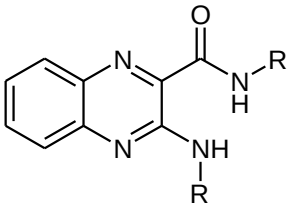

Table 11: Summary of 3-(amino)quinoxaline-2-carbonyl amide derivatives against *Mtb* $H_{37}R_V$ strain

Entry	R-component	Product	MIC_{90} (µM) *Mtb* $H_{37}R_V$ strain
1	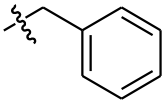	101C	>100
2	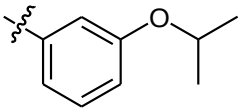	101D	>100

Similarly, both the 3-chloroquinoxaline-2-carbonyl amide derivatives **101A – B** and 3-(amino)quinoxaline-2-carbonyl amide derivatives **101C – D** in **table 10** and **11** were found to be inactive against *Mtb* $H_{37}R_V$ strain. Three of the amide derivatives were found to exhibit activity at MIC_{90} >100 µM. However, compound **101C** was found to exhibit activity at MIC_{90} of 40.66 µM.

2.5.2 *In-vitro* antiproliferative activity of quinoxaline derivatives against cancer cell lines

A preliminary study of antiproliferative activity was conducted on compounds **86A** (LA-55), **86C** (LA-65C3), **87A** (LA-39B) and **90A** (LA-16A). The *in-vitro* cell survival

experiment were performed at the University of Limpopo, Biochemistry Department against cervical cancer (HeLa), breast cancer (MCF-7), lung cancer (A549) and Raw 2647 cell lines using MTT assay with Actinomycin D used as a positive control. The preliminary data obtained is shown in **Figure 44.**

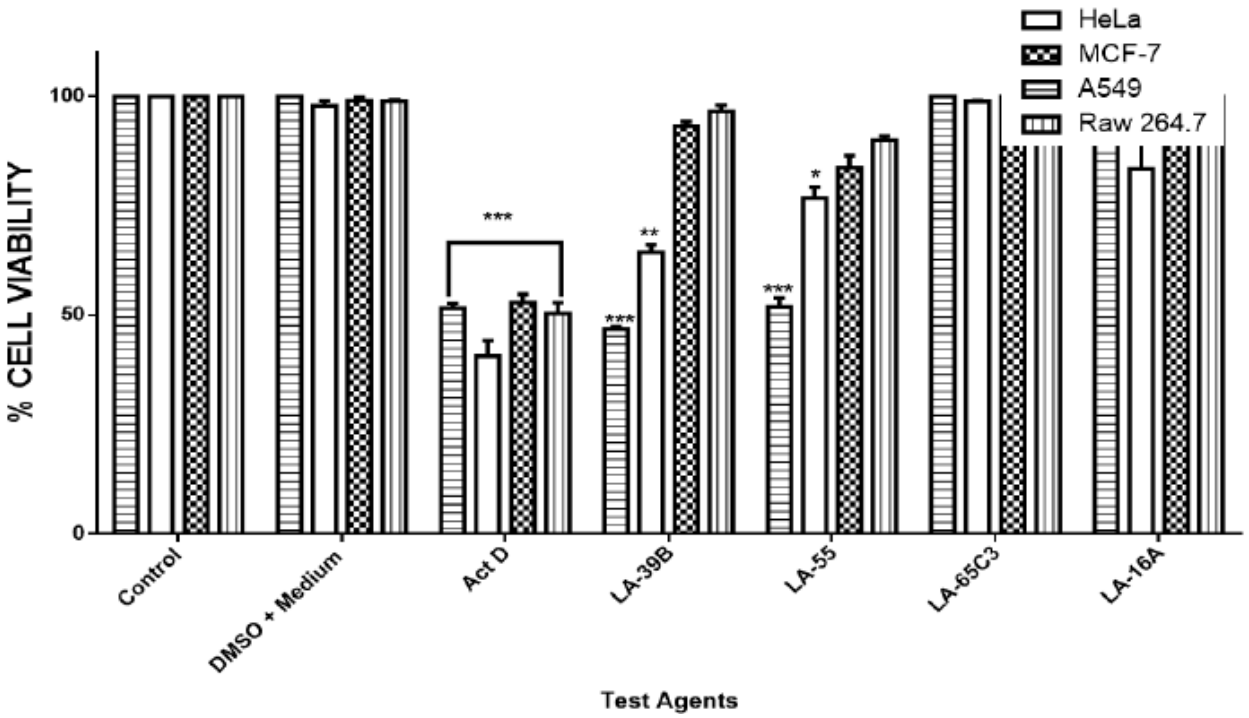

Figure 44: The comparative effect of quinoxaline derivatives on cell viability of HeLa, MCF-7, A549, and Raw 2647 cells at concentration of 25 µM.

Quinoxaline derivatives have been previously reported to play a significant role in cancer therapy [15, 16]. As a result, the presence of an alkynyl group on the quinoxaline moiety is reported to exhibit potential antiproliferative activity [16]. **Figure 44** shows the percentage viability of the four listed quinoxaline derivatives at concentration of 25 µM against the four cancer cell lines. According to the results obtained, the four quinoxaline alkynyl derivatives were found to be nontoxic against Raw 2647 cells. The results show a dose dependent inhibition of cell viability in the cancer cell lines. Compounds **86A** and **87A** were found to exhibit the highest viability-inhibition abilities in all cancer cell lines. Moreover, compounds **86A** and **87A** were found to exhibit potential antiproliferative

activity against A549 lung cancer cell lines as compare to compounds **86C** and **90A** which were found to be inactive against A549 and the three other cancer cell lines. In addition, among the four quinoxaline alkynyl derivatives **87A** was found to be the most active against A549 cell line showing 50% viability-inhibition at 25 µM [17].

References

[1] Nxumalo, W. and Dinsmore, A., 2013. Preparation of 6-ethynylpteridine derivatives by Sonogashira coupling. *Heterocycles: an International Journal for Reviews and Communications in Heterocyclic Chemistry*, *87*(1), pp.79-89.

[2] Ndlovu, N. and Nxumalo, W., 2016. Nucleophilic Substitution on 2-Monosubstituted Quinoxalines Giving 2, 3-Disubstituted Quinoxalines: Investigating the Effect of the 2-Substituent. *Molecules*, *21*(10), pp.1304.

[3] Nxumalo, W. and Dinsmore, A., 2013. Negishi coupling of pteridine-O-sulfonates. *South African Journal of Chemistry*, *66*(1), pp.42-46.

[4] Mokgoathana, H.D., 2015. Sonogashira coupling of quinoxaline-o-sulfonates leading to heterocyclic compounds with potential medicinal properties against TB (MSc dissertation). http://hdl.handle.net/10386/1633.

[5] Kang, F.A., Lanter, J.C., Cai, C., Sui, Z. and Murray, W.V., 2010. Direct dehydrative cross-coupling of tautomerizable heterocycles with alkynes via Pd/Cu-catalyzed phosphonium coupling. *Chemical Communications*, *46*(8), pp.1347-1349.

[6] Armengol, M. and Joule, J.A., 2001. Synthesis of thieno [2, 3-b] quinoxalines and pyrrolo [1, 2-a] quinoxalines from 2-haloquinoxalines. *Journal of the Chemical Society, Perkin Transactions 1*, (9), pp.978-984.

[7] Derosa, J., Cantu, A.L., Boulous, M.N., O'Duill, M.L., Turnbull, J.L., Liu, Z., De La Torre, D.M. and Engle, K.M., 2017. Palladium (II)-Catalyzed Directed anti-Hydrochlorination of Unactivated Alkynes with HCl. *Journal of the American Chemical Society*, *139*(14), pp.5183-5193.

[8] Alphonse, F.A., Karim, R., Cano-Soumillac, C., Hebray, M., Collison, D., Garner, C.D. and Joule, J.A., 2005. A bis (η5-cyclopentadienyl) cobalt complex of a bis-dithiolene: a chemical analogue of the metal centres of the DMSO reductase family of molybdenum and tungsten enzymes, in particular ferredoxin aldehyde oxidoreductase. *Tetrahedron*, *61*(46), pp.11010-11019.

[9] Naeimi, H., Safari, J. and Heidarnezhad, A., 2007. Synthesis of Schiff base ligands derived from condensation of salicylaldehyde derivatives and synthetic diamine. *Dyes and Pigments*, *73*(2), pp.251-253.

[13] Hati, S., Holzgrabe, U. and Sen, S., 2017. Oxidative dehydrogenation of CC and CN bonds: A convenient approach to access diverse (dihydro) heteroaromatic compounds. *Beilstein Journal of Organic Chemistry*, *13*, pp.1670-1692.

[14] Seitz, L.E., Suling, W.J. and Reynolds, R.C., 2002. Synthesis and antimycobacterial activity of pyrazine and quinoxaline derivatives. *Journal of Medicinal Chemistry*, *45*(25), pp.5604-5606.

[15] Gu, W., Wang, S., Jin, X., Zhang, Y., Hua, D., Miao, T., Tao, X. and Wang, S., 2017. Synthesis and evaluation of new quinoxaline derivatives of dehydroabietic acid as potential antitumor agents. *Molecules*, *22*(7), pp.1154.

[16] Hajri, M., Esteve, M.A., Khoumeri, O., Abderrahim, R., Terme, T., Montana, M. and Vanelle, P., 2016. Synthesis and evaluation of in vitro antiproliferative activity of new ethyl 3-(arylethynyl) quinoxaline-2-carboxylate and pyrido [4, 3-b] quinoxalin-1 (2H)-one derivatives. *European Journal of Medicinal Chemistry*, *124*, pp.959-966.

[17] Sibiya, M.A., Raphoko, L., Mangokoana, D., Makola, R., Nxumalo, W. and Matsebatlela, T.M., 2019. Induction of Cell Death in Human A549 Cells Using 3-(Quinoxaline-3-yl) Prop-2-ynyl Methanosulphonate and 3-(Quinoxaline-3-yl) Prop-2-yn-1-ol. *Molecules*, *24*(3), pp.407.

Chapter 3

3.1 Conclusion

Several reactions in an attempt to synthesise quinoxaline-ferrocene compounds via reductive amination (method A and B), etherification (method C) and esterification (method D) were unsuccessful. However, esterification reaction (method E) via nucleophillic substitution of quinoxaline alkynyl alcohols **86A** and **86B** were successful. As a result, a series of quinoxaline alkynyl ester derivatives together with two quinoxaline-ferrocene compounds were synthesised. The successfully synthesised compounds were evaluated for *in-vitro* antimycobacterial ativity against *Mtb* $H_{37}R_V$ strain.

The preliminary *in-vitro* antimycobacterial activity results obtained demonstrate quinoxaline derivatives with potent antimycobacterial activity. The quinoxaline alkynyl intermediates (**87 – 93**) were found to exhibit antimycobacterial activity at MIC_{90} ranging from 1.13 – 68.58 µM. Within this series, three of the eight intermediates exhibited excellent antimycobacterial activity at MIC_{90} < 10 µM, with compound **90B** showing the highest activity at MIC_{90} of 1.13 µM. In addition, the ester derivatives obtained from both **86A** and **86B** were found to exhibit potential antimycobacterial activity against *Mtb* $H_{37}R_V$ strain. Among the esters obtained, the 6-chloroquinoxaline ester derivatives were found to exhibit poor activity at MIC_{90} ranging from 19.36 – 63.31 µM as compared to the parent quinoxaline derivative **86B** with MIC_{90} of 1.16 µM. On the other hand, ester derivatives obtained from **86A** were found to exhibit promising activity at MIC_{90} ranging from 16.18 – 28.01 µM. Within the ester derivatives, three compounds were found to exhibit antimycobacterial activity at MIC_{90} < 20 µM with compound **97A-ii** showing the highest activity at MIC_{90} of 16.18 µM, followed by **97A-i** and **97B-iii** showing MIC_{90} of 18.05 and 19.36 µM, respectively. Consequently, the two quinoxaline-ferrocene ester derivatives obtained within this series were found to exhibit antimyocobacterial activity against Mtb $H_{37}R_V$ strain. However, compound **97B-iv** was found to be inactive against *Mtb* $H_{37}R_V$ strain as it showed MIC_{90} > 100 µM. On the other hand, compound **97A-iv** was found to exhibit an improved antimycobacterial activity at MIC_{90} of 39.39 µM as compared to the parent quinoxaline derivative **86A** with MIC_{90} of 57.22 µM. The 3-chloroquinoxaline-2-

carbonyl ester and amide derivatives were found to be inactive against *Mtb* $H_{37}R_V$ strain. This compounds were found to exhibit antimycobacterial activity at MIC_{90} > 100 µM therefore regarded as inactive. However, compound **101C** a 3-(amino)quinoxaline-2-carbonyl amide derivative was found to possess antimycobacterial activity at MIC_{90} of 40.66 µM.

The preliminary *in-vitro* antiproliferative activity of compounds **86A**, **86C**, **87A** and **90A** demonstrated the potential of quinoxaline as anticancer agents. The four quinoxaline derivatives were found to be nontoxic against Raw 2647 cell lines. In addition compounds, **86A** and **87A** were found to exhibit excellent antiproliferative activity against lung cancer cell lines. It is worth noting that, compound **86A** and **87A** exhibited promising antimycobaterial and antiproliferative activity. This shows that quinoxaline derivatives are multifaceted and serve as potential antitubercular and anticancer agents.

3.2 Future work.

In future, evaluation for *in-vitro* antiproliferative activity against cancer cell lines for **86B**, **87B**, **90B**, **93A – B**, **97A – B**, **100A – C** and **101A – D** will be performed. In addition, compounds showing promising antimycobacterial and antiproliferative activity will be evaluated for cytotoxicity to determine the safety of the compounds. The alkynyl moiety observed between *C*-9 and *C*-10 of quinoxaline alkynyl derivatives can be explored for activity against *Mtb* $H_{37}R_V$ strain, by reducing the alkynyl bond to an alkene. Furthermore, new derivatives containing electron withdrawing groups (F, Br and NO_2) at *C*-6 can be explored for antimycobacterial activity against *Mtb* $H_{37}R_V$ strain.

Chapter 4

4. Experimental procedures

4.1 General information

Commercially available reagents and solvents were purchased from Sigma Aldrich and Merck (South Africa). All chemicals were used as received, unless otherwise stated. Tetrahydrofuran (THF) was distilled over sodium metal lumps and benzophenone under nitrogen atmosphere before use. The structural properties of the compounds were recorded and confirmed by: High-resolution mass spectra were recorded using Waters Synapt G2, ESI probe, ESI Pos, Cone Voltage 15 V (Waters Corp., Milford, MA, USA) at the University of Stellenbosch Central Analytical Facility; Melting points were obtained using Lasec/SA-melting point apparatus from Lasec company, SA (Johannesburg, South Africa); IR spectra were recorded using Anglient technologies carry 600 series, FTIR spectrometer; and Nuclear Magnetic Resonance (NMR) (Bruker Ascend 400 MHz Topspin 3.2); ^{1}H NMR and ^{13}C NMR spectra were referenced internally using solvent signals, ^{1}H NMR: 7.250 ppm for $CDCl_3$, 2.500 ppm for DMSO-d_6; ^{13}C NMR: 77.00 ppm for $CDCl_3$, 39.40 ppm for DMSO-d_6, respectively which were used as the solvents at room temperature. Chemical shifts are expressed in δ-values parts per million (ppm) and the coupling constants (*J*) in Hertz (Hz). Multiplicity of the signals is given as follows: brs = broad singlet, s = singlet, d = doublet, dd = doublet of doublets, t = triplet, sept = septet and m = multiplet.

4.2 Synthesis

4.2.1 Synthesis of quinoxalin-2-ol 82A.

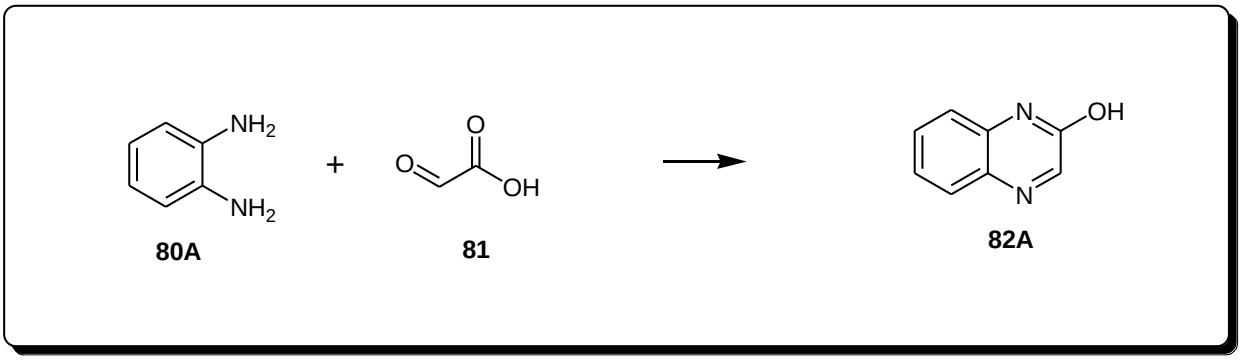

O-phenylenediamine **80A** (0.093 mol, 10 g) was dissolved in 10 mL acetic acid and 10 mL methanol in a 100 mL flask charged with a stirrer bar. The reaction was cooled to 0 ºC and treated with glyoxylic acid **81** (0.093 mol,10 mL) added drop wise over 20 minutes. The reaction was allowed to warm to room temperature and stirred for 2 hours. Thereafter, the mixture was filtered and washed with 10 mL water followed by 10 mL methanol. The residues were recrystalised from DMF to give quinoxalin-2-ol **82A** as a tan solid (9.40 g, 70%); mp = 265-267 ˚C (Lit. 266-267 ˚C): δ_H (400 MHz, DMSO-d_6) 7.25 (2 H, m), 7.55 (1H, m), 7.77 (1H, m), 8.17 (1 H, s), 12.45 (1H, brs); δ_C (100 MHz, DMSO-d_6) 116.2, 123.8, 129.2, 131.2, 132.2, 132.5, 152.0, 155.4. Spectroscopic data agree with those reported in literature [1].

4.2.2 Synthesis of 6-chloroquinoxalin-2-ol 82B

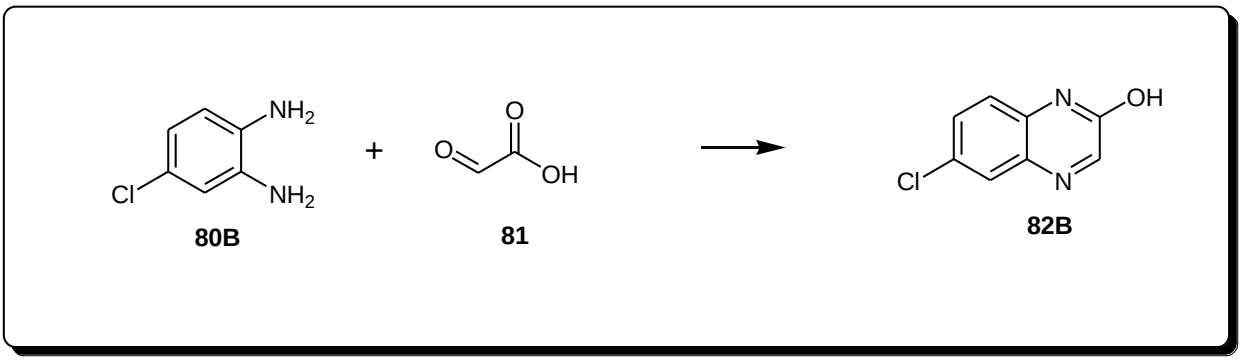

6-chloroquinoxalin-2-ol **82B** was synthesised following similar procedure as **82A:** 4-chloro-*O*-phenylenediamine **80B** (0.093 mol, 10 g) was dissolved in 10 mL acetic acid and 10 mL methanol in a 100 mL flask charged with a stirrer bar. The reaction was cooled to 0 ºC and treated with glyoxylic acid **82** (0.093 mol, 10 mL) added drops wise of over 20 minutes. The residues were recrystalised from DMF to give 6-chloroquinoxalin-2-ol **82B** as a purple solid (9.40 g, 70%); mp = 318 – 320 ºC. δ_H (400 MHz, DMSO-d_6, ppm) 7.31 (1H, *J* = 8.8 Hz, d), 7.61 (1H, ^3J = 8.8 Hz and ^4J = 2.4 Hz, dd), 7.85 (1H, *J* = 2.4 Hz, d), 8.21 (1H, s), 12.55 (1H, brs); δ_C (100 MHz, DMSO-d_6, ppm) 118.3, 127.9, 128.6, 131.6, 133.3, 153.7, 155.6;

4.2.3 Synthesis of quinoxalin-3-yl benzenesulfonate 83A

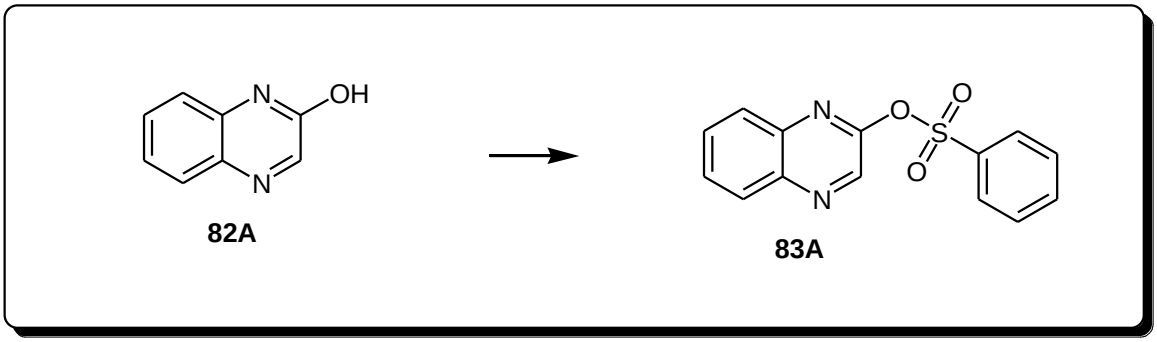

To a 100 mL flask equipped with a stirrer bar, was added a mixture of quinoxalin-2-ol **82A** (0.014 mol, 2.05 g), DMAP (10 mol%, 1.40 mmol, 180 mg) and $PhSO_2Cl$ (2 equiv., 0.03 mmol, 3.18 mL) in 25 mL DCM and stirred for 5 minutes. The reaction was cooled to 0 ºC and Et_3N (2.6 equiv., 0.04 mol, 5.27 mL) was added drop wise over 5 minutes. The reaction was allowed to warm to room temperature and stirred for an hour. The reaction was quenched by adding 25 mL saturated aqueous $NaHCO_3$ and the layers were separated. The aqueous layer was washed with DCM (3 × 15 mL), the combined organic layers were dried over $MgSO_4$ and concentrated. The crude product was purified on flash column using DCM and gave quinoxalin-3-yl benzenesulfonate **83A** as a white solid (3.335 g, 83%); mp = 89-92 ˚C (Lit 91 ˚C); δ_H (400 MHz, $CDCl_3$) 7.58 (2H, m), 7.77 (3H, m), 7.90 (1H, m), 8.17 (3H, m), 8.67 ppm (1H, s): δ_C (100 MHz, $CDCl_3$), 128.5, 128.6, 129.0, 129.2, 129.8, 131.2, 134.6, 136.5, 139.2, 139.7, 141.31, 150.9 ppm. Spectroscopic data agree with those reported in literature [1].

4.2.4 Synthesis of 6-chloroquinoxalin-3-yl benzenesulfonate 83B

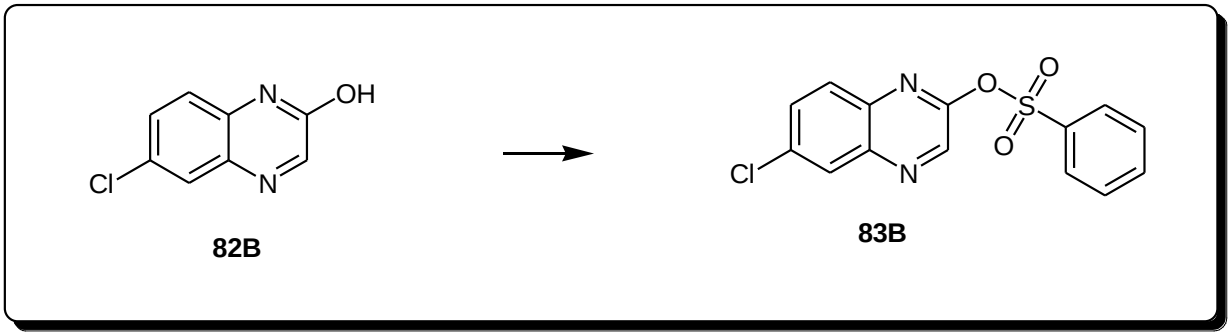

6-chloroquinoxalin-2-yl benzenesulfonate **83B** was synthesised following similar procedure as **83A:** A mixture of 6-chloroquinoxalin-2-ol **82B** (1.67 mmol, 300 mg), DMAP (10 mol%, 0.17 mmol, 2 mg) and $PhSO_2Cl$ (2 equiv., 3.32 mmol, 0.42 mL) in 25 mL DCM was stirred for 5 minutes. The reaction was cooled to 0 ºC and Et_3N (2.6 equiv., 4.32 mmol, 0.60 mL) was added drop wise over 5 minutes. After the aqueous work up, the crude product was purified on flash column using MeOH/DCM (0.5:9.5) and gave 6-chloroquinoxalin-3-yl benzenesulfonate **83B** as a pink powder (219 mg, 41%); mp = 143.7 – 146.5 ºC. δ_H (400 MHz, $CDCl_3$, ppm) 7.60 (2H, m), 7.71 (2H, m), 7.82 (1H, J = 9.2 Hz, d), 8.123 (3H, m), 8.65 (1H, s); δ_C (100 MHz, $CDCl_3$, ppm) 128.2, 129.0, 129.2, 129.6, 132.1, 134.8, 135.7, 136.2, 138.2, 140.1, 141.4, 150.9.

4.2.5 General procedure for Sonogashira cross-coupling reactions of quinoxalinyl sulfonate intermediates 83

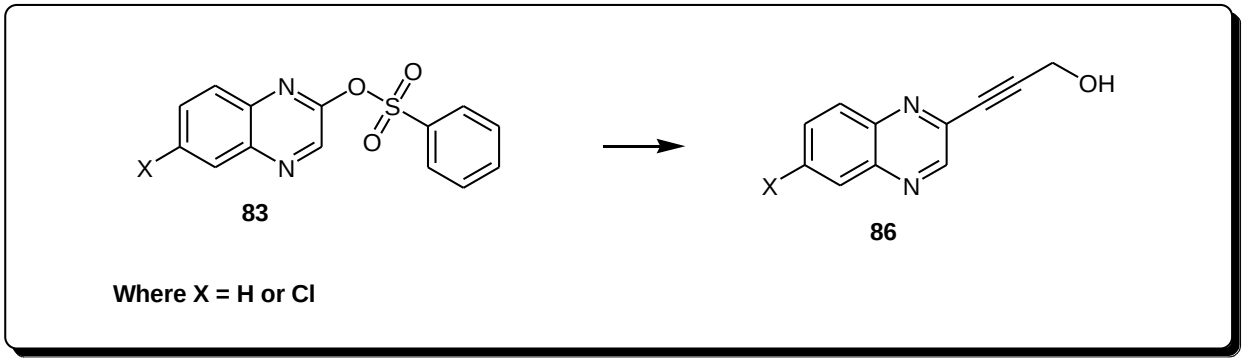

To an oven dried 2 neck flask equipped with a stirrer bar, was added quinoxalin-3-yl benzenesulfonate **83** (4.09 mmol), $PdCl_2(PPh_3)_2$ (5 mol%) and CuI (10 mol%) was dissolved in dry THF followed by an addition of Et_3N (2 equiv.) and propargyl alcohol (1.2 equiv.). The reaction mixture was refluxed and stirred 18 hours under nitrogen atmosphere. The reaction was quenched by adding ethyl acetate/water (3:1). The layers were separated and the aqueous layer was washed with ethyl acetate (20 mL × 3). The combined organic layers were dried over anhydrous $MgSO_4$, filtered and concentrated. The crude was purified by recrystallisation from acetone and gave **86A – C**.

4.2.5.1 Synthesis of 3-(quinoxalin-3-yl)prop-2-yn-1-ol 86A

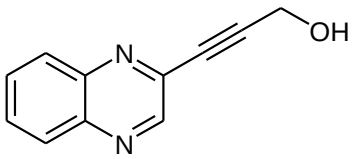

86A

A mixture of quinoxalin-3-yl benzenesulfonate **83A** (4.09 mmol, 1 g), $PdCl_2(PPh_3)_2$ (5 mol%, 0.21 mmol, 150 mg) and CuI (10 mol%, 0.41 mmol, 83 mg) was dissolved in 15 mL dry THF followed by an addition of Et_3N (2 equiv., 8.18 mmol, 1.14 mL) and propargyl alcohol (1.2 equiv., 4.98 mmol, 0.29 mL). After the aqueous work up, the crude was purified by recrystalisation from acetone and gave 3-(quinoxalin-3-yl)prop-2-yn-1-ol **86A** as a brown solid (451 mg, 60%), mp = 139 - 141 ºC (Lit 140-141 ºC); δ_H (400 MHz, $CDCl_3$, ppm) 4.61 (2H, s), 7.79 (2H, m), 8.08 (2H, m) and 8.89 (1H, s); δ_C (100 MHz, $CDCl_3$, ppm) 51.4, 83.0, 91.9, 128.4, 129.2, 130.7, 132.0, 138.7, 141.2, 141.9 and 146.9; V_{max} (FT-IR) 758, 946, 1014, 1127, 1229, 1429, 1694, 2228, 2922, 3275 cm^{-1}; Calculated for ($C_{11}H_8N_2O$) 184.0637; HRMS (ESI): $[M+H]^+$, $C_{11}H_8N_2O$, found 185.0431. Spectroscopic data agree with those reported in literature [2].

4.2.5.2 Synthesis of 3-(6-chloroquinoxalin-2-yl)prop-2-yn-1-ol 86B

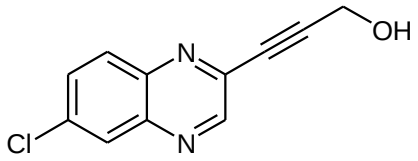

86B

A mixture of 6-chloroquinoxalin-3-yl benzenesulfonate **83B** (4.68 mmol, 1.50 g), $PdCl_2(PPh_3)_2$ (5 mol%, 0.234 mmol, 0.164 g) and CuI (10 mol%, 0.468 mmol, 89 mg) was dissolved in 25 mL dry THF followed by an addition of Et_3N (2 equiv., 9.630 mmol, 1.30 mL) and propargyl alcohol (1.2 equiv., 5.62 mmol, 0.33 mL). After the aqueous work up, the crude was purified by recrystalisation from acetone and gave 3-(6-chloroquinoxalin-2-yl)prop-2-yn-1-ol **86B** as a brown solid (499 mg, 49%); mp = 137.1 – 142.9 ºC; δ_H (400 MHz, $CDCl_3$, ppm) 4.60 (2H, s), 7.72 (1H, *J* = 8.8 Hz and 2.4 Hz, dd), 7.98 (1H, *J* = 8.8 Hz, d), 8.07 (1H, *J* = 2.4 Hz, d), 8.86 (1H, s); δ_C (100 MHz, $CDCl_3$, ppm) 51.1, 83.0, 88.4, 128.2, 130.5, 132.2, 136.86, 138.4, 140.5, 144.4, 147.8; V_{max} (FT-IR) 534, 644, 795, 1007, 1260, 1292, 1594, 2157, 2911, 3266 cm^{-1}; Calculated for ($C_{11}H_7N_2OCl$) 218.0247; HRMS (ESI); $[M+H]^+$, $C_{11}H_7N_2O^{35}Cl$, found 219.1902.

4.2.5.3 Synthesis of 2-methyl-4-(quinoxalin-3-yl)but-3-yn-2-ol 86C

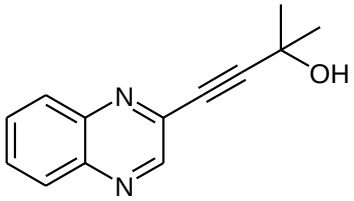

86C

A mixture of quinoxalin-3-yl benzenesulfonate **83A** (6.99 mmol, 2.04 g), $PdCl_2(PPh_3)_2$ (5 mol%, 0.35 mmol, 1 g) and CuI (10 mol%, 0.699 mmol, 133 mg) was dissolved in 25 mL dry THF followed by an addition of Et_3N (2 equiv., 0.014 mol, 1.95 mL) and 2-methylbut-3-yn-2-ol (1.2 equiv., 8.39 mmol, 0.81 mL). After the aqueous work up, the crude was purified by recrystalisation from acetone and gave 2-methyl-4-(quinoxalin-3-yl)but-3-yn-2-ol **86C** as a brown solid (1.165 g, 78%), mp = 155.3 - 158.4 ºC; δ_H (400 MHz, $CDCl_3$, ppm) 1.70 (6H, s), 7.78 (2H, m), 8.08 (2H, m), 8.87 (1H, s); δ_C (100 MHz, $CDCl_3$, ppm) 31.1, 65.5, 79.84, 98.2, 129.1, 129.2, 130.6, 130.8, 139.0, 140.9, 141.9 and 147.1; V_{max}

(FT-IR) 762, 960, 1050, 1229, 1301, 1488, 1538, 2230, 2982, 3290 cm^{-1}; Calculated for ($C_{13}H_{12}N_2O$) 212.0950; HRMS (ESI): $[M+H]^+$, $C_{13}H_{12}N_2O$ found, 213.1023. Spectroscopic data agree with those reported in literature [3].

4.2.6 General procedure for mesylation of 3-(quinoxalin-3-yl)prop-2-yn-1-ol 86A and 3-(6-chloroquinoxalin-3-yl)prop-2-yn-1-ol 86B.

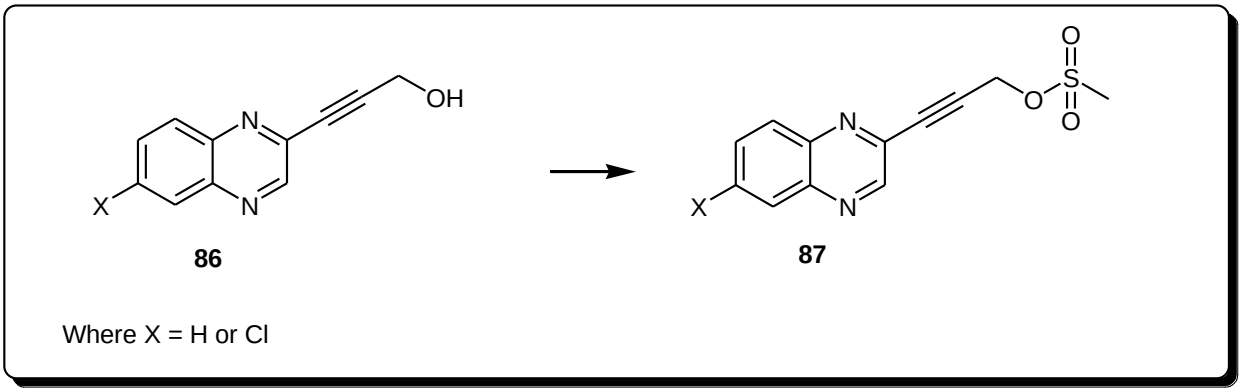

To an oven dried two neck flask under nitrogen atmosphere equipped with a stirrer bar, was added 3-(quinoxalin-3-yl)prop-2-yn-1-ol **86** (1 equiv.) and Et_3N (3.2 equiv.) dissolved in DCM. The reaction mixture was cooled to 0 ºC, and $MeSO_2Cl$ (1.2 equiv.) was added drop wise into the flask. The reaction was maintained at 0 ºC for 2.5 hours under nitrogen atmosphere. The reaction was quenched by adding aqueous saturated solution of $NaHCO_3$ into the reaction mixture, the layers were separated and the aqueous layer was extracted with DCM. The combined organic layers were dried over anhydrous $MgSO_4$, filtered and concentrated. The crude product was purified on prep TLC eluting with ethyl acetate/n-hexane (3:7) and yielded the desired products **87A – B**.

4.2.6.1 Synthesis of 3-(quinoxalin-3-yl) prop-2-ynyl methanesulfonate 87A

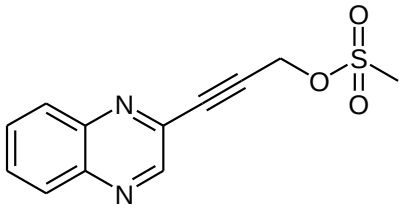

87A

A mixrure of 3-(quinoxalin-3-yl)prop-2-yn-1-ol **86A** (1.91 mmol, 500 mg) and Et_3N (3.2 equiv., 8.67 mmol, 1.21 mL) dissolved in 10 mL DCM. The reaction mixture was cooled to 0 ºC, and $MeSO_2Cl$ (1.2 equiv., 3.26 mmol, 0.25 mL) was added drop wise into the flask. The reaction was maintained at 0 ºC for 2.5 hours under nitrogen atmosphere. After the aqueous work up, the crude product was purified on prep TLC eluting with ethyl acetate/n-hexane (3:7) and gave 3-(quinoxalin-3-yl) prop-2-ynyl methanesulfonate **87A** as a brown solid (423 mg, 59%), mp = 93.8 - 96.7 ºC; δ_H (400 MHz, $CDCl_3$, ppm) 3.19 (3H, s), 5.16 (2H, s), 7.80 (2H, m), 8.07 (2H, m), 8.89 (1H, s); δ_C (100 MHz, $CDCl_3$, ppm) 38.9, 57.1, 84.5, 86.1, 129.3, 131.0, 131.2, 137.6, 141.3, 141.9, 146.6; V_{max} (FT-IR) 523, 649, 765, 801, 938, 1008, 1172, 1355, 1490, 2953 cm^{-1}; Calculated ($C_{12}H_{10}N_2O_3S$) 262.0412; HRMS (ESI): $[M+H]^+$, $C_{12}H_{10}N_2O_3S$, found 263.0481.

4.2.6.2 Synthesis of 3-(6-chlororquinoxalin-2-yl)prop-2-ynylmethanesulfonate 87B

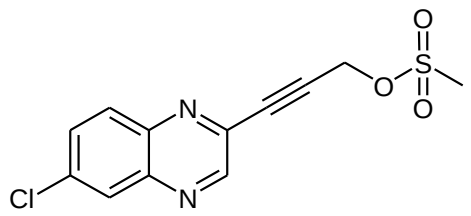

87B

A mixture of 3-(6-chloroquinoxalin-3-yl)prop-2-yn-1-ol **86B** (2.71 mmol, 500 mg) and Et_3N (3.2 equiv., 8.67 mmol, 1.21 mL) dissolved in 10 mL DCM. The reaction mixture was cooled to 0 ºC and $MeSO_2Cl$ (1.2 equiv., 3.26 mmol, 0.25 mL) was added drop wise into the flask. The reaction was maintained at 0 ºC for 2.5 hours under nitrogen atmosphere. After the aqueous work up, the crude product was purified on prep TLC eluting with ethyl acetate/n-hexane (3:7) and gave 3-(6-chlororquinoxalin-2-yl)prop-2-ynylmethanesulfonate **87B** as brown solid (75 mg, 55%); mp = 97.5 – 99.6 ºC; δ_H (400MHz, $CDCl_3$, ppm) 3.20 (3H, s), 5.16 (2H, s), 7.75 (1H, ^3J = 8.8 Hz and ^4J =2.4 Hz, dd), 8.00 (1H, J = 8.8 Hz, d), 8.20 (1H, J = 2.4 Hz, d), 8.89 (1H, s); δ_C (100 MHz, $CDCl_3$, ppm) 38.9, 56.9, 85.14, 85.9, 128.1, 128.3, 130.5, 130.6, 132.2, 137.7, 140.6, 141.6, 146.8,147.5; V_{max} (FT-IR) 443, 519, 792, 1033, 1165, 1219, 1305, 1486, 1601, 2919 cm^{-}

[1]; Calculated ($C_{12}H_9N_2O_3SCl$) 296.0022; HRMS (ES); $[M+H]^+$, $C_{12}H_9N_2O_3S^{35}Cl$, found 297.0256.

4.2.7 General procedure for oxidation of quinoxaline 3-(quinoxalin-3-yl)prop-2-yn-1-ol 86A and 3-(6-chloroquinoxalin-3-yl)prop-2-yn-1-ol 86B.

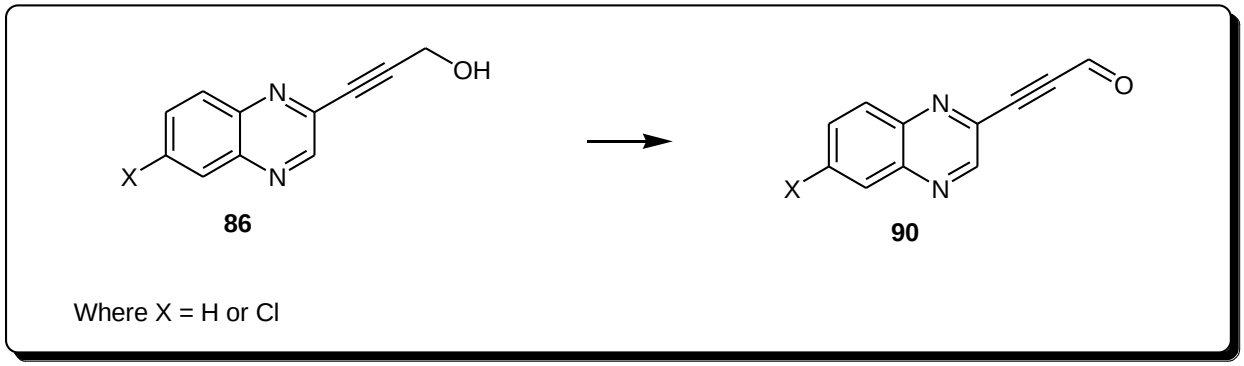

A mixture of Dess-Martin Periodinane (1.5 equiv.) and 3-(quinoxalin-3-yl)prop-2-yn-1-ol **86** (0.804 mmol) in 50 mL round bottom flask containing 10 mL DCM was stirred for 1 hour at room temperature. After this time 10% aqueous solution of $Na_2S_2O_3 \times 5H_2O$ and aqueous saturated solution $NaHCO_3$ were added into the reaction mixture and stirred for further 5 min. The reaction mixture was transferred into a separation funnel and extracted with DCM. The organic layers were combined, dried over anhydrous $MgSO_4$, filtered and concentrated. The crude product was purified on prep TLC eluting with ethyl acetate/n-hexane (3:7) and yielded the desired products **90A – B**.

4.2.7.1 Synthesis of 3-(quinoxalin-3-yl)propiolaldehyde 90A

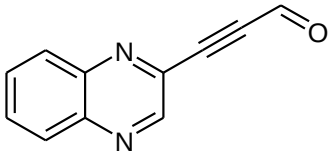

90A

A mixture of Dess-Martin Periodinane (1.5 equiv., 1.21 mmol, 515 mg) and 3-(quinoxalin-3-yl)prop-2-yn-1-ol **86A** (0.804 mmol, 148 mg), were mixed in 50 mL round bottom flask containing 10 mL DCM and stirred for 1 hour at room temperature. After the aqueous

work up, the crude product was purified on prep TLC eluting with ethyl acetate/n-hexane (3:7) and gave 3-(quinoxalin-3-yl)propiolaldehyde **90A** as brown powder (40 mg, 28%), mp = 122.2 - 124.8 ºC; δ_H (400 MHz, $CDCl_3$, ppm) 7.87 (2H, m), 8.14 (2H, m), 9.02 (1H, s) and 9.53 (1H, s); δ_C (100 MHz, $CDCl_3$, ppm) 88.2, 89.3, 129.5, 129.7, 131.4, 132.2, 136.4, 141.9, 124.3, 147.1 and 175.9; V_{max} (FT-IR) 752, 955, 1024, 1090, 1122, 1295, 1367, 1485, 1662, 2200 cm^{-1}; Calculated for ($C_{11}H_6N_2O$) 182.0480; HRMS (ESI): $[M+H]^+$, $C_{11}H_6N_2O$, found 183.0550. Spectroscopic data agree with those reported in literature [4].

4.2.7.2 Synthesis of 3-(6-chloroquinoxalin-2-yl)propiolaldehyde 90B

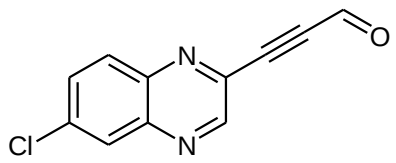

90B

A mixture of Dess-Martin reagent (1.5 equiv., 2.75 mmol, 1.167 g) and 3-(6-chloroquinoxalin-3-yl)prop-2-yn-1-ol **86B** (1.83 mmol, 400 mg)**,** were mixed in 50 mL round bottom flask containing 10 mL dichloromethane and stirred for 30 min at room temperature. After the aqueous work up, the crude product was purified on prep TLC eluting with ethyl acetate/n-hexane (3:7) and gave 3-(6-chloroquinoxalin-2-yl)propiolaldehyde **90B** as brown solid (53 mg, 13%); mp = 126.3 – 128.7 ºC; δ_H (400 MHz, $CDCl_3$, ppm) 7.795 (1H, ^3J = 9.2 Hz and ^4J = 2.4 Hz, dd), 8.06 (1H, J= 9.2 Hz, d), 8.14 (1H, J = 2.4 Hz, d), 8.99 (1H, s) and 9.52 (1H, s); δ_C (100 MHz, $CDCl_3$, ppm) 88.5, 88.8, 128.4, 130.8, 132.6, 136.5,138.3, 140.8, 142.0, 147.9 and 175.8; V_{max} (FT-IR) 573, 714, 790, 1012, 1257, 1463, 1595, 1657, 2203, 2961 cm^{-1}; Calculated for ($C_{11}H_7N_2Cl$) 216.0090, HRMS (ESI); $[M+H]^+$, $C_{11}H_7N_2{}^{35}Cl$, found 217.1046.

4.2.8 General procedure for chlorination of quinoxaline 3-(quinoxalin-3-yl)prop-2-yn-1-ol 86A and 3-(6-chloroquinoxalin-3-yl)prop-2-yn-1-ol 86B

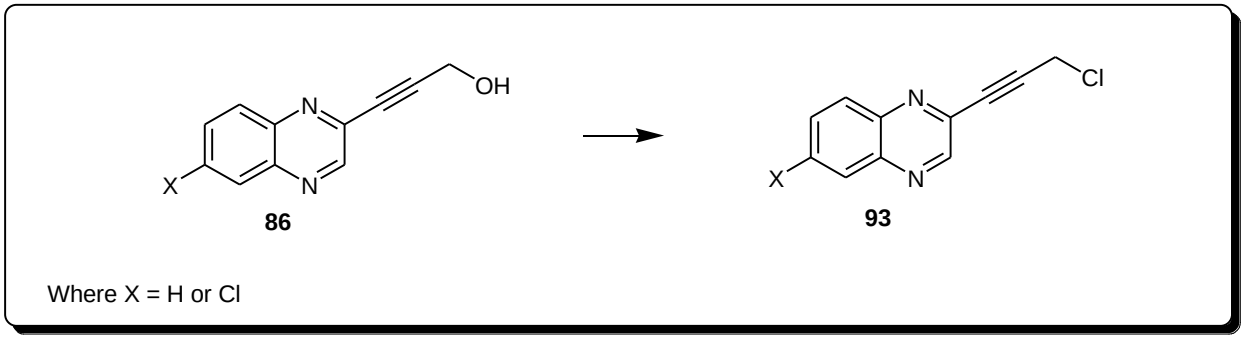

A mixture of $SOCl_2$ (10 mL) and 3-(quinoxalin-3-yl)prop-2-yn-1-ol **86** (1.63 mmol) were added into a 50 mL round bottom flask and refluxed for 4 hours a. After this time, the reaction was allowed to cool to room temperature and poured onto 15g of ice. The aqueous solution was extracted with ethyl acetate. The organic layers were combined then washed with 10mL brine, dried over $MgSO_4$ and concentrated. The crude product was purified on prep TLC eluting with ethyl acetate/n-hexane (3:7) and yielded the desired products **93A – B**.

4.2.8.1 Synthesis of 2-(3-chloroprop-1-ynyl)quinoxaline 93A

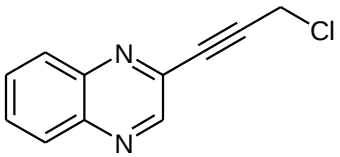

93A

A mixture of $SOCl_2$ (10 mL) and 3-(quinoxalin-3-yl)prop-2-yn-1-ol **86A** (1.63 mmol, 0.300 g) were added into a 50 mL round bottom flask and refluxed for 4 hours. After the aqueous work up, the crude product was purified on prep TLC eluting with ethyl acetate/n-hexane (3:7) and gave 2-(3-chloroprop-1-ynyl)quinoxaline **93A** as a brown solid (19 mg, 17%); mp = 126.5 – 131.7 ºC; δ_H (400 MHz, $CDCl_3$, ppm) 5.44 (1H, *J* = 15.6 Hz, d), 5.88 (1H, *J* = 15.6 Hz, d), 7.83 (2H, m), 8.14 (2H, m) and 9.60 (1H, s); δ_C (100 MHz, $CDCl_3$, ppm)

83.4, 129.3, 129.7, 131.1, 131.5, 137.3, 141.6, 141.7, 142.9, 143.1 and 143.5; V_{max} (FT-IR) 596, 685, 777, 978, 1129, 1259, 1448, 1637, 1729, 2915 cm^{-1}; Calculated for ($C_{11}H_7N_2Cl$) 202.0298; HRMS (ESI); $[M+H]^+$, $C_{11}H_7N_2{}^{35}Cl$, found 203.0097.

4.2.8.2 Synthesis of 6-chloro-2-(3-chloroprop-1-ynyl)quinoxaline 93B

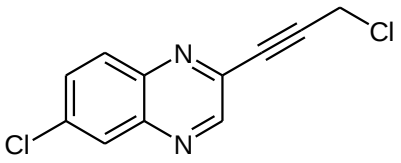

93B

A mixture of $SOCl_2$ (10 mL) and 3-(6-chloroquinoxalin-3-yl)prop-2-yn-1-ol **86B** (0.686 mmol, 150 mg) were added into a 50 mL round bottom flask and refluxed for 4 hours . After the aqueous work up, the crude product was purified on prep TLC eluting ethyl acetate/n-hexane (3:7) and gave 6-chloro-2-(3-chloroprop-1-ynyl)quinoxaline **93B** as brown power (31 mg, 19%); mp = 128.2 – 132.7 ºC ; δ_H (400 MHz, $CDCl_3$, ppm) 5.45 (1H, *J* = 16 Hz, d), 5.88 (1H, *J* = 16 Hz, d), 7.78 (1H, ^3J = 9.2 Hz and ^4J = 2.4 Hz, dd), 8.07 (1H, *J* = 8.8 Hz, d) 8.17 (1H, *J* = 2.4 Hz, d), 9.59 (1H, s); δ_C (100 MHz, $CDCl_3$, ppm) 83.9, 129.8, 130.3, 131.5, 131.9, 137.3, 141.6, 141.7, 142.9, 143.1 and 143.8; V_{max} (FT-IR) 598, 658, 788, 1067, 1146, 1260, 1483, 1635, 1720, 2921 cm^{-1}; Calculated for ($C_{11}H_6N_2Cl_2$) 235.9908; HRMS (ESI); $[M+Na]^+$, $C_{11}H_6N_2{}^{35}Cl_2Na$, found 258.9601.

4.2.9 General procedure for esterification of 3-(quinoxalin-3-yl)prop-2-yn-1-ol 86A and 3-(6-chloroquinoxalin-3-yl)prop-2-yn-1-ol 86B

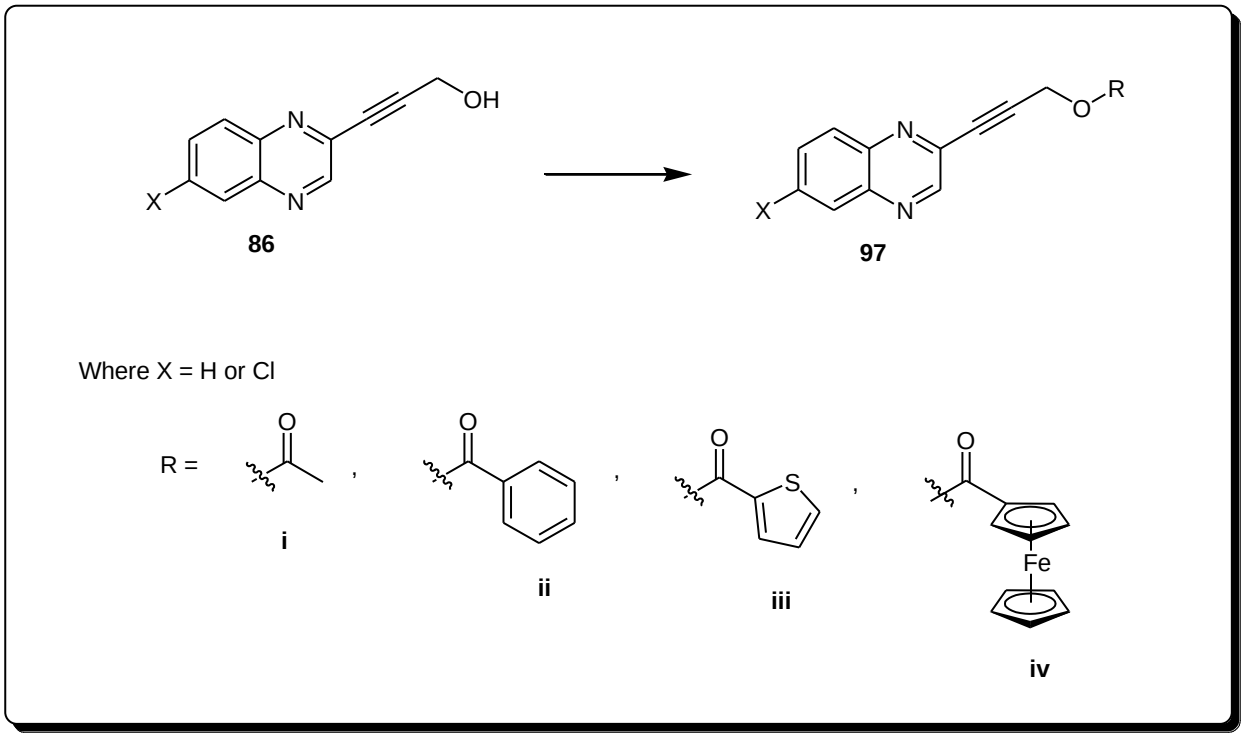

To an oven dried 2 neck flask equipped with a stirrer bar, was added 3-(quinoxalin-3-yl)prop-2-yn-1-,ol **86** (0.33 mmol), DMAP (10 mol%) and acid chloride (1 equiv.) dissolved in DCM. The reaction mixture was cooled to 0 ºC and Et_3N (3 equiv.) was added drop wise into the flask. The reaction was allowed to warm to room temperature and stirred for 3 hours under nitrogen atmosphere. The reaction was quenched by adding aqueous saturated solution of $NaHCO_3$ into the reaction mixture, the layers were separated and the aqueous layer was extracted with DCM. The combined organic layers were dried over anhydrous $MgSO_4$, filtered and concentrated. The crude product was purified on prep TLC eluting with ethyl acetate/n-hexane (3:7) yielding the desired products **97A - B**.

4.2.9.1 Synthesis of 3-(quinoxalin-3-yl)prop-2-ynyl acetate 97A-i

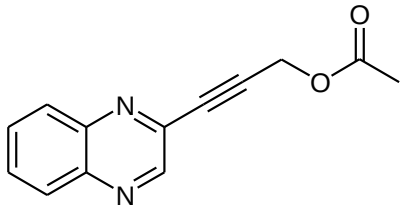

97A-i

A mixture of 3-(quinoxalin-3-yl)prop-2-yn-1-ol **86A** (0.33 mmol, 60 mg), DMAP (10 mol%, 0.03 mmol, 4 mg) and acetyl chloride (1 equiv., 0.33 mmol, 0.02 mL) was dissolved in 10 mL DCM. The reaction mixture was cooled to 0 ºC and Et_3N (3 equiv., 0.99 mmol, 0.14 mL) was added drop wise into the flask. After the aqueous work up, the crude was purified on prep TLC eluting with ethyl acetate/ hexane (3:7) and gave 3-(quinoxalin-3-yl)prop-2-ynyl acetate **97A-i** as brown solid (64 mg, 84%); mp = 64.5 – 65.9 ºC ;δ_H (400 MHz, $CDCl_3$, ppm) 2.15 (3H, s), 4.99 (2H, s), 7.78 (2H, m), 8.07 (2H, m), 8.88 (1H, s); δ_C (100 MHz, $CDCl_3$) 20.7, 52.2, 83.7, 87.3, 129.2, 129.2, 130.8, 138.4, 141.2, 141.9, 146.9, 170.1; V_{max} (FT-IR) 515, 598, 764, 914, 1030, 1127, 1220, 1358, 1732, 2928 cm^{-1}; Calculated for ($C_{13}H_{10}N_2O_2$) 226.0742; HRMS (ESI); $[M+H]^+$, $C_{13}H_{10}N_2O_2$, found 227.0819.

4.2.9.2 Synthesis of 3-(quinoxalin-3-yl)prop-2-ynyl benzoate 97A-ii

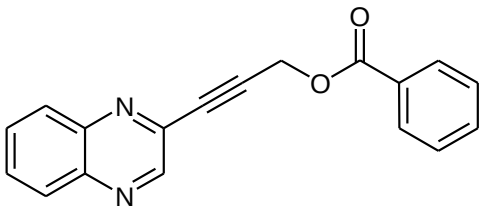

97A-ii

A mixture of 3-(quinoxalin-3-yl)prop-2-yn-1-ol **86A** (0.54 mmol, 100 mg), DMAP (10 mol%, 0.05 mmol, 6.63 mg) and benzoyl chloride (1 equiv., 0.54 mmol, 0.06 mL) was dissolved in 10 mL DCM. The reaction mixture was cooled to 0 ºC and Et_3N (3 equiv., 1.62 mmol, 0.23 mL) was added drop wise into the flask. After the aqueous work up, the

crude product was purified on prep TLC eluting with ethyl acetate/hexane (3:7) and gave 3-(quinoxalin-3-yl)prop-2-ynyl benzoate **97A-ii** as a brown solid (118 mg,76%); mp = 95 – 97.2 ºC (Lit 94 - 97 ºC) [2]; δ_H (400 MHz, $CDCl_3$, ppm) 5.26 (2H, s), 7.47 (2H, m), 7.59 (1H, m), 7.80 (2H, m), 8.09 (4H, m), 8.92 (1H, s); δ_C (100 MHz, $CDCl_3$, ppm) 52.7, 83.9, 87.4, 128.5, 129.2, 129.3, 130.8, 133.5, 13.4, 141.20, 142.0, 146.8, 165.8; V_{max} (FT-IR) 537, 708, 763, 795, 1013, 1089, 157, 1485, 1708, 2921 cm^{-1}; Calculated for ($C_{18}H_{12}N_2O_2$) 288.0899; HRMS (ESI); $[M+H]^+$, $C_{18}H_{12}N_2O_2$, found 289.0561.

4.2.9.3 Synthesis of 3-(quinoxalin-3-yl)prop-2-ynyl thiophene-2-carboxylate 97A-iii

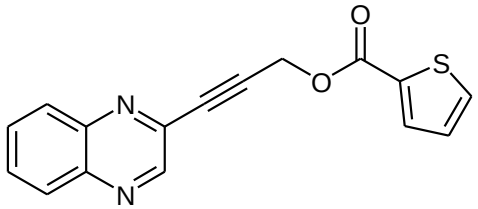

97A-iii

A mixture of 3-(quinoxalin-3-yl)prop-2-yn-1-ol **86A** (0.54 mmol, 100 mg), DMAP (10 mol%, 0.05 mmol, 6.63 mg) and thiophene-2-carbonyl chloride (1 equiv., 0.54 mmol, 0.06 mL) was dissolved in 10 mL DCM. The reaction mixture was cooled to 0 ºC and Et_3N (3 equiv., 1.629 mmol, 0.23 mL) was added drop wise into the flask. After the aqueous work up, the crude was purified on prep TLC eluting with ethyl acetate (3:7) and gave 3-(quinoxalin-2-yl)prop-2-ynyl thiophene-2-carboxylate **97A-iii** as a yellow solid (60 mg, 38%); mp = 97.3 – 99.3 ºC; δ_H (400 MHz, $CDCl_3$, ppm) 5.21 (2H, s), 7.12 (1H, ^3J = 4.8 Hz and ^3J = 4 Hz, dd), 7.61 (1H, ^3J = 4.8 Hz and ^4J = 1.2 Hz, dd), 7.79 (2H, m), 7.88 (1H, ^3J = 3.6 Hz and ^4J = 1.2 Hz, dd), 8.07 (2H, m), 8.90 (1H, s); δ_C (100 MHz, $CDCl_3$, ppm) 52.7, 83.9, 87.1, 127.9, 129.2, 130.8, 132.4, 133.3, 134.4, 138.4, 141.2, 141.9, 146.9, 161.3; V_{max} (FT-IR) 526, 611, 742, 1080, 1268, 1414, 1704, 2104, 2340, 3095 cm^{-1} ; Calculated for ($C_{16}H_{10}N_2OS$) 294.0463; HRMS (ESI); $[M+Na]^+$, $C_{16}H_{10}N_2OSNa$, found 317.1025.

4.2.9.4 Synthesis of 3-(quinoxalin-3-yl)prop-2-ynyl ferrocetate 97A-iv

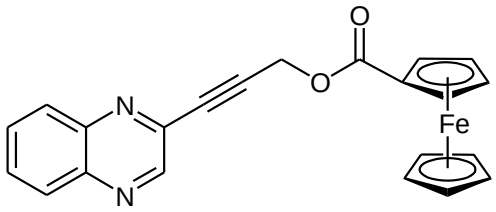

97A-iv

A mixture of 3-(quinoxalin-3-yl)prop-2-yn-1-ol **86A** (0.33 mmol, 60 mg), DMAP (10 mol%, 0.033 mmol, 4 mg) and ferrocenoyl chloride (1 equiv., 0.33 mmol, 81.6 mg) was dissolved in 10 mL DCM. The reaction mixture was cooled to 0 ºC and Et_3N (3 equiv., 0.99 mmol, 0.14 mL) was added drop wise into the flask. The reaction mixture was allowed to warm to room temperature and stirred for 18 hours under nitrogen atmosphere. After the aqueous work up, the crude product was purified on prep TLC eluting with ethyl acetate/n-hexane (3:7) and gave 3-(quinoxalin-3-yl)prop-2-ynyl ferrocetate **97A-iv** as orange powder (49 mg, 42%); mp = 148.9 – 150.8 ºC; δ_H (400 MHz, $CDCl_3$) 4.26 (5H, s), 4.45 (2H, *J* = 4 Hz, t), 4.88 (2H, *J* = 3.6 Hz, t), 5.14 (2H, s), 7.78 (2H, m), 8.67 (2H, m), 8.92 (1H, s); δ_C (100 MHz, $CDCl_3$, ppm) 51.9, 69.5, 69.9, 70.4, 71.8, 83.5, 88.2, 129.3, 129.3, 130.8, 138.5, 141.2, 142.1, 146.8, 171.1; V_{max} (FT-IR) 482, 505, 759, 796, 1026, 1113, 1257, 1373, 1451, 1709, 2921 cm^{-1}; Calculated for ($C_{22}H_{16}N_2O_2Fe$) 396.0561; HRMS (ESI); $[M+H]^+$, $C_{22}H_{16}N_2O_2Fe$, found 397.0634.

4.2.9.5 Synthesis of 3-(6-chloroquinoxalin-2-yl)prop-2-ynyl acetate 97B-i

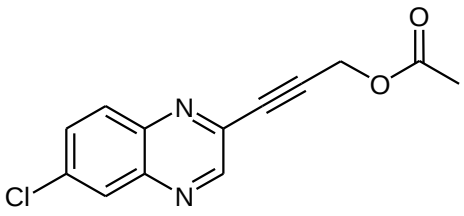

97B-i

A mixture of 3-(6- chloroquinoxalin-3-yl)prop-2-yn-1-ol **86B** (0.27 mmol, 60 mg), DMAP (10 mol%, 0.027 mmol, 3.35 mg) and acetyl chloride (1 equiv., 0.27 mmol, 0.019 mL) was

dissolved in 10mL DCM. The reaction mixture was cooled to 0 ºC and Et_3N (3 equiv., 0.81 mmol, 0.11 mL) was added drop wise into the flask. After the aqueous work up, the crude product was purified on prep TLC eluting with ethyl acetate/hexane (3:7) and gave 3-(6-chloroquinoxalin-2-yl)prop-2-ynyl acetate **97B-i** as a pink solid (64 mg, 91%); mp = 166.1 – 169.9 ºC; δ_H (400MHz, $CDCl_3$) 2.15 (3H, s), 4.98 (1H, s), 7.72 (1H, ^3J = 8.8 Hz and ^4J = 2.4 Hz, dd), 7.98 (1H, *J* = 8.8 Hz, d), 8.07 (1H, *J* = 2.4 Hz, d), 8.86 (1H, s); δ_C (100 MHz, $CDCl_3$) 20.7, 52.1, 83.4, 87.9, 128.2, 130.5, 131.9, 136.8, 138.5, 140.5, 141.4, 147.7, 170.1; V_{max} (FT-IR) 464, 570, 827, 1027, 1235, 1361, 1741, 2026, 2161, 3058 cm^{-1}; Calculated for ($C_{13}H_9N_2O_2Cl$) 260.0353; HRMS (ESI); $[M+H]^+$, $C_{13}H_9N_2O_2{}^{35}Cl$, found 261.0426.

4.2.9.6 Synthesis of 3-(6-chloroquinoxalin-2-yl)prop-2-ynyl benzoate 97B-ii

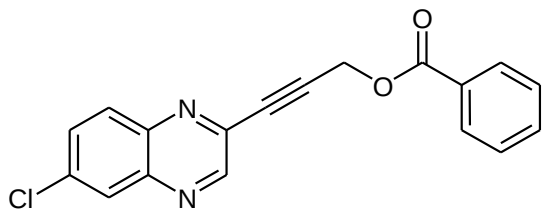

97B-ii

A mixture of 3-(6-chloroquinoxalin-3-yl)prop-2-yn-1-ol **86B** (0.457 mmol, 100 mg), DMAP (10 mol%,0.0457 mmol, 5.58 mg) and benzoyl chloride (1 equiv., 0.457 mmol, 0.05 mL) was dissolved in 10 mL DCM. The reaction mixture was cooled to 0 ºC and Et_3N (3 equiv., 1.371 mmol, 0.19 mL) was added drop wise into the flask. After the aqueous work up, the crude was purified on prep TLC eluting with DCM and gave 3-(6-chloroquinoxalin-2-yl)prop-2-ynyl benzoate **97B-ii** as a tan solid (19 mg, 13%); mp = 143.2 – 144.2 ºC ;δ_H (400 MHz, $CDCl_3$) 5.25 (2H, s), 7.47 (2H, m), 7.58 (1H, m), 7.73 (1H, ^3J = 8.8 Hz and ^4J = 2.4 Hz, dd), 8.00 (1H, *J* = 8.8 Hz, d), 8.09 (3H, m), 8.90 (1H, s); δ_C (100 MHz, $CDCl_3$, ppm) 52.7, 83.6, 88.1, 128.2, 128.5, 129.1, 129.9, .130.5, 131.9, 133.5, 136.8, 138.5, 140.5, 141.4, 147.8, 165.7; V_{max} (FT-IR) 408, 566, 702, 785, 1069, 1259, 1452, 1600, 1715, 2921 cm^{-1}; Calculated for ($C_{18}H_{11}N_2O_2Cl$) 322.0509; HRMS (ESI); $[M+H]^+$, $C_{18}H_{11}N_2O_2{}^{35}Cl$, found 323.0590.

4.2.9.7 Synthesis of 3-(6-chloroquinoxalin-2-yl)prop-2-ynyl thiophene-2-carboxylate 97B-iii.

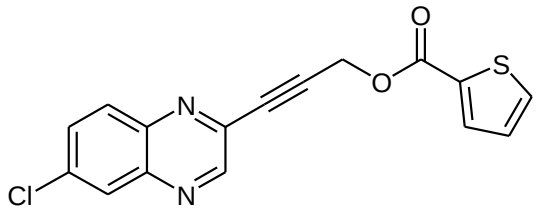

97B-iii

A mixture of 3-(6-chloroquinoxalin-3-yl)prop-2-yn-1-ol **86B** (0.457 mmol, 100 mg), DMAP (10 mol%, 0.0457 mmol, 5.58 mg) and thiophene-2-carbonyl chloride (1 equiv., 0.457 mmol, 0.05 mL) was dissolved in 10 mL DCM. The reaction mixture was cooled to 0ºC and Et_3N (3 equiv., 1.371 mmol, 0.19 mL) was added drop wise into the flask. After the aqueous work up, the crude was purified on prep TLC eluting with DCM and gave 3-(6-chloroquinoxalin-2-yl)prop-2-ynyl thiophene-2-carboxylate **97B-iii** as tan solid (55 mg, 37%); mp = 138.4 – 140.7 ºC; δ_H (400 MHz, $CDCl_3$) 5.22 (2H, s), 7.14 (1H, ^3J = 5.2 Hz and ^3J = 4 Hz, dd), 7.62 (1H, ^3J = 4.8 Hz and ^4J = 1.2 Hz, dd), 7.73 (1H, ^3J = 8.8 Hz and ^4J = 2.4 Hz, dd), 7.89 (1H, ^3J = 3.6 Hz and ^4J = 1.2 Hz, dd), 8.00 (1H, J = 9.2 Hz, d), 8.09 (1H, J = 2.4 Hz, d), 8.90 (1H, s); δ_C (100 MHz, $CDCl_3$, ppm) 52.7, 83.7, 87.8, 127.9, 128.2, 130.4, 131.9, 132.4, 133.4, 134.4, 136.8, 138.5, 140.5, 141.4, 147.8, 161.3: V_{max} (FT-IR) 571, 714, 832, 1097, 1255, 1374, 1418, 1521, 1704, 2922 cm^{-1}; Calculated for ($C_{16}H_9N_2O_2SCl$) 328.0073; HRMS (ESI); $[M+H]^+$, $C_{16}H_9N_2O_2S^{35}Cl$, found 329.0156.

4.2.9.8 Synthesis of 3-(6-chloroquinoxalin-2-yl)prop-2-ynyl ferrocetate 97B-iv

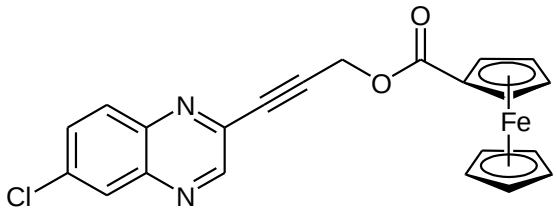

97B-iv

A mixture of 3-(6-chloroquinoxalin-3-yl)prop-2-yn-1-ol **86B** (0.18 mmol, 40 mg), DMAP (10 mol%, 0.018 mmol, 2.2 mg) and ferrocenoyl chloride (1 equiv., 0.18 mmol, 45 mg) was dissolved in 10 mL DCM. The reaction mixture was cooled to 0 ºC and Et_3N (3 equiv., 1.371 mmol, 0.19 mL) was added drop wise into the flask. The reaction was allowed to warm to room temperature and stirred for 18 hours under nitrogen atmosphere. After the aqueous work up, the crude product was purified on prep TLC eluting DCM and gave 3-(6-chloroquinoxalin-2-yl)prop-2-ynyl ferrocetate **97B-iv** as an orange solid (34 mg, 43%); mp = 189.8 – 192.8 ºC; δ_H (400 MHz, $CDCl_3$, ppm) 4.26 (5H, s), 4.45 (2H, J = 4 Hz, t), 4.88 (2H, *J* = 4 Hz, t), 5.14 (2H, s), 7.72 (1H, ^3J = 8.8 Hz and ^4J = 2.4 Hz, dd), 7.99 (1H, *J* = 8.8 Hz, d), 8.08 (1H, *J* = 2 Hz, d), 8.90 (1H, s); δ_C (100 MHz, $CDCl_3$, ppm) 51.8, 69.5, 69.9, 70.4, 71.8, 83.2, 88.8, 128.2, 130.5, 131.9, 136.7, 138.6, 140.6, 141.4, 147.7, 171.1; V_{max} (FT-IR) 485, 503, 794, 1020, 1119, 1168, 1262, 1454, 1712, 2920 cm^{-1}; Calculated for ($C_{22}H_{15}N_2O_2FeCl$) 430.0171; HRMS (ESI); $[M+H]^+$, $C_{22}H_{15}N_2O_2Fe^{35}Cl$, found 431.0255.

4.2.10 Synthesis of 3-chloroquinoxaline-2-carbonyl chloride 99

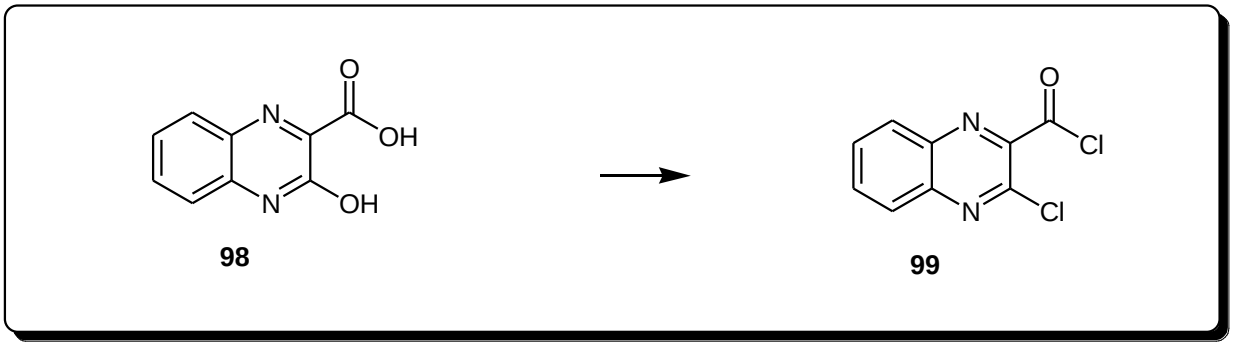

A solution of 3-hydroxyquinoxaline-2-carboxylic acid **98** (0.500 g, 2.63 mmol) in 30 mL $SOCl_2$ and 10 drops of DMF was added into l00 mL flask and heated to reflux for 18 hours. After this time, the reaction mixture was cooled to room temperature and 50 g of ice was added and precipitates were formed. The precipitates were filtered off, dried under vacuum and gave 3-chloroquinoxaline-2-carbonyl chloride **99** as yellow solid (552 mg, 93%); mp 142.5 - 144.8 ºC; δ_H (400MHz, $CDCl_3$, ppm) 7.91 (1H, m), 7.98 (1H, m), 8.11 (1H, *J* = 8.2 Hz, d), 8.26 (1H, *J* = 8.2 Hz, d); δ_C (100MHz, $CDCl_3$, ppm) 128.4, 129.2, 130.2, 131.7, 134.4, 138.4, 139.5, 142.9, 158.9 ; V_{max} (FT-IR) 525, 601, 765, 901, 1027,

1130, 1344, 1455, 1519, 1651,1770 cm^{-1}; Calculated for ($C_9H_4N_2OCl_2$) 226.9701; HRMS (ESI-); [M-(-COCl)], $C_8H_4N_2{}^{35}Cl$, found 163.0064.

4.2.11 General procedure for esterification of 3-chloroquinoxaline-2-carbonyl chloride substrate

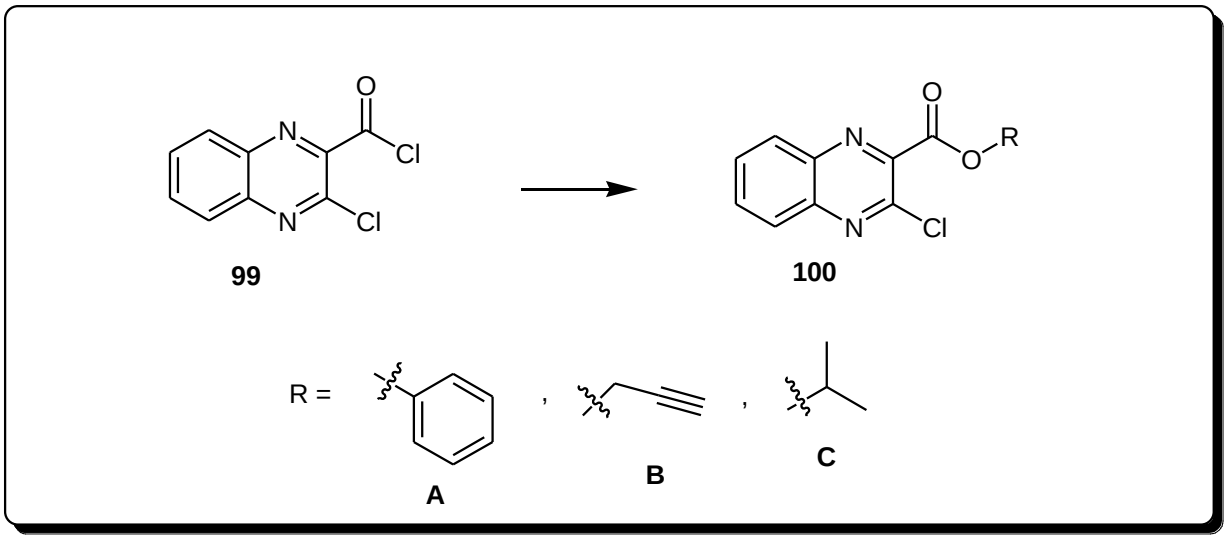

To an oven dried 2 neck flask under nitrogen was equipped with a stirrer bar, was added an alcohol (1.1 equiv.), DMAP (10 mol%) and 3-chloroquinoxaline-2-carbonyl chloride **99** (0.221 mmol) dissolved in DCM. The reaction mixture was stirred for 5 minutes, cooled to 0 ºC and Et_3N (3 equiv.) was added drop wise. The reaction was allowed to warm to room temperature and stirred for 18 hours. The reaction was quenched by adding aqueous saturated solution of $NaHCO_3$ and the layers were separated. The aqueous layer was washed with DCM. The combined organic layers dried over $MgSO_4$, concentrated and purified on prep TLC eluting with 3:7 ethyl acetate/ n-hexane yielding the desired products **100A – C**.

4.2.11.1 Synthesis of phenyl 3-chloroquinoxaline-2-carboxylate 100A

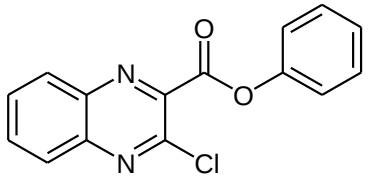

100A

A mixture of phenol (1.1 equiv., 0.24 mmol), DMAP (10 mol%, 0.0221 mmol, 2.7 mg) and 3-chloroquinoxaline-2-carbonyl chloride **99** (50 mg, 0.221 mmol) was dissolved in 10 mL DCM. The reaction mixture was stirred for 5 min, cooled to 0 ºC and Et_3N (3 equiv., 0.663 mmol, 0.09 mL) was added drop wise. After the aqueous work up, the crude product was purified on prep TLC eluting with ethyl acetate/hexane (3:7) and gave phenyl 3-chloroquinoxaline-2-carboxylate **100A** as a white solid (42 mg, 67%); mp = 115.7 - 117.4 ºC; δ_H (400 MHz, $CDCl_3$, ppm) 7.34 (3H,m), 7.48 (2H, m), 7.89 (2H,m), 8.11 (1H, *J* = 8 Hz, d), 8.25 (1H, *J* = 7.8 Hz, d); δ_C (100 MHz, $CDCl_3$, ppm) 121.4, 126.7, 128.4, 129.7, 129.8, 131.3, 133.1, 133.1, 139.7, 142.4, 143.8, 144.0, 150.4, 162.2; V_{max} (FT-IR) 454, 592, 686, 762, 1020, 1178, 1328, 1462, 1755, 2915 cm^{-1}; Calculated for ($C_{15}H_9N_2O_2Cl$) 284.0353; HRMS (ESI); $[M+H]^+$, $C_{15}H_9N_2O_2{}^{35}Cl$, found 285.0415

4.2.11.2 Synthesis of prop-2-ynyl 3-chloroquinoxaline-2-carboxylate 100B

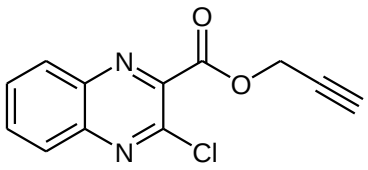

100B

A mixture of propargyl alcohol (1.1 equiv., 0.24 mmol), DMAP (10 mol%, 0.0221 mmol, 2.7 mg) and 3-chloroquinoxaline-2-carbonyl chloride **99** (50 mg, 0.221 mmol) was dissolved in 10 mL DCM. The reaction mixture was stirred for 5 minutes, cooled to 0 ºC and Et_3N (3 equiv., 0.663 mmol, 0.09 mL) was added drop wise. After the aqueous work up the crude product was purified on prep TLC eluting with ethyl acetate/hexane (3:7) and gave prop-2-ynyl 3-chloroquinoxaline-2-carboxylate **100B** as a white solid (43 mg,

78%); mp = 121.9 - 123.5 ºC; δ_H (400 MHz, $CDCl_3$, ppm) 2.61 (1H, *J* = 4.8 Hz, t), 5.08 (2H, *J* = 2.8 Hz, d), 7.88 (2H, m), 8.07 (1H, *J* = 8 Hz, d), 8.20 (1H, *J* = 7.7 Hz, d); δ_C (100MHz, $CDCl_3$, ppm) 54.0, 128.4, 129.8, 131.2, 133.0, 139.6, 142.2, 144.0, 163.6; V_{max} (FT-IR) 598, 689, 755, 942, 1043, 1116, 1317, 1724, 2914, 3228 cm^{-1}; Calculated for ($C_{12}H_7N_2O_2Cl$) 246.0196; HRMS (ESI); $[M+Na]^+$, $C_{12}H_7N_2O_2{}^{35}Cl$, found 269.0140.

4.2.11.3 Synthesis of isopropyl 3-chloroquinoxaline-2-carboxylate 100C

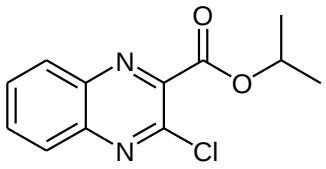

100C

A mixture of propan-2-ol (1.1 equiv., 0.24 mmol), DMAP (10 mol%, 0.0221 mmol, 2.7 mg) and 3-chloroquinoxaline-2-carbonyl chloride **99** (50 mg, 0.221 mmol) was dissolved in 10 mL DCM. The reaction mixture was stirred for 5 minutes, cooled to 0ºC and Et_3N (3 equiv., 0.663 mmol, 0.09 mL) was added drop wise. After the aqueous work up the crude product was purified on prep TLC eluting with ethyl acetate /hexane (3:7) and gave isopropyl 3-chloroquinoxaline-2-carboxylate **100C** as a white solid (16 mg, 30%); mp = 71.8 - 73.5 ºC; δ_H (400 MHz, $CDCl_3$, ppm) 1.46 (6H, *J* = 6.4 Hz, d), 5.43 (1H, sept), 7.85 (2H, m), 8.05 (1H, *J* = 7.7 Hz, d), 8.18 (1H, *J* = 7.9 Hz, d); δ_C (100 MHz, $CDCl_3$, ppm) 21.7, 71.3, 128.3, 129.6, 130.9, 132.5, 139.7, 1427, 143.66, 145.3 and 163,6; V_{max} (FT-IR) 461, 493, 759, 1026, 1179, 1226, 1318, 1462, 1732, 2982 cm^{-1}; Calculated for ($C_{12}H_{11}N_2O_2Cl$) 250.0509 ; HRMS (ESI); $[M+Na]^+$, $C_{12}H_{11}N_2O_2{}^{35}ClNa$, found 273.0408.

4.2.12 General procedure for amidation of 3-chloroquinoxaline-2-carbonyl chloride substrate

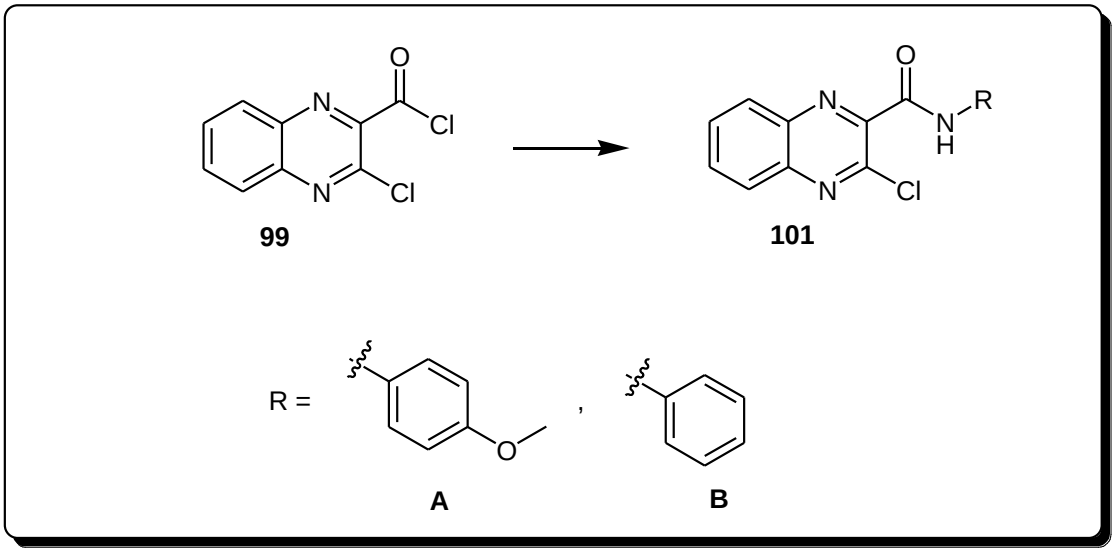

To an oven dried 2 neck flask under nitrogen was equipped with a stirrer bar, was added an amine (1.1 equiv.), DMAP (10 mol%) and 3-chloroquinoxaline-2-carbonyl chloride **99** (0.221 mmol) followed by DCM. The reaction mixture was stirred for 5 minutes, cooled to 0 ºC and Et_3N (3 equiv.) was added drop wise. The reaction was allowed to warm to room temperature and stirred for 18 hours, quenched by adding aqueous saturated solution of $NaHCO_3$ and the layers were separated. The aqueous layer was washed with DCM. The combined organic layers dried over $MgSO_4$, concentrated and purified on prep TLC eluting with ethyl acetate/ n-hexane (3:7) yielding the desired products **101A – B**.

4.2.12.1 Synthesis of 3-chloro-N-(4-methoxyphenyl)quinoxaline-2-carboxamide 101A

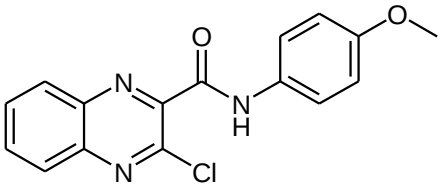

101A

A mixture of P-anisidine (1.1 equiv., 0.243 mmol), DMAP (10 mol%, 0.0221 mmol, 2.7 mg) and 3-chloroquinoxaline-2-carbonyl chloride **99** (50 mg, 0.221 mmol) was dissolved

in 10 mL DCM. The reaction mixture was stirred for 5 minutes, cooled to 0 ºC and Et_3N (3 equiv., 0.663 mmol, 0.09 mL) was added drop wise. After the aqueous work up, the crude product was purified on prep TLC eluting with ethyl acetate/hexane (3:7) and gave 3-chloro-N-(4-methoxyphenyl)quinoxaline-2-carboxamide **101A** as an orange solid (37 mg, 53%); mp = 168.5 – 172.7 ºC; δ_H (400 MHz, $CDCl_3$, ppm) 3.83 (3H, s), 6.94 (2H, *J* = 8.8 Hz, d), 7.71 (2H, *J* = 9.2 Hz, d), 7.90 (2H, m), 8.11 (1H, *J* = 9.6 Hz, d), 8.17 (1H, *J* = 9.2 Hz, d), 9.44 (1H, brs); δ_C (100 MHz, $CDCl_3$, ppm) 55.5, 114.3, 121.6, 128.4, 129.1, 130.5, 131.2, 132.9, 138.7, 142.2, 142.7, 145.5, 156.8, 159.5; V_{max} (FT-IR) 442, 597, 716, 820, 1021, 1110, 1244, 1530, 1659, 3257 cm^{-1}; Calculated for ($C_{16}H_{12}N_3O_2Cl$) 313.0618; HRMS (ES); $[M+H]^+$, $C_{16}H_{12}N_3O_2{}^{35}Cl$, found 314.0695.

4.2.12.2 Synthesis of 3-chloro-N-phenylquinoxaline-2-carboxamide 101B

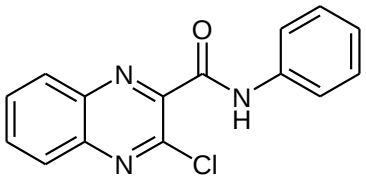

101B

A mixture of aniline (1.1 equiv., 0.243 mmol), DMAP (10 mol%, 0.0221 mmol, 2.7 mg) and 3-chloroquinoxaline-2-carbonyl chloride **99** (50 mg, 0.221 mmol) was dissolved in 10 mL DCM. The reaction mixture was stirred for 5 minutes, cooled to 0 ºC and Et_3N (3 equiv., 0.663 mmol, 0.09 mL) was added drop wise. After the aqueous work up the crude product was purified on prep TLC eluting with ethyl acetate/hexane (3:7) and gave 3-chloro-N-phenylquinoxaline-2-carboxamide **101B** as a yellow solid (27 mg, 43%); mp =168.2 – 170.3 ºC; δ_H (400 MHz, $CDCl_3$, ppm) 7.20 (1H, m), 7.28 (2H, m), 7.79 (2H, *J* = 7.6 Hz, d), 7.915 (2H, m), 8.11 (1H, *J* = 8 Hz, d), 8.19 (1H, *J* = 7.8 Hz, d), 9.57 (1H, brs); δ_C (100 MHz, $CDCl_3$, ppm) 118.9, 123.9, 127.4, 128.2, 130.3, 132.1, 136.3, 137.6, 140.9, 141.8, 158.8; V_{max} (FT-IR) 442, 596, 690, 747, 1035, 1257, 1441, 1531, 1672, 3263, 3380 cm^{-1}; Calculated ($C_{15}H_{10}N_3OCl$) 283.0512; HRMS (ESI); $[M+H]^+$, $C_{15}H_{10}N_3O^{35}Cl$, found 284.0245.

4.2.12.3 Synthesis of N-benzyl-3-(benzylamino)quinoxaline-2-carboxamide 101C

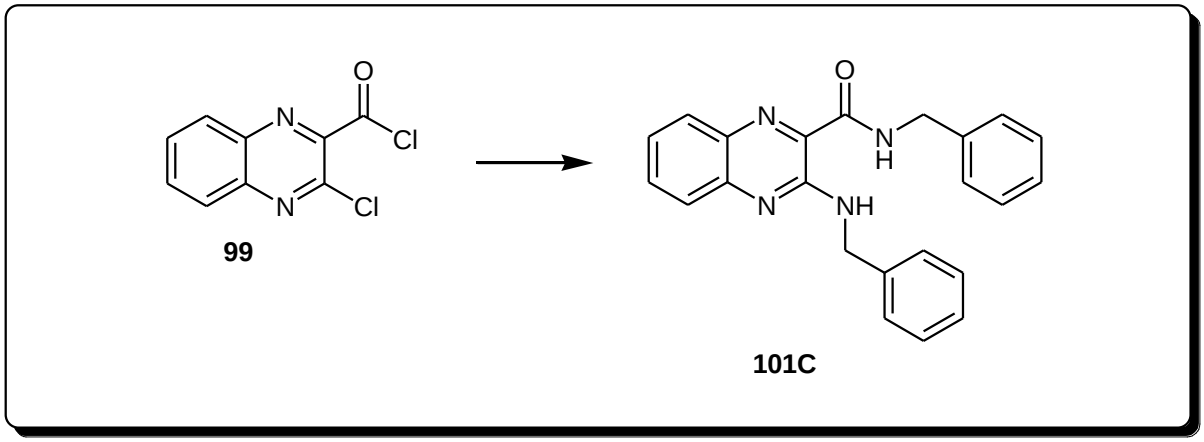

Synthesis of N-benzyl-3-(benzylamino)quinoxaline-2-carboxamide **101C** followed similar procedure as **101A**: A mixture of benzylamine (1.1 equiv., 0.243 mmol), DMAP (10 mol%, 0.0221 mmol, 2.7 mg) and 3-chloroquinoxaline-2-carbonyl chloride **99** (50 mg, 0.221 mmol) was dissolved in 10 mL DCM. The reaction mixture was stirred for 5 minutes, cooled to 0ºC and Et_3N (3 equiv., 0.663 mmol, 0.09 mL) was added drop wise. After the aqueous work up, the crude product was purified on prep TLC eluting with ethyl acetate/hexane (3:7) and gave N-benzyl-3-(benzylamino)quinoxaline-2-carboxamide **101C** as a yellow solid (4 mg, 61%); mp = 99.5 – 101.8 ºC; δ_H (400 MHz, $CDCl_3$, ppm) 4.65 (2H, *J* = 6 Hz, d), 4.82 (2H, *J* = 5.6 Hz, d), 7.32 (9H, m), 7.45 (2H, *J* = 8.8 Hz, d), 7.60 (1H, m), 7.67 (1H, *J* = 8.1 Hz, d), 7.77 (1H, *J* = 8.1 Hz, d), 8.5879 (1H, brs), 9.21 (1H, brs); δ_C (100 MHz, $CDCl_3$, ppm) 43.3, 44.6, 124.5, 126.1, 127.1, 127.7, 127.8, 127.9, 128.6, 128.8, 129.2, 131.3, 131.9, 134.7, 137.7, 138.9, 144.5, 151.9, 165.6; V_{max} (FT-IR) 639, 723, 1014, 1136, 1257, 1450, 1524, 1664, 2916, 3364 cm^{-1}; Calculated for ($C_{23}H_{20}N_4O$) 368.1637; HRMS (ESI); $[M+H]^+$, $C_{23}H_{20}N_4O$, found 369.1713.

4.2.12.4 Synthesis of 3-(3-isopropoxyphenylamino)-N-(3-isopropoxyphenyl)quinoxaline-2-carboxamide 101D

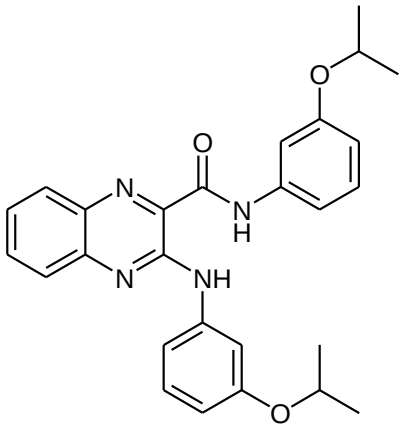

101D

3.2.16.4 Synthesis of 3-(3-isopropoxyphenylamino)-N-(3-isopropoxyphenyl)quinoxaline-2-carboxamide **101D** followed similar procedure as **101A**: A mixture of isopropoxyaniline (1.1 equiv., 0.243 mmol), DMAP (10 mol%, 0.0221 mmol, 2.7 mg) and 3-chloroquinoxaline-2-carbonyl chloride **99** (50 mg, 0.221 mmol) was dissolved in 10 mL DCM. The reaction mixture was stirred for 5 minutes, cooled to 0 ºC and Et_3N (3 equiv., 0.663 mmol, 0.0 9mL) was added drop wise. After the aqueous work up, the crude product was purified on prep TLC eluting with ethyl acetate/hexane (3:7) and gave 3-(3-isopropoxyphenylamino)-N-(3-isopropoxyphenyl)quinoxaline-2-carboxamide **101D** as orange solid (22 mg, 30%); mp = 379.6 – 380.6 ºC; δ_H (400 MHz, $CDCl_3$, ppm) 1.39 (12H, m), 4.63 (2H, sept), 6.64 (1H, *J* = 8.2 Hz, d), 6.75 (1H, *J* = 6.6 Hz, d), 7.29 (3H, m), 7.41 (1H, *J* = 7.9 Hz, d), 7.51 (2H, m), 7.71 (1H, m), 7.81 (2H, m), 7.93 (1H, *J* = 8.2 Hz, d), 10.23 (1H, brs), 11.29 (1H, brs); δ_C (400MHz, $CDCl_3$, ppm) 22.1, 22.2, 69.9, 70.0, 107.6, 107.9, 110.9, 112.3, 112.5, 112.6, 125.9, 126.8, 129.1, 129.5, 129.9, 131.2, 132.4, 134.9, 138.1, 140.6, 143.7, 149.6, 158.4, 158.6, 163.4; V_{max} (FT-IR) 687, 781, 1076, 1260, 1493, 1537, 1599, 1677, 2968, 3340 cm^{-1}; Calculated for ($C_{27}H_{28}N_4O_3$) 456.2161; HRMS (ESI); $[M+H]^+$, $C_{27}H_{28}N_4O_3$, found 457.2234.

4.3 Biological evaluation

4.3.1 Broth micro-dilution method

The synthesised compounds were evaluated for *in-vitro* antimycobacterial activity against *Mtb* $H_{37}R_V$ strain. The inhibitory activity against *Mtb* was achieved at the University of Cape Town, drug discovery and development centre (H3-D), following broth micro-dilution method. The broth micro-dilution method allows a range of antibiotic concentrations to be tested on a single 96-well microtitre plate in order to determine the minimum inhibitory concentration (MIC). Briefly, a 10 mL culture of a mutant *Mtb* ($H_{37}R_V$) strain constitutively expressing recombinant alamar blue assay of a plasmid integrated at the *attB* locus is grown to an OD600 of 0.6–0.7. The *Mtb*. $H_{37}R_V$ strain culture is then diluted 1:100 in 7H9 GLU CAS TX. In a 96-well microtitre plate, 50 µL of 7H9 GLU CAS TX medium is added to all wells from Rows 2-12. The compounds to be tested are added to Row 2-12 in duplicate, at a final concentration of 640 µM (stocks are made up to a concentration of 12.8 mM in DMSO, and diluted to 640 µM in 7H9 GLU CAS TX medium). A two-fold serial dilution is prepared, by transferring 50 µL of the liquid in Row 1 and 2 to mix. 50 µL of the liquid in Row 2 is then transferred to Row 3 and aspirated. The procedure is repeated until Row 12 is reached, from which 50 µL of the liquid is discarded to bring the final volume in all wells to 50 µL. Finally, 50 µL of the 1:100 diluted *Mtb* cultures are added to all wells in Rows 2-12. Row 1 serves as a contamination control which includes media, 5% DMSO and rifampicin. The microtitre plate is stored in a secondary container and incubated at 37 °C with humidifier to prevent evaporation of the liquid. The lowest concentration of compounds which inhibit growth of more than 90% of the bacterial population is considered to be the MIC_{90}. The pellet data is reported as visual score and calculated MIC during 14 day post inoculation [5].

4.3.2 MTT Assay

The synthesised compounds were evaluated for *in-vitro* antiproliferative activity against Raw 264.7, A549, HeLa, and MCF-7 cancer cell lines. Cell viability was determined using

MTT [3-(4,5-Dimethylthiazol-2-yl)-2,5-diphenyltetrazolium Bromide] assay which is principled on the ability of mitochondrial succinyl dehydrogenase in viable cells to convert soluble yellow tetrazolium salt into an insoluble formazan product. Briefly, cells (Raw 264.7, A549, HeLa, or MCF-7) were seeded at a density of 6 × 104 pre-well in a 96 well-plate and incubated overnight. Cells were then treated with various concentrations of quinoxaline derivatives (25 µM, 50 µM, 100 µM, and 200 µM), 0.5% DMSO in culture medium and 20 µg/mL Actinomycin-D for 24 hours. Prior to the addition of the MTT reagent, cell imaging was conducted. MTT of 5 mg/mL (Sigma Aldrich, Saint Louis, MI, USA) was added and after 4 h of incubation the aqueous medium was replaced with 100 µL DMSO. The blue formazan crystals were allowed to dissolve in DMSO by incubating in the dark for 30 min. Absorbance was then measured at 570 nm using GloMax-Multi microplate reader.

Reference

[1] Nxumalo, W. and Dinsmore, A., 2013. Preparation of 6-ethynylpteridine derivatives by Sonogashira coupling. *Heterocycles: an international journal for reviews and communications in heterocyclic chemistry*, *87*(1), pp.79-89.

[2] Armengol, M. and Joule, J.A., 2001. Synthesis of thieno [2, 3-b] quinoxalines and pyrrolo [1, 2-a] quinoxalines from 2-haloquinoxalines. *Journal of the Chemical Society, Perkin Transactions 1*, (9), pp.978-984.

[3] Kang, F.A., Lanter, J.C., Cai, C., Sui, Z. and Murray, W.V., 2010. Direct dehydrative cross-coupling of tautomerizable heterocycles with alkynes via Pd/Cu-catalyzed phosphonium coupling. *Chemical Communications*, *46*(8), pp.1347-1349.

[4] Alphonse, F.A., Karim, R., Cano-Soumillac, C., Hebray, M., Collison, D., Garner, C.D. and Joule, J.A., 2005. A bis (η5-cyclopentadienyl) cobalt complex of a bis-dithiolene: a chemical analogue of the metal centres of the DMSO reductase family of molybdenum and tungsten enzymes, in particular ferredoxin aldehyde oxidoreductase. *Tetrahedron*, *61*(46), pp.11010-11019.

[5] Yang, J., Pi, W., Xiong, L., Ang, W., Yang, T., He, J., Liu, Y., Chang, Y., Ye, W., Wang, Z. and Luo, Y., 2013. 3H-1, 2, 4-Dithiazol-3-one compounds as novel potential affordable antitubercular agents. *Bioorganic & Medicinal Chemistry Letters*, *23*(5), pp.1424-1427.